

**The Computational Role of Short-Term Plasticity and the
Balance of Excitation and Inhibition in Neural Microcircuits**
– Experimental and Theoretical Analysis –

Tiago Jorge de Pinho Carvalho

Oeiras, February 2009



Dissertation presented to obtain the
Doutoramento (Ph.D.) degree in Biology at the
Instituto de Tecnologia Química e Biológica
da Universidade Nova de Lisboa.

ISBN: 978-989-20-1525-5

Com o apoio financeiro da FCT e do FSE no âmbito do Quadro Comunitário de apoio, BD nº SFRH/BD/15211/2004

How does the brain work?

President of the Jury:

- Professor Miguel Nuno Sepúlveda Gouveia Teixeira, Instituto de Tecnologia Química e Biológica, Universidade Nova de Lisboa.

Members of the Jury:

- Professor Dean Buonomano, University of California, Los Angeles, USA;
- Professor Alex Reyes, New York University, USA;
- Dr. Rui Costa, National Institutes of Health, USA;
- Professor Ana Maria Ferreira de Sousa Sebastião, Faculdade de Medicina, Universidade de Lisboa;
- Dr. Sukalyan Chatterjee, Centro de Neurociências e Biologia Celular, Universidade de Coimbra;
- Professor Jorge Carneiro, Instituto de Tecnologia Química e Biológica, Universidade Nova de Lisboa.

Oeiras, February 9th 2009



Provas de doutoramento em Biologia
Candidato: Lic^o. Tiago Jorge de Pinho Carvalho
Data: 9 de Fevereiro de 2009

Voto

Aprovado

Recusado

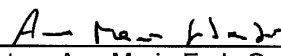
Justificação:

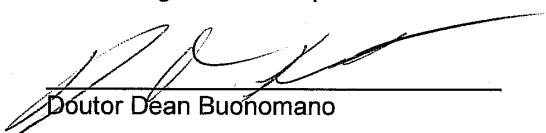
O candidato Tiago Jorge de Pinho Carvalho defendeu com sucesso a sua tese intitulada: "The Computational Role of Short-Term Plasticity and the Balance of Excitation and Inhibition in Neural Microcircuits: Experimental and Theoretical Analysis", no dia 9 de Fevereiro de 2009.

O candidato demonstrou ter um conhecimento do campo de trabalho em que realizou a teses, demonstrou ter um poder de síntese para escolher as experiências mais importantes para a sua tese, e escreveu uma tese muito clara.

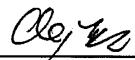
O candidato demonstrou ter pensamento crítico e ser capaz de realizar experiências e interpretar os resultados que obteve. Mais, o Candidato discutiu experiências que não resultaram, o que demonstrou maturidade científica. É nosso entendimento que o candidato merece o grau de doutorado.

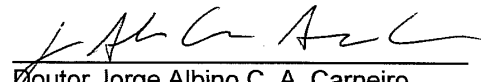

Doutor Miguel Nuño Sepúlveda G. Teixeira


Doutora Ana Maria F. de Sousa Sebastião


Doutor Dean Buonomano


Doutor Sukalyan Chatterjee


Doutor Alex Reyes


Doutor Jorge Albino C. A. Carneiro

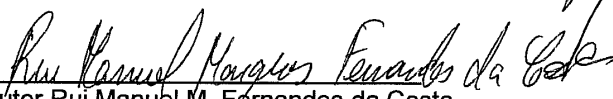

Doutor Rui Manuel M. Fernandes da Costa

TABLE OF CONTENTS

TABLE OF CONTENTS	<i>i</i>
ACKNOWLEDGEMENTS	<i>v</i>
SUMMARY (English)	<i>vii</i>
SUMÁRIO (Português)	<i>ix</i>
CHAPTER 1 Introduction	<i>1</i>
Basic General Concepts	<i>5</i>
Balance of Excitation and Inhibition in Neural Microcircuits	<i>9</i>
EPSP-Spike potentiation	<i>11</i>
Gain Modulation.....	<i>13</i>
Scope of Chapter 2.....	<i>15</i>
Short-Term Synaptic Plasticity (STP).....	<i>17</i>
Mechanisms of STP.....	<i>18</i>
Computational Models Incorporating STP	<i>19</i>
Scope of Chapter 3.....	<i>20</i>
Final Introductory Remarks	<i>21</i>
CHAPTER 2 Differential effects of excitatory and inhibitory plasticity on synaptically-driven neuronal Input-Output functions	<i>23</i>
Abstract	<i>27</i>
Introduction	<i>29</i>
Results	<i>33</i>
Discussion.....	<i>51</i>
Methodology.....	<i>57</i>

Supplemental Figures	61
Supplemental Information Regarding the Mechanisms Underlying Gain Control.....	67
Supplemental Methods.....	75
Acknowledgments	81
CHAPTER 3 Short-term plasticity and metaplasticity of short-term plasticity enhance the discrimination of spatiotemporal stimuli in simulated neural networks	83
Abstract	87
Introduction.....	89
Methodology.....	91
Results	99
Discussion	115
Acknowledgements	119
CHAPTER 4 Final Discussion.....	121
APPENDIX A Spike-Timing-Dependent Plasticity (STDP)	127
APPENDIX B Neural Dynamics in Organotypic Cortical Networks	135
Summary	137
Methods.....	139
Results	143
Discussion	155
REFERENCES	157

ACKNOWLEDGEMENTS

First and foremost, I would like to thank my close family for their unconditional support in these difficult times. In particular, I thank my mom, who has revealed herself as a strong and truly extraordinary human being that constantly leaves me full of admiration for her tenderness, tolerance and wise decisions. To my brother, whom I do not think is aware of how much I love and care about him. To my dad, while I am sure that he is very proud and would like to enjoy this moment with me, I just hope he will one day re-connect with the simple people that truly care about him.

I am happy for finally having the chance to properly acknowledge Professor Arnaldo Videira for the opportunities and trust he gave me, and Margarida Duarte for her patience and dedication in the beginning of my scientific career. I feel extraordinarily lucky to have had such a supportive start, from which everything else developed.

Naturally, there are people that had a more direct role in contributing to the success of this Ph.D., as supervisors but above all as mentors. To Sukalyan I am in debt for his support and for his clarity and rationality of thoughts, especially in times where everything seemed so cloudy and complicated. Sukalyan's lessons extend well beyond science and I was fortunate enough to have benefited from his "human-being lessons" as well. To Dean, well... these were years of intense scientific learning! I knew nothing about neuroscience and Dean was audacious enough to accept me in his lab. We shared long hours trying to figure out "how the brain works", during which my imagination often drifted to implausible scenarios. But as a true mentor teaching his apprentice, Dean kept patiently pulling me back down to earth to steer my focus to the biologically meaningful explanations. Dean is an extraordinary and truly genuine scientist, and he is completely passionate

about the mysteries of the brain. Let there be no doubts that the final outcome of this thesis project would not be the same if it were not for Dean's feedback, support and motivation, both inside the lab as well as outside of it. Of course these acknowledgements extend naturally to everyone else in the lab, whom I had the pleasure to work with.

To my eternal roommate Cleide, for her friendship and for making my life in Los Angeles so pleasant and colorful.

And finally, for everything that it encompasses, my touched thank you to Lotta who has shared with me the vast majority of the intense up and down moments, and helped me deal with some of the burden of this intense Ph.D. trip. The most important memories and lessons I learned from these last four and a half years extend well outside the scope of this thesis and I was very fortunate to have Lotta sharing her feelings with me while being my safe harbor when work in the lab was not going as well (as it always happens with any serious research – otherwise where are the problems to be solved?). My mood and motivation would not have endured such a journey if it was not for such special companionship and heart felt love. Love you!

Needless to say, the extraordinary financial support from FCT provides students with a competitive advantage that is very much appreciated.

SUMMARY (English)

The computations performed by the brain ultimately rely on the functional connectivity between neurons embedded in complex networks. It is well known that the neuronal connections, the synapses, are plastic, i.e. the contribution of each presynaptic neuron to the firing of a postsynaptic neuron can be independently adjusted. The modulation of effective synaptic strength can occur on time scales that range from tens or hundreds of milliseconds, to tens of minutes or hours, to days, and may involve pre- and/or post-synaptic modifications. The collection of these mechanisms is generally believed to underlie learning and memory and, hence, it is fundamental to understand their consequences in the behavior of neurons.

Virtually all neurons in the brain receive inputs from excitatory and inhibitory synapses, and their response to a brief stimulus is determined by the magnitude and net balance of fast excitatory and inhibitory currents. While it is well established that both synapse types are plastic, the computational benefit of their concerted regulation is not understood. Computer simulations showed that excitatory plasticity primarily controls the threshold of the neuronal input-output function, while balanced changes in excitation and inhibition modify the gain, independently of the threshold. These theoretical results generated testable predictions that were confirmed experimentally in rat hippocampal slices with a collection of electrophysiological techniques. These data support the existence of two types of functional synaptic plasticity: threshold and gain plasticity.

In addition to these long-term changes in synaptic strength it is known that the effective synaptic efficacy between two neurons can dynamically decrease or increase in a use-dependent manner, on a time scale on the order of tens to hundreds of milliseconds. Here, it is shown that this phenomenon,

known as short-term synaptic plasticity (STP), enhances the ability of small networks of neurons to discriminate time-varying stimuli, such as Poisson spike patterns. Additionally, it is proposed that STP may be governed by specific learning rules in which synapses ‘learn’ *when* to be strong – i.e., whether to express short-term synaptic depression or facilitation. Computer simulations show how the discrimination of spatiotemporal patterns greatly benefits from metaplasticity of short-term plasticity.

Together, the work presented here contributes to bridging the gap between the understanding of synaptic and cellular properties and neural systems, by studying network dynamics and plasticity at the level of isolated neuronal circuits.

SUMÁRIO (Português)

As computações efectuadas pelo cérebro dependem, em última análise, das conexões entre neurónios embebidos em redes complexas. É sabido que estas conexões, as sinapses, são plásticas, i.e. a contribuição de cada neurónio pré-sináptico para a activação do neurónio pós-sináptico pode ser ajustada independentemente. O controlo do peso efectivo de cada sinapse pode ocorrer a diferentes níveis – em escalas de dezenas ou centenas de milisegundos, até minutos, horas ou dias – e pode envolver modificações pré- e/ou pós-sinápticas. Está estabelecido que os fenómenos de memória e aprendizagem dependem do conjunto destes mecanismos e, portanto, é fundamental conhecer e perceber as consequências de todas estas modificações sinápticas no comportamento dos neurónios.

Praticamente todos os neurónios no cérebro recebem informação de sinapses excitatórias e inibitórias, e, portanto, a resposta dos neurónios a estímulos transientes é determinada pela magnitude e pelo balanço entre as correntes excitatórias e inibitórias rápidas. Enquanto que está estabelecido que ambas as sinapses são plásticas, não é conhecido qual o benefício computacional da sua regulação concertada. Simulações computacionais mostraram que a plasticidade excitatória controla principalmente o limiar da função de entrada-saída (I/O) do neurónio, enquanto que modificações paralelas da excitação e inibição modificam o ganho, independentemente do limiar. Estes resultados teóricos geraram hipóteses testáveis e que foram confirmadas experimentalmente em fatias de hipocampo de rato, através de um conjunto de técnicas electrofisiológicas diferentes. Estes dados sugerem a existência de dois tipos de plasticidade sináptica funcional: plasticidade do limiar e do ganho do neurónio.

Para além das modificações de longo termo da força sináptica é sabido que a eficácia efectiva entre dois neurónios pode decrescer ou aumentar dinamicamente dependendo da actividade, numa escala da ordem das dezenas às centenas de milisegundos. Aqui mostra-se que este fenómeno, denominado de plasticidade sináptica de curto termo, aumenta a capacidade de pequenas redes de neurónios de discriminarem estímulos temporais, tais como padrões de Poisson. Adicionalmente, é proposto que a plasticidade de curto termo pode ser governada por regras específicas em que as sinapses “aprendem” quando ser fortes – i.e., quando expressar depressão ou facilitação de curta duração. Simulações computacionais mostram que a discriminação de padrões espacio-temporais beneficia desta metaplasticidade da plasticidade de curta duração.

No seu conjunto o trabalho aqui apresentado contribui para preencher o vazio entre o conhecimento das propriedades sinápticas e celulares e o comportamento de redes neurais complexas, ao estudar plasticidade sináptica e as suas consequências funcionais em circuitos neuronais simples.

CHAPTER 1

Introduction

The brain is the center of the nervous systems of all vertebrate animals (Kandel and Schwartz, 1985). The human brain weights approximately 1,400 grams (Byrne, 2003) and is the most complex biological structure known (Shepherd, 1994), with its 100 billion neurons, each of which connecting to as many as 1,000 - 10,000 other cells (Kandel and Schwartz, 1985). It is now generally accepted that human behavior, consciousness, feelings and emotion are intrinsically dependent and related to brain activity (Damásio, 1994). Nevertheless, what constitutes the human essence is still a point of scientific and philosophical debate (Czerner, 2001; Stevens, 2005).

From a scientific point of view, it is safe to say that animal behavior (in which humans are included) is limited by the biological substrate of the nervous system, namely the number and types of cells and their connectivity patterns. Through this highly complex structure flow patterns of neuronal activity that on one hand carry representations of the sensorial world and, on the other hand, determine and execute the behavioral interaction with the external world.

One of the fundamental goals of neuroscientists is to understand how the brain transmits and processes information, i.e. to 'crack the neural code'. To achieve this goal there is a need to understand how and when 'simple' cellular phenomena become meaningful *neural computations*. This thesis is positioned somewhere in between the details of molecular biology or biochemistry and the large-scale neuronal patterns observable with fMRI or EEG, and it attempts to describe how certain subcellular events directly modulate the neural output, which ultimately determines behavior.

Basic General Concepts

There are two main categories of cells in the brain: neurons and glial cells. While each of the following properties may not be exclusive of each category, in general, neurons differ from glial cells by their ability to generate propagated action potentials (also called spikes) and in their ability to communicate with other neurons through specialized subcellular structures called the *synapses*. Neurons are polarized cells in the sense that their citoarchitecture is divided into specialized compartments with different biological functions: the dendrites and the axon (usually one). Neurons receive information from certain locations in the dendritic plasma membrane that contain neurotransmitter receptors; and release neurotransmitter at specialized locations in the axon (the presynaptic terminal) (Byrne, 2003).

The work presented here focuses exclusively on neurons as they may be the main contributors to information propagation in the brain. There are many different cellular types of neurons, but they can be broadly classified into two general groups according to the neurotransmitter they release: excitatory and inhibitory neurons (Miles, 2000).

Due to the action of constantly active ionic pumps ($\text{Na}^+\text{-K}^+\text{-ATPases}$), the intracellular side of neurons is negatively charged with relation to the extracellular milieu, which generates a difference in potential (Wright, 2004) (reference values may be around -60 to -70 mV). Thus, if positive ions enter the cell the membrane potential will become less negative and the neuron depolarizes. Conversely, if negative ions enter the neuron its potential will become more negative and the cell hyperpolarizes (Brock et al., 1952a, b).

When excitatory neurons become active they generate an action potential that travels down the axon, causing the release of glutamate from the *presynaptic* terminals. The released glutamate binds to AMPA (α -amino-3-

hydroxyl-5-methyl-4-isoxazole-propionate) channels on the *postsynaptic* side resulting in the influx of Na^+ , causing the postsynaptic neuron to depolarize slightly and transiently, i.e., producing an excitatory postsynaptic potential (EPSP) (Brock et al., 1952b). If there are sufficient (~10-30) presynaptic terminals releasing glutamate in close temporal proximity (~5-20 ms) the summed depolarization in the postsynaptic neuron might reach threshold (~ -40 mV) and triggers the generation of an action potential in the postsynaptic neuron. This flow of neuronal activity throughout networks of neurons is related to information transmission in the brain.

Roughly 20% of the neurons in the brain are inhibitory (Beaulieu et al., 1992) and the mechanisms of synaptic transmission and action potential generation are similar to described above. However, when inhibitory neurons elicit an action potential it is generally the neurotransmitter GABA (Gamma-aminobutyric acid) that is released instead of glutamate. GABA binds to GABAA receptors on the surface of the postsynaptic neuron, causing an inflow of Cl^- (an inhibitory postsynaptic potential – IPSP) (Brock et al., 1952b), causing the neuron to hyperpolarize..

Each cortical neuron receives inputs from many excitatory and inhibitory synapses, and during active cortical processing neurons receive a barrage of excitatory and inhibitory inputs (Hirsch et al., 1998; Destexhe and Pare, 1999; Steriade, 2001). In simple terms, it is the compound interaction between the depolarizing and hyperpolarizing effects of EPSPs and IPSPs that will determine whether or not the postsynaptic neuron will elicit an action potential (Pouille and Scanziani, 2001; Wehr and Zador, 2003; Wilent and Contreras, 2005).

Another prominent feature of neurons is *synaptic plasticity*, which means that the ability of synapses to depolarize (or hyperpolarize) a neuron can increase or decrease. Activity-dependent forms of synaptic plasticity

induce changes in the strength of synapses in a way determined by the patterns of pre- and/or postsynaptic activity (Malenka and Bear, 2004; Caporale and Dan, 2008).

There are many forms of synaptic plasticity, but here the focus will be on short-term forms of synaptic plasticity (STP), which last tens to hundreds of milliseconds, and long-term forms of synaptic plasticity (long-term potentiation, LTP; or long-term depression, LTD), which persist for tens of minutes or longer. Collectively, the multiple forms of synaptic plasticity are responsible for the dynamics of neural circuit function and are thought to play important roles in learning and memory (Buonomano and Merzenich, 1998b).

Balance of Excitation and Inhibition in Neural Microcircuits

A virtually ubiquitous network motif in the brain is the disynaptic microcircuit, in which an input generates an EPSP via a direct excitatory synapse followed by a fast IPSP, via an indirect feed-forward inhibitory synapse (Buzsaki and Eidelberg, 1981; Buzsaki, 1984; Ferster, 1986; Pouille and Scanziani, 2001; Wehr and Zador, 2003; Wilent and Contreras, 2005; Kapfer et al., 2007).

Both the excitatory (Bliss and Lomo, 1973; Dudek and Bear, 1992; Malenka and Bear, 2004) and inhibitory (Komatsu, 1994; Xie et al., 1995; McLean et al., 1996; Lu et al., 2000; Gaiarsa et al., 2002; Chevaleyre and Castillo, 2003) synapses are known to undergo long-term plasticity, suggesting that the tuning of each plays a critical role in controlling the response of the post-synaptic neuron. Previous experimental evidence indicates that excitation and inhibition (Ex-Inh) are balanced or co-tuned (Galarreta and Hestrin, 1998; Wehr and Zador, 2003, Gabernet and Scanziani), suggesting that this balance is important for cortical function and that there are mechanisms in place to actively maintain it.

Wehr and Zador (Wehr and Zador, 2003) recorded intracellularly from neurons in primary auditory cortex of anaesthetized rats and analyzed the response of the neuron to brief auditory tones (25-70 ms duration). By recording the total synaptic current evoked by the auditory stimulation, while voltage-clamping the neuron at different holding potentials, they were able to decompose the synaptic response into excitatory and inhibitory conductances. Their main observation was that excitatory and inhibitory conductances were co-tuned for sound frequency and intensity. In other words, they observed that

the stimuli that elicited maximal excitatory synaptic drive would also evoke maximal inhibitory synaptic drive.

More recently, Froemke et al. (Froemke et al., 2007) also recorded the response evoked by brief auditory tones (50 ms duration), from neurons in the auditory cortex of anaesthetized rats. After determining the excitatory and inhibitory synaptic conductances at different sound frequencies, they paired nucleus basalis stimulation (the main source of cortical acetylcholine) with tones at a frequency different than the preferred one. They observed that this protocol rapidly potentiated tone-evoked EPSCs and depressed IPSCs at the paired sound frequency. Interestingly however, they observed that tens of minutes after the pairing there was a gradual increase in the IPSCs elicited by the paired frequency, thus re-balancing again EPSCs and IPSCs.

The functional significance of this balance has not been fully elucidated yet, but a number of non-mutually exclusive hypothesis have been put forth regarding the function of balanced Ex-Inh, including:

- keeping excitation in check and preventing epileptic-like activity (Freund and Buzsaki, 1996; Galarreta and Hestrin, 1998);
- controlling the period over which effective EPSP summation can occur – the temporal integration window (Wehr and Zador, 2003; Gabernet et al., 2005; Wilent and Contreras, 2005);
- balanced Ex-Inh is critical for computations such as temporal processing (Buonomano, 2000);

EPSP-Spike potentiation

Since the discovery of potentiating and depressing forms of long-term synaptic plasticity (Bliss and Lomo, 1973; Dudek and Bear, 1992), there has been extensive molecular and physiological characterization of these phenomena. Physiological studies classically focus on the enhancement or depression of excitatory subthreshold responses; specifically, by looking at the slope of EPSPs before and after the plasticity inducing protocol. The initial slope of the EPSP is a measure of the synaptic excitatory drive onto the cell (Wigstrom and Gustafsson, 1985; McCormick et al., 1993) and thus it is a valid measure to assess the changes induced by the plasticity protocols.

Aside from the debate regarding the fine details of long-term synaptic plasticity, it is important to realize that *changes in EPSP strength are only functionally significant when they translate into changes in the firing patterns of the postsynaptic neuron*. Accordingly, early in the development of the field there was an interest in understanding the relationship between evoked extracellular EPSPs (field EPSPs or fEPSPs – a measure of neuronal input), and the simultaneously recorded extracellular population spike amplitude (Pop. Spike – the *output* of the neurons). After the induction of LTP there is an increase in the slope of fEPSPs, but it was not known how that would relate with the Pop. Spike amplitude.

Andersen et al. (Andersen et al., 1980) observed that tetanization of the Schaffer collaterals in acute hippocampal slices induced a long lasting *left-shift* of this E-S function (fEPSP slope vs. Pop. Spike amplitude). Functionally, this would mean that after the LTP induction protocol a fEPSP of the same slope could drive more neurons to fire action potentials, and hence the term E-S potentiation.

Kairiss et al. (Kairiss et al., 1987) confirmed these results in the perforant path synapse of the dentate gyrus but in addition to the left-shift of

the E-S relationship it was also observed a decrease in the E-S *slope*. The slope of these types of Input/Output (I/O) functions is related to the sensitivity or *gain* of the neuronal response: a smaller gain means that a given change in the fEPSP is accompanied by a smaller change of the population spike. Kairiss et al. suggested that the LTP inducing protocol may also be inducing a parallel increase in the strength of inhibitory synapses, which could be the cause of the slope change of the E-S curve.

A commonality in these earlier studies is that the protocol used to induce synaptic plasticity (extracellular tetanic stimulation) was likely to induce plasticity at excitatory synapses, but may also induce plasticity of excitatory-to-inhibitory and inhibitory-to-excitatory synapses as well.

More recently, Marder and Buonomano (Marder and Buonomano, 2004) re-examined the issue of E-S potentiation with the goal of determining the mechanisms underlying the observed left-shift of the E-S function. Marder and Buonomano performed *single-cell* intracellular recordings and plotted the EPSP slope versus the action potential probability for a series of increasing stimulation intensities. Intracellular I/O functions can be defined by two parameters: the *gain* (similar to extracellular I/O functions) and the *threshold* (the EPSP slope that elicits action potentials with 50% probability), which is a measure of the position of the curve on the x-axis. To induce LTP Marder and Buonomano used an associative pairing protocol, which was shown to elicit plasticity at the excitatory synapses with no changes in IPSPs or intrinsic excitability. As expected, LTP caused an increase in the EPSP slope, but when the stimulation intensity is reduced until the EPSP slope is back to the original levels there is also a reduction in the activation of feed-forward inhibitory neurons. Thus, after LTP the *same EPSP slope* is accompanied by less inhibition and thus the neuron has an increased probability of firing an action potential, explaining the *left-shift* of the E-S function.

Gain Modulation

Finally, another line of research that has received considerable attention, and that relates to the work presented here, concerns the gain modulation of the neuronal Input/Output function. Above, it was discussed that increases in excitatory synaptic *strength* could induce leftward shifts of the I/O function (E-S potentiation). Given that, during active cortical processing, neurons are being constantly bombarded with excitatory and inhibitory inputs from other neurons, we will consider in this section the impact of that background synaptic activity on the neuronal I/O characteristics. Gain modulation consists in changing the sensitivity of neurons without changing their selectivity or, in other words, changing the slope of the relationship between input 'intensity' and spike output (Cardin et al., 2008).

Chance et al. (Chance et al., 2002) analyzed the mechanisms underlying gain modulation by recordings from layer 5 pyramidal neurons, in rat brain slices, in dynamic clamp mode (Robinson and Kawai, 1993; Sharp et al., 1993) with two whole-cell somatic recording electrodes. Briefly, using this configuration Chance et al. were able to measure the voltage through one electrode and simultaneously inject current through the other electrode, directly into the soma of the neuron. To simulate background synaptic noise they modeled independent excitatory and inhibitory conductances from many 'synapses', and the computer would calculate in a continuous fashion how much current should be injected through the electrode to mimic that synaptic activity.

In their definition of the neuronal I/O function Chance et al. considered the output *firing rate* of the neuron versus an injected step of constant depolarizing current (2-3 sec.). After determining a 'basal' I/O response they injected the simulated noisy currents and observed that balanced increases in

the excitatory and inhibitory ‘synaptic’ conductances had a divisive gain modulation effect (the slope of the curve decreases). To determine the mechanistic causes underlying this gain modulation they analyzed separately the shunting and the membrane potential (Vm) fluctuation contributions, caused by increased background activity. They concluded that increased shunting shifts additively the curve to the right, while increased Vm fluctuations facilitate responses at all depolarizing levels, but more so for smaller driving currents. The combination of these two effects results in divisive gain modulation.

The work of Chance et al. was followed up by Shu et al. (Shu et al., 2003), where they used UP states in cortical slices to emulate physiologically increases in background synaptic activity, essentially confirming the previous results.

Recently, Cardin et al. (Cardin et al., 2008) attempted to further elucidate the cellular mechanisms of gain modulation in vivo. They performed intracellular recordings in primary visual cortex of anesthetized cats and analyzed the effects on the neuronal I/O function of two different visual stimuli (drifting grating and broadband stimuli), which elicit background synaptic inputs with different characteristics. The neuronal I/O function was again defined as the mean firing rate caused by constant depolarizing current pulses (100 ms) of different intensities.

Increasing the contrast of drifting grating stimuli caused non-linear increases in the Vm standard deviation, membrane depolarization and decrease in the input resistance of neurons. Accordingly with previous results (Chance et al., 2002; Shu et al., 2003), drifting grating visual stimuli of increasing contrast caused a decrease in the slope of the I/O function (gain modulation). On the other hand, broadband stimuli of increasing contrasts did not induce membrane depolarization or change the input resistance in the

recorded neurons, but still caused a linear increase in the Vm standard deviation. Curiously, this visually evoked increase in Vm fluctuations alone failed to affect neuronal gain, raising the hypothesis that the mechanisms of gain modulation in vivo may involve other properties besides input noise caused by the input.

Scope of Chapter 2

All together, these brief descriptions of some previous work give an idea of the state of the art in the fields that relate to the work presented in Chapter 2.

The gain modulation observed in the studies just mentioned (Chance et al., 2002; Shu et al., 2003; Cardin et al., 2008) relied on background synaptic input, which may be caused by changes in the state of the animal and thus allowing for rapid and online modulation of neural computations. However, during longer-term processes, such as learning and memory, it should also be possible to modulate the gain of neurons in a more permanent manner. Here, it will be considered whether synaptic plasticity could mediate such an effect.

Accordingly, we analyzed the changes induced by excitatory and inhibitory synaptic plasticity in *synaptically* determined I/O functions of single neurons. In the context of the E-S potentiation field, we contribute by analyzing not only the LTP-induced left shifts of I/O functions, but by also analyzing the changes in gain, thus completing the possible modifications that may occur to the I/O function. In addition, we also determine the contribution of inhibitory synaptic plasticity in the modulation of single-neuron I/O functions.

These results establish a framework to understand the effects of excitatory and inhibitory plasticity on both the gain and threshold shifts of the neuronal I/O function. They relate to the balance of excitation and inhibition

because they may provide answers to intriguing questions such as: why are there plasticity protocols that potentiate both EPSPs and IPSPs onto the same postsynaptic neuron? (Brown et al., 1990; Komatsu, 1994; Xie et al., 1995; Shew et al., 2000, Froemke Merzenich). What is the computational benefit of this apparently self-defeating form of plasticity? From a computational perspective, what is the functional difference between potentiating excitatory and depressing inhibitory inputs?

One concept that is fundamental throughout this thesis is that, whether one is considering small or large networks of neurons, the computations that can be performed are ultimately dependent on the conversion of input to output by each individual neuron that makes up the network.

Here, we propose that one of the functions of the feed-forward neuronal circuit architecture, along with the presence of plasticity at both the excitatory and inhibitory branches, is to allow neurons to control independently the two features that ultimately determine their role in a local computation: the gain and threshold of their I/O function.

Short-Term Synaptic Plasticity (STP)

In the second chapter of this thesis we focused on how long-term synaptic plasticity affects the *output* of neurons, with regards to brief and transient synaptically activated *inputs* (I/O function). The changes in gain and threshold that are presented are possible because synapses are plastic and their strength can increase or decrease in an activity dependent manner (Malenka and Bear, 2004; Caporale and Dan, 2008). In this framework synapses are simple communication channels, that increase or decrease how 'loud' they transmit, and the computations and integration of information are performed by the neuron, which is often considered the computational unit of the brain (Abbott and Regehr, 2004).

However, another noteworthy property of synapses is their ability to keep track of their history of prior activity through a phenomenon called Short-Term synaptic Plasticity (STP), in which the *effective* synaptic strength between two neurons can also dynamically decrease or increase but in a *use-dependent manner*, on a time scale on the order of tens to hundreds of milliseconds.

During active cortical processing, neurons (and thus synapses) are active at rates between 5-20 Hz, or even higher (Abbott et al., 1997; Steriade et al., 2001). Thus, due to the ubiquitous presence of STP, the *effective* synaptic strength between two neurons in the brain will change dynamically depending on the frequency of firing of the presynaptic neuron and on the specific characteristics of each synapse (Markram and Tsodyks, 1996; Abbott et al., 1997; Reyes et al., 1998).

While STP was discovered long time ago (in the neuromuscular junction, Eccles et al., 1941; Eccles and Mac, 1949), a quick search in Pubmed suggests that it has received less attention compared to long-term

forms of synaptic plasticity, even though its computational effects in the brain may be no less important.

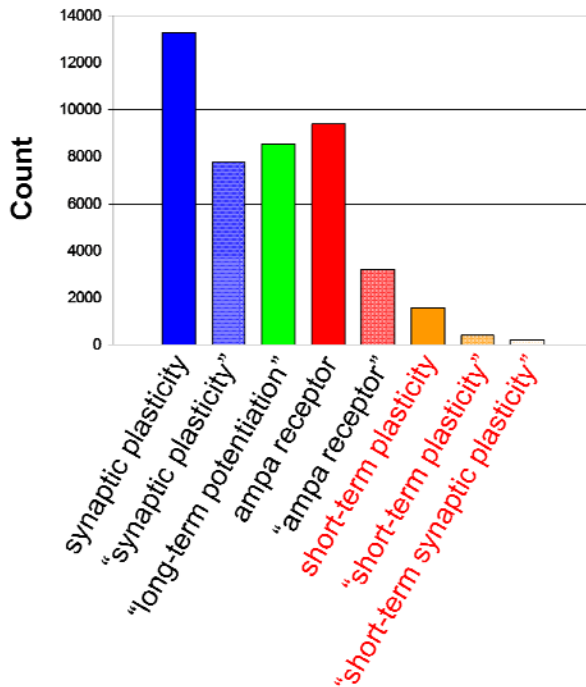


Figure 1 – Number of Pubmed results for the respective search term. Searching with quotes forces phrase searching.

Mechanisms of STP

The mechanisms underlying short-term synaptic plasticity have not been completely unraveled yet, but there is a growing consensus that synaptic depression due to long trains of stimulating pulses may be attributed to depletion of the readily releasable pool of synaptic vesicles (Rosenmund and Stevens, 1996; Schneggenburger et al., 2002; Zucker and Regehr, 2002). However, paired-pulse depression may rely on alternate mechanisms

(Sullivan, 2007). Synapses that have a low probability of vesicle release are likely to show some degree of short-term facilitation (Dobrunz and Stevens, 1997). In these cases, trains of action potentials may cause accumulation of residual calcium, which binds to sensor proteins that trigger transmitter release, thus enhancing synaptic transmission (Katz and Miledi, 1968; Zucker and Regehr, 2002).

A recent alternative is that, in some systems, depression and facilitation may be caused by common mechanisms, involving Ca^{2+} -dependent regulation of Ca^{2+} sensor proteins that regulate the presynaptic calcium channels responsible for triggering transmitter release (Mochida et al., 2008).

Computational Models Incorporating STP

Buonomano and Merzenich (Buonomano and Merzenich, 1995) showed through computer simulations that STP (specifically, paired-pulse facilitation, PPF), together with slow IPSPs, could allow networks of neurons to discriminate time-varying stimuli such as brief-pulse intervals, input rates, simple temporal patterns or even phonemes. In their paper, the input layer feeds to a model of LIV, which in turn feeds a model of LII/III. Importantly, each brief, tap-like, stimulus activates the *same* set of input neurons to make sure that the network is not using spatial information, i.e., *which* input neurons get activated. Equally important is the fact that there was no learning or changes in the synaptic weights but, due to the time-dependent properties of PPF and slow IPSPs, the *second* stimulus of a pair coming at either 100 or 200 ms after the first will elicit different patterns of activation in each layer. A set of output neurons was connected to LII/III and a simple supervised learning rule was used in those synapses, so that the output neurons could learn the different patterns elicited by each of the different stimuli, and in this manner become detectors of the trained stimulus.

Other studies have proposed a computational role for STP including temporal processing (Buonomano, 2000), working memory (Mongillo et al., 2008) and gain control (Abbott et al., 1997; Chance et al., 1998; Galarreta and Hestrin, 1998). However, most of these studies have not considered synapse specific STP, nor ‘plasticity’ of STP itself.

Scope of Chapter 3

It is well established that each of the multiple spikes in a train do not contribute equally to the depolarization of the post synaptic cell, due to STP (Markram and Tsodyks, 1996; Reyes et al., 1998). Given that neurons in the cortex are active at high firing rates, it is likely that STP plays a role in shaping information processing and transmission. In Chapter 3, we consider the computational potential of STP for the discrimination of spatiotemporal spike patterns in simple feed-forward neural networks.

In addition, multiple forms of STP have been observed in the brain, in a synapse specific manner (Markram et al., 1998; Reyes et al., 1998; Rozov et al., 2001; Zucker and Regehr, 2002). We propose that this diversity may be the result of ‘adaptive’ (or plastic) mechanisms that determine how much and for how long a synapse should depress or facilitate, depending on the computation at hand. This would imply that STP is much more than a general mechanism to regulate gain control or other general properties but takes an active role in performing computations, in a synapse specific manner. Indeed, we propose that STP itself may be plastic and propose a learning rule for this metaplasticity of short-term plasticity.

Final Introductory Remarks

Throughout this work, we considered two well known properties of biological neural networks, namely long-term (Chapter 2) and short-term (Chapter 3) forms of synaptic plasticity. We show, using a combination of experiments and computer simulations, how the dynamics of synaptic plasticity may determine the *output* of neurons and propose specific examples of how these properties could be used by the brain to perform computations.

CHAPTER 2

Differential effects of excitatory and inhibitory plasticity on synaptically-driven neuronal Input-Output functions

Differential effects of excitatory and inhibitory plasticity on synaptically-driven neuronal Input-Output functions

Tiago P. Carvalho^{1,2} & Dean V. Buonomano^{2,3,4}

¹*Gulbenkian Ph.D. Program in Biomedicine, P-2781-901 Oeiras, Portugal.*

²*Departments of Neurobiology and ³Psychology, and ⁴Brain Research Institute, University of California, Los Angeles, CA 90095, USA.*

Correspondence should be addressed to D.V.B. (dbuono@ucla.edu)



Abstract

Ultimately, whether or not a neuron produces a spike determines its contribution to local computations. In response to brief stimuli the probability a neuron will fire can be described by its input-output function, which depends on the net balance and timing of excitatory and inhibitory currents. While excitatory and inhibitory synapses are plastic, most studies examine plasticity of subthreshold events. Thus, the effects of concerted regulation of excitatory and inhibitory synaptic strength on neuronal input-output functions are not well understood. Here, theoretical analyses reveal that excitatory synaptic strength controls the threshold of the neuronal input-output function, while inhibitory plasticity alters the threshold and gain. Experimentally, changes in the balance of excitation and inhibition in CA1 pyramidal neurons also altered their input-output function as predicted by the model. These results support the existence of two functional modes of plasticity that can be used to optimize information processing: threshold and gain plasticity.

Introduction

A large number of studies have characterized the mechanisms and learning rules underlying synaptic plasticity, and it is generally accepted that changes in synaptic strength contribute to learning and memory (Martin et al., 2000; Malenka and Bear, 2004). However, since alterations in behavior must ultimately be caused by changes in neuronal firing, it is not synaptic plasticity *per se*, but how synaptic plasticity modifies the *output* of neurons, that underlies learning. Thus, to understand the relationship between synaptic plasticity and learning it is important to elucidate how synaptic plasticity alters the input-output characteristics of neurons.

We use the term *neuronal Input-Output (I/O) function* to refer to the relationship between the excitatory input to a neuron and the probability it will generate an action potential (**Fig. 1B,C**) (Daoudal and Debanne, 2003; Staff and Spruston, 2003; Marder and Buonomano, 2004; Campanac and Debanne, 2008). A neuron's I/O curve, generally represented as a sigmoidal function, is characterized by two components: the threshold and the gain. Here we define the I/O threshold as the EPSP slope that elicits a spike 50% of the time (this usage is similar to that in the artificial neural network literature in which threshold refers to the midpoint of the activation function, Rumelhart et al., 1986). The gain refers to the rate of change or sensitivity of the I/O function (**Fig. 1C**). The I/O threshold and gain of a neuron are directly related to its computational role, as both of these features can be used to quantify the ability of neurons to discriminate sensory stimuli (Mountcastle and Powell, 1959; Maffei and Fiorentini, 1973; Dean et al., 2005) and optimize the encoding of sensory information (Laughlin, 1981). Indeed, at the psychophysical level similar measures are used to quantify behavioral performance, where the threshold and gain are related to the point of subjective equality and just noticeable difference, respectively (Morrone et al., 2005; Lapid et al., 2008).

Previous studies have established that LTP alters the threshold of the I/O function – a phenomenon referred to as EPSP-spike (E-S) potentiation (Andersen et al., 1980). Specifically, an EPSP of the same strength (as measured by the slope), that was not effective in eliciting spikes, can fire the cell after the induction of LTP. While the mechanisms underlying the LTP-induced shift in the I/O function continue to be debated (Daoudal and Debanne, 2003; Frick et al., 2004; Marder and Buonomano, 2004; Campanac and Debanne, 2008), the balance of excitation and inhibition is known to be an important contributing factor. For example, one reason that an EPSP of a given size can elicit a spike after LTP, but not before, is due to an increase in the excitation/inhibition ratio. After LTP, a smaller stimulation intensity is required to elicit the same size EPSP and consequently fewer inhibitory neurons will be recruited and those that are will have a longer latency, which facilitates the generation of the action potential (Marder and Buonomano, 2004). However, in contrast to the threshold, previous studies have not examined how excitatory plasticity influences the gain of neuronal I/O functions. Additionally, to date no general framework exists as to how excitatory and inhibitory synaptic plasticity interact to control the I/O function of a neuron.

To understand how synaptic plasticity alters the behavior of neurons it is necessary to characterize the I/O function in response to *synaptically* evoked activity. It is important to note that the issue of long-term changes in I/O functions produced by synaptic plasticity is distinct from the rapid ‘online’ changes in gain of the firing rate curve – such as the modulation produced by the position of the eyes (Trotter and Celebrini, 1999) or attention (McAdams and Reid, 2005) – that are critical for many sensory and motor computations (Salinas and Thier, 2000). It has been shown that the gain modulation of the firing rate curves is dependent on background synaptic activity (Chance et al., 2002; Murphy and Miller, 2003; Prescott and De Koninck, 2003; Cardin et al., 2008). These studies typically examine steady-state firing rate in response to

injected depolarizing current steps, and address how firing rate is modulated on a rapid time scale for online computations. The distinct question addressed here pertains to the probability a neuron will spike in response to a brief stimulus depending on the *strength* of the active excitatory and inhibitory synapses. The focus on the early response to stimuli is important, particularly in sensory systems, because it is the transient response that is critical to many sensory computations (Durstewitz and Deco, 2008; Rabinovich et al., 2008) and brief sensory stimuli often elicit only one or a few spikes (DeWeese et al., 2003; Wang et al., 2005). Indeed, in many cases steady-state responses are unlikely to contribute to computations (Rolls and Tovee, 1994; Thorpe et al., 1996; Hung et al., 2005; Rabinovich et al., 2008).

While it is established that both EPSPs (Bliss and Lomo, 1973; Dudek and Bear, 1992) and IPSPs (Komatsu, 1994; McLean et al., 1996; Lu et al., 2000; Gaiarsa et al., 2002; Chevaleyre and Castillo, 2003) undergo LTP and LTD, the trade-off between different types of synaptic plasticity and the computation being performed is not understood. For example, from a computational perspective, what is the functional difference between potentiating excitatory inputs and depressing inhibitory ones? What is the computational benefit of potentiating both EPSPs and IPSPs onto the same postsynaptic neuron (Kairiss et al., 1987; Komatsu, 1994; Xie et al., 1995; Shew et al., 2000; Lamsa et al., 2005; Froemke et al., 2007), which superficially seems self-defeating?

To address these questions we first developed a computational model which shows that the threshold and gain of neuronal I/O functions can be independently controlled by change in excitatory and/or inhibitory synaptic strength. We next examined experimentally the prediction of the model by determining the I/O function of neurons in response to manipulation of excitatory and inhibitory synaptic strengths. Our findings indicate that excitatory plasticity in isolation alters the threshold of a neuron's I/O function

while keeping the gain constant. On the other hand, balanced changes in synaptic excitation and inhibition can adjust the gain of the neuron's I/O function while maintaining a constant threshold. This study establishes a framework for understanding the potential function and trade-off between invoking excitatory and inhibitory plasticity in isolation or in parallel, and proposes that I/O function plasticity could be used to optimize the encoding of information.

Results

Theoretical analysis of the effects of excitatory and inhibitory plasticity on neuronal I/O functions

To examine the effects of changing excitatory and inhibitory synaptic strengths on the neuronal I/O function, we simulated a feed-forward disynaptic circuit (**Fig. 1A**) and examined the response of a single postsynaptic excitatory neuron (Ex) to increasing input intensity, which we represented as an increase in the number of active excitatory and inhibitory synapses (**Fig. 1B**; see Methods). In accordance with real neurons, the likelihood of eliciting an action potential is probabilistic as a result of an incorporated “noise” current – representing background synaptic activity and other stochastic processes. The estimation of the spike probability across increasing intensities was fit with a sigmoid function and, as observed experimentally, high intensities led not only to an increased probability of firing but also to a decrease in the spike latency (Pennartz and Kitai, 1991) (**Fig. 1B,C**).

FIG. 1

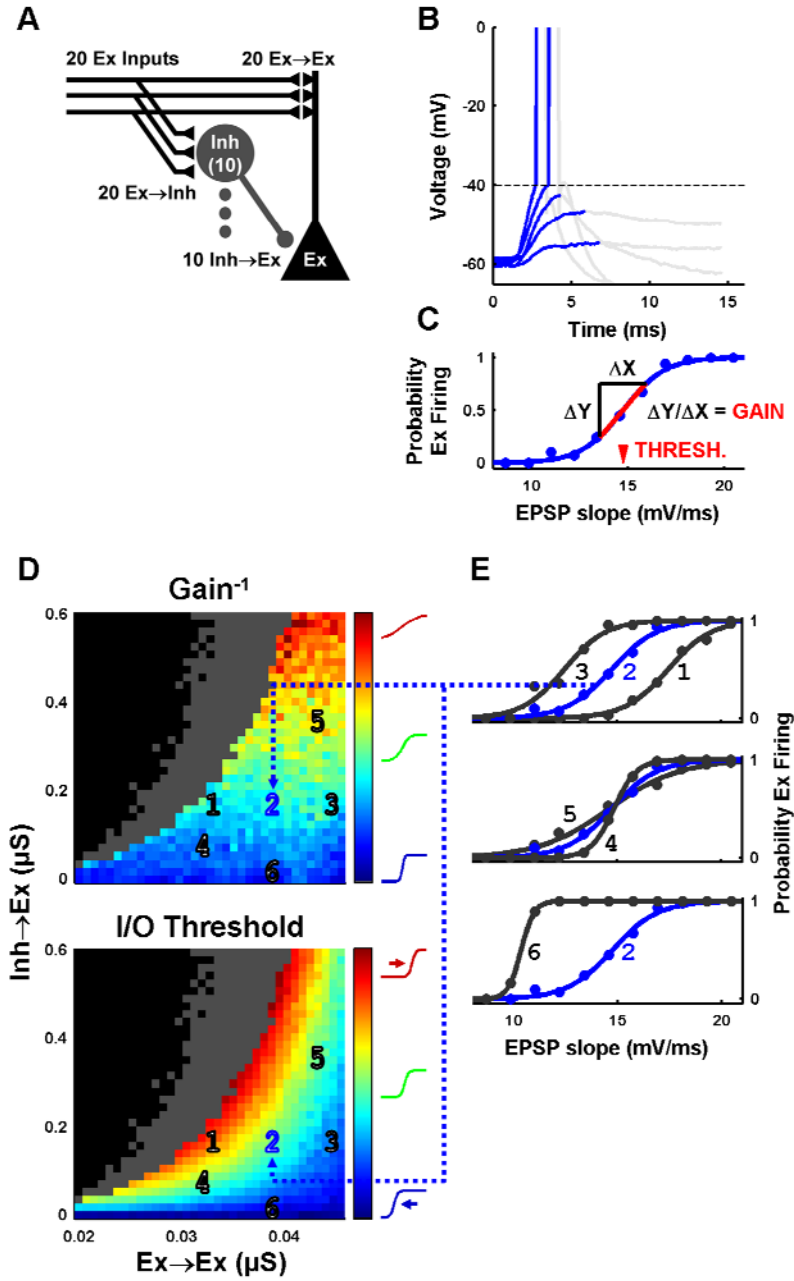


Fig. 1: Excitatory and inhibitory synaptic strengths control the gain and threshold of the neuronal input-output function.

A) Topology of the simulated feed-forward inhibitory circuit.

B) Sample voltage responses of the Ex unit at different input intensities (see text), for a particular combination of Ex→Ex and Inh→Ex synaptic weights (number 2 in panel D). Voltage traces were colored gray after the peak to ease the visualization of overlapping lines.

C) I/O function of the Ex unit in panel B, obtained by plotting the action potential probability versus the EPSP slope of the voltage traces (in bins, see text and Experimental Procedures).

D) Parameter scan of the excitatory and inhibitory synapse space. At each coordinate an I/O function was determined for the corresponding Ex→Ex and Inh→Ex synaptic weights. The numbers in the foreground depict the individual I/O functions plotted in panel E. *Top*: the gain (inverse) of each I/O function is plotted in color (range: [0.09 1.10] ms/mV). Hot colors depict an I/O function with a shallow slope, while cold colors depict an I/O function with a very sharp slope. Black depicts coordinates in which the inhibitory synapses were so strong that the Ex unit never fired. In gray the Ex unit fired occasionally, but not yielding enough points to be fitted with a sigmoid. *Bottom*: as above, but plotting the threshold of the same I/O curves (range: [10 20] mV/ms). Hot colors depict I/O functions with high threshold while cold colors depict I/O functions with low threshold. The dashed arrow highlights that a single I/O function is defined by two properties (gain and threshold).

E) Sample individual I/O functions. The gain *and* threshold of these sigmoids are highlighted in the corresponding plots in panel D by the corresponding numbers.

To understand how different excitatory and inhibitory synaptic weights, corresponding to LTD or LTP of EPSPs and/or IPSPs, modify the I/O function of a neuron, we parametrically varied the strength of Ex→Ex and Inh→Ex synapses. For each pair of synaptic weights, we plotted the threshold and gain of the corresponding I/O function, hence describing the behavior of the neuron across synapse space (**Fig. 1D**). These results show that, for fixed levels of inhibitory synaptic strength, modifying the strength of a neuron's excitatory synapses shifts the threshold to the left or right, but has little effect on the gain of the I/O function (**Fig. 1E, top**). The horizontal shift in the threshold indicates that some of the previously subthreshold EPSPs are now suprathreshold. This is because, as excitatory synapses get stronger, it is possible to elicit the same size EPSP at lower intensities, thus recruiting less inhibition (Marder and

Buonomano, 2004). This scenario is equivalent to LTP of the Ex→Ex synapses in the absence of other forms of plasticity. In contrast, inhibitory plasticity alone altered both the threshold and gain of the I/O function (**Fig. 1E, bottom**). Interestingly, regulating the excitatory *and* inhibitory synaptic weights in a *balanced* manner allowed neurons to change the gain of their I/O function while maintaining the same threshold, essentially establishing an ‘iso-threshold’ band along the diagonal of the excitatory and inhibitory synapse space (**Fig. 1E, middle**). In contrast to the previously observed shifts in the threshold, the change in the gain as a function of excitatory and inhibitory *synaptic strength* has not been previously described experimentally or theoretically.

These theoretical results suggest that one reason excitatory and inhibitory synapses are plastic is to allow for the *independent control* of the gain and threshold of neuronal I/O functions. That is, if the gain has to be changed while maintaining the threshold, parallel excitatory and inhibitory plasticity should be engaged, whereas if the threshold should be changed while maintaining the gain, only excitatory plasticity should be induced.

Synaptic inhibition increases the threshold and gain of I/O functions in CA1 pyramidal neurons

To test the above predictions, we performed experiments in which we analyzed the I/O function of CA1 pyramidal neurons in hippocampal slices in response to manipulations of the strength of the excitatory or inhibitory synapses. Like most neurons, CA1 pyramidal cells receive robust feed-forward excitation and inhibition; however, in contrast to the majority of cortical areas, the CA1 subfield has little recurrent connectivity, thus providing a reasonable approximation to the simulated disynaptic circuit used above. Effective synaptic strength was manipulated using pharmacology, hyperpolarization,

and directly through the induction of single-cell LTP. Given the difficulty in inducing plasticity exclusively at Inh→Ex synapses, uncertainties regarding the protocols that induce inhibitory plasticity, and the variability of results (Xie et al., 1995; Lu et al., 2000; Shew et al., 2000; Gaiarsa et al., 2002; Chevaleyre and Castillo, 2003), we limited our manipulations of inhibitory strength to pharmacological means to alter Inh→Ex transmission independently of the Ex→Ex and Ex→Inh strengths.

While recording in whole-cell configuration, we first examined the effects of low concentrations (2-3 μM) of the GABA_A antagonist bicuculline on the neuronal I/O function. As already reported (Abraham et al., 1987; Marder and Buonomano, 2003), there was a robust leftward shift of the threshold (**Fig. 2B,C**, dark blue vs. red, 9.9 ± 1.1 vs. 4.6 ± 0.6 mV/ms, $p < 0.001$). Here we show that in agreement with the above simulations (**Fig. 1E, bottom**), there was also an increase in the gain of the I/O function (0.40 ± 0.06 vs. 0.94 ± 0.08 ms/mV, $p < 0.001$). Upon washout of the drug, the threshold and gain of the I/O function returned to baseline (**Fig. 2B,C**, light blue, gain: 0.42 ± 0.05 ms/mV, threshold: 10.0 ± 1.0 mV/ms). The same results were also observed using 10-15 μM picrotoxin (baseline threshold: 8.4 ± 0.43 mV/ms, gain: 0.60 ± 0.14 ms/mV; PTX threshold: 2.0 ± 0.30 , gain: 1.30 ± 0.23 ; $n=3$; data not shown).

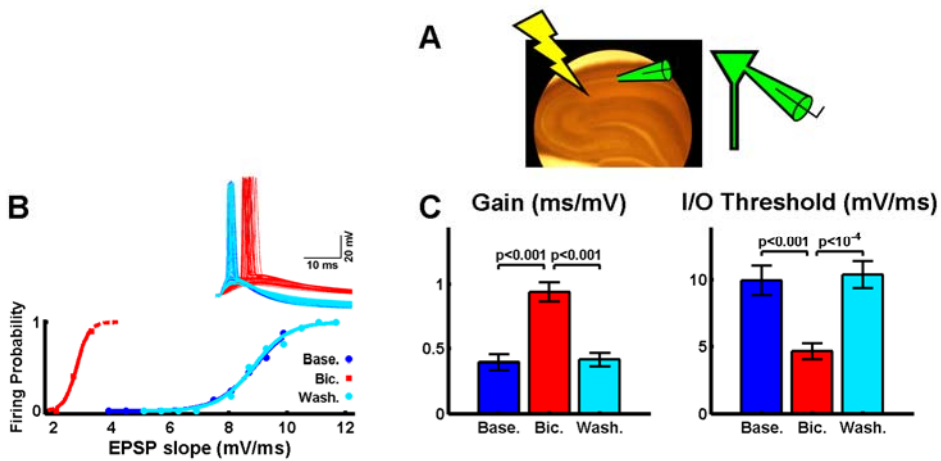


Fig. 2: Decrease in inhibitory strength decreases the threshold but increases the gain of neuronal I/O functions.

A) Schematic placement of the stimulating and whole-cell recording electrodes.

B) Example of a bicuculline experiment. *Dark blue*: I/O function of an intracellularly recorded CA1 pyramidal neuron, in standard ACSF. *Red*: I/O function of the same neuron in the presence of 3 μ M bicuculline. *Light blue*: I/O function after 10 min. washout of bicuculline. Inset: Sample voltage traces for each of the conditions.

C) Average gain and threshold for the manipulations described in panel B (n=8).

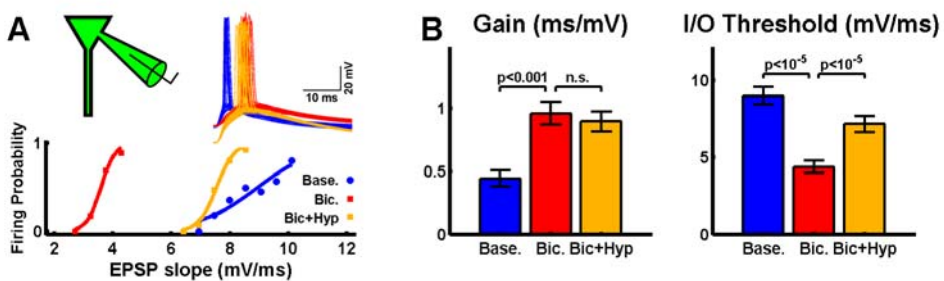


Fig. 3: Dissociation of changes in gain and threshold.

A) Bicuculline followed by hyperpolarization experiment. *Dark blue*: I/O function of an intracellularly recorded CA1 pyramidal neuron, in whole-cell mode in standard ACSF. *Red*: I/O function of the same neuron in the presence of 3 μ M bicuculline. *Orange*: I/O function of the same neuron in the presence of bicuculline and hyperpolarized by 12 mV. Inset: Sample voltage traces for each of the conditions.

B) Average gain and threshold for the manipulations described in panel A (n=12). Notice that the hyperpolarization, associated with the increase in stimulation intensity necessary to make the neuron fire, increases the I/O threshold in a statistically significant manner, without inducing significant changes in the gain.

Experimental dissociation of shifts in threshold and changes in gain

In the above experiments it could be argued that an increase in gain is inextricably linked to the leftward shift in threshold. To establish that it is possible to dissociate changes in threshold and gain, we tonically hyperpolarized the cells (mean: 9.7 ± 2.2 mV; range: 5-13 mV) after collecting the baseline and bicuculline I/O curves (**Fig. 3A,B**). Tonic hyperpolarization will alter all synaptic driving forces, however, under reduced inhibition (due to bicuculline) its primary functional effect is a decrease in excitation (i.e., even though EPSP amplitude may be larger, a neuron that was firing will cease to do so because the peak EPSP is farther from action potential threshold). Thus, hyperpolarization together with the necessary increase in stimulation intensity to make the neuron fire shifts the I/O curve rightwards, towards values closer to baseline but, interestingly, does not affect the gain (**Fig. 3A,B**, red vs. orange, gain: 0.96 ± 0.09 vs. 0.90 ± 0.08 ms/mV, $p > 0.50$, threshold: 4.4 ± 0.4 vs. 7.2 ± 0.5 mV/ms, $p < 10^{-5}$). These results show that changes in threshold and gain can be dissociated and, indirectly, support the proposal that parallel changes in excitation and inhibition may serve to maintain a constant threshold while modifying the gain of the I/O function of a neuron (**Fig. 1E, middle**).

LTP alters the threshold while maintaining the gain of I/O functions

Early studies on LTP established that it produces a leftward shift of the I/O curve (Bliss and Lomo, 1973; Andersen et al., 1980; Bliss et al., 1983). The mechanisms underlying the leftward shift remain incompletely understood, in part because some of the induction protocols used (e.g., presynaptic high frequency stimulation) may induce plasticity at other synapses (Ex→Inh and/or Inh→Ex) (Kairiss et al., 1987; Komatsu, 1994; Xie et al., 1995; Shew et al., 2000) as well as changes in intrinsic excitability or dendritic integration (Chavez-Noriega et al., 1990; Daoudal and Debanne, 2003; Xu et al., 2005; Campanac and Debanne, 2008). Nevertheless, it has been shown that single-cell associative pairing protocols can also induce left shifts in the I/O function (Marder and Buonomano, 2004), which is consistent with our theoretical framework. However, the effect of LTP of excitatory synapses on the gain of the neuronal I/O function has not been addressed.

To examine this issue we performed intracellular experiments with high resistance micropipettes (70-90 M Ω) to prevent washout of LTP (Lamsa et al., 2005). LTP was induced in single neurons with a pairing protocol that has previously been shown not to induce changes in inhibition or intrinsic excitability (Barrionuevo and Brown, 1983; Gustafsson et al., 1987; Marder and Buonomano, 2004). Specifically, pairing intracellular depolarization (100 ms) with a train of 4 presynaptic stimuli (40Hz; 60 pairings at 0.2Hz) resulted in a 79 \pm 17% increase in the EPSP slope (we only included experiments with LTP > 10% in this analysis). The induction of LTP caused a left shift (7.4 \pm 0.5 vs. 5.6 \pm 0.8 mV/ms, p <0.05) and, in agreement with the theoretical predictions, did not induce any change in the gain (0.59 \pm 0.07 vs. 0.57 \pm 0.07 ms/mV, p >0.80) of the neuronal I/O function (**Fig. 4B,C**).

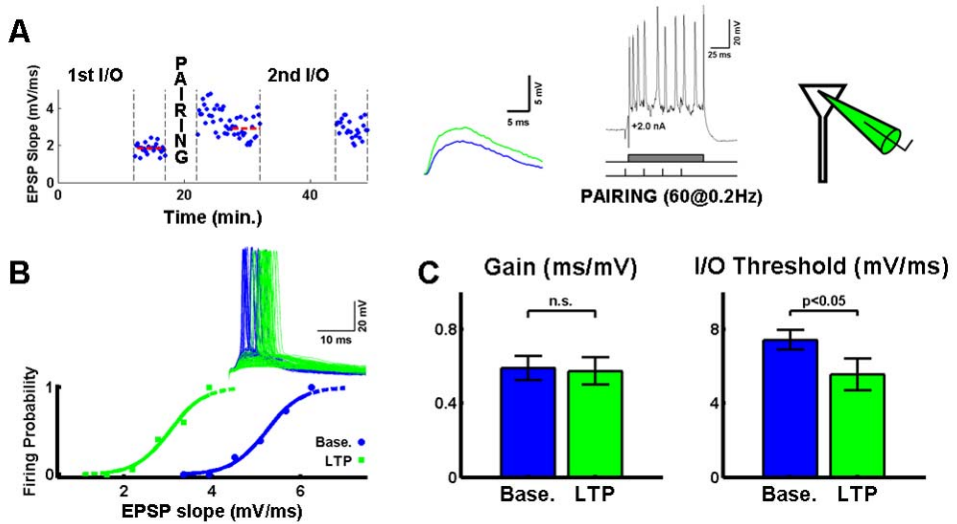


Fig. 4: Potentiation of the excitatory strength decreases the threshold without changing the gain of neuronal I/O functions.

A) EPSP slopes recorded with a sharp microelectrode during the course of an associative LTP experiment. Voltage traces on the middle represent average sample PSPs from 5 min. after the 1st I/O and 5 min. before the 2nd I/O. The voltage trace on the right shows a sample of the pairing depolarization.

B) I/O functions before and after the associative LTP pairing protocol. The threshold of the I/O function decreases (left shift), but the gain is left unchanged. *Inset:* Sample voltage traces for each of the conditions

C) Average gain and threshold of baseline and LTP I/O curves ($n=11$). The associative pairing protocol results in a decrease in the threshold and no changes in gain of the neuronal I/O functions.

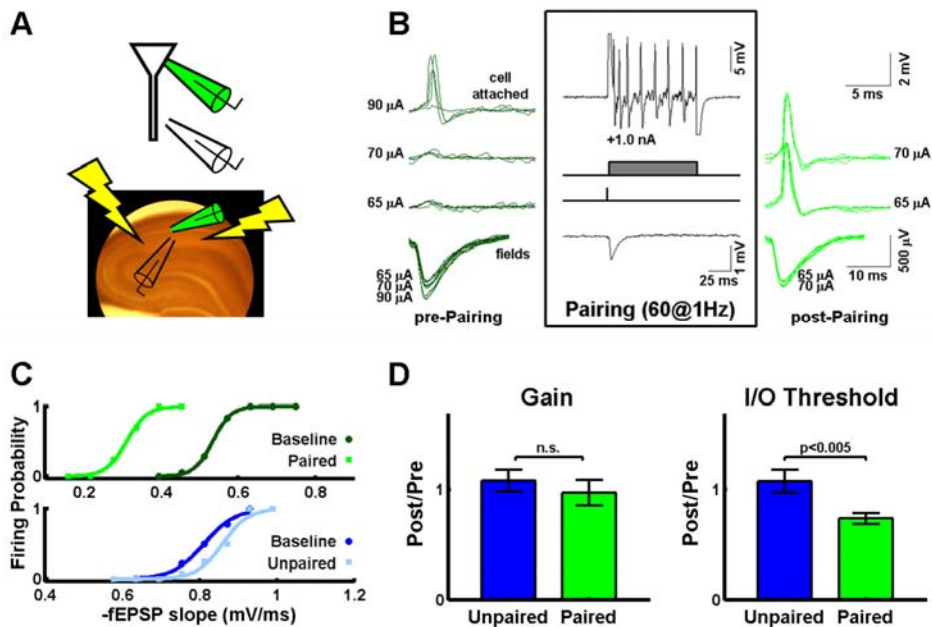


Fig. 5: LTP induced threshold left shifts with constant gain are not due to global changes in excitability.

A) Schematic placement of the stimulating and cell-attached and field recording electrodes.

B) Example of the potentiation protocol. *Left*: Sample voltage traces recorded from the cell-attached (top) and field (bottom) electrodes at 3 different intensities. There are four traces per intensity. *Middle*: Associative pairing protocol. Presynaptic stimulation was paired with 100 ms postsynaptic depolarization 60 times at 1Hz. *Right*: Voltage traces for the same intensities as before (the highest intensity was no longer used to optimize the estimation of the I/O functions). Notice the increased action potential probability.

C) Sample I/O functions before and after the associative pairing protocol illustrated in panel B. *Top*: Paired pathway. The threshold of the I/O function decreases (left shift), but the gain is left unchanged. *Bottom*: Control pathway. The I/O function is unchanged supporting the existence of no global changes in excitability.

D) Average change in gain and threshold, relative to baseline, for the paired and unpaired pathways ($n = 13$). The associative pairing protocol results in a decrease in threshold and no changes in gain of the neuronal I/O functions. In contrast, the unpaired pathway shows no changes in either the threshold or gain.

As mentioned above the mechanisms underlying the left shift in the I/O function (E-S potentiation) remain controversial and other groups have suggested that it could be due to changes in intrinsic excitability (Sourdret et al., 2003; Frick et al., 2004; Losonczy et al., 2008). A further complicating set of issues is that intracellular techniques can alter the neuronal I/O function as a result of washout (Kato et al., 1993; Staff and Spruston, 2003; Lamsa et al., 2005; Xu et al., 2005), changes in cell input resistance, or changes in the balance of excitation and inhibition (Zhang et al., 1991; Staley and Smith, 2001). To avoid any potential methodological artifacts and determine if global changes in intrinsic excitability could have influenced the above results we performed experiments in tight-seal cell-attached configuration – which does not rupture the cellular membrane – and included a second unpaired control pathway in the LTP experiments. Given that the cell-attached technique does not allow recording subthreshold responses, we estimated the average input to the neuron by recording the field EPSP from an electrode placed in stratum radiatum in a line perpendicular with the cell body layer (**Fig. 5A**) (Andersen et al., 1980; Zalutsky and Nicoll, 1990). The high resistance cell-attached configuration does not rupture the membrane (seal > 1 G Ω), but still allows the injection of positive current through the electrode and the recording of the spikes (Perkins, 2006; Houweling and Brecht, 2008) (**Fig. 5B**, middle). By pairing this depolarization (100 ms) with single presynaptic stimuli (60 pairings at 1Hz), we consistently observed leftward shifts in the I/O functions (11/13 experiments) and, in agreement with the previous results, no change in gain (**Fig. 5C,D**; threshold: $74\pm 5\%$ $p < 0.001$, gain: $97\pm 12\%$ $p > 0.80$). Importantly, the unpaired control pathway onto the same cell showed no horizontal shift or change in gain (threshold: $108\pm 10\%$ $p > 0.70$; gain: $108\pm 10\%$ $p > 0.70$). There was a significant difference in the threshold between the paired and unpaired pathways ($p < 0.005$), but no difference in the gain ($p > 0.50$, **Fig. 5D**). These results establish that the pairing-LTP induced left shift is not a result of general changes in intrinsic excitability. Additionally, as in the LTP experiments shown

in **Figure 4**, the fact that there was no change in the gain of the I/O function is consistent with the prediction made in **Figure 1**. However, it should be stressed that the interpretation of I/O function in these cell-attached experiments is constrained by the fact that the extracellular fEPSP was used to construct the I/O function.

Together these results demonstrate that LTP produces a leftward shift in the absence of a change in gain, and that this effect is not likely to be a result of any cell-wide form of intrinsic plasticity. In contrast, a decrease in inhibition is accompanied by a change in gain, in addition to the change in threshold.

Mechanisms of the changes in gain and threshold induced by synaptic plasticity

The simulations and experiments above indicate that increasing excitatory (E-LTP) or decreasing inhibitory synaptic strength (I-LTD) both produce left shifts in the threshold of the I/O function; however, the latter also induces an increase in the gain (the potential computational relevance of these forms of plasticity is addressed in the Discussion). Next, we used the computational model to understand the origin of the change in gain associated with changes in synaptic inhibitory strength. It is important to point out that excitatory and inhibitory synaptic plasticity produce fundamentally different changes in the post-synaptic potential (PSP) waveform: excitatory plasticity changes the slope and peak of the PSP, while changes in inhibition alter the peak and width of the PSP (Fig. S1, Buonomano and Merzenich, 1998a; Pouille and Scanziani, 2001). As a consequence of the inherent asymmetry between excitatory and inhibitory plasticity, imposed primarily by the delay of inhibition in relation to excitation, small changes in excitation are proportionally more effective in altering the PSP peak than changes in inhibition (**Fig. S1**).

On the other hand, the fact that inhibitory plasticity determines the width of the PSP is an important factor in determining the gain of the I/O function because the wider the PSP the longer it borders action potential threshold – hence, subsequent small increases in the PSP slope will result in sharp increases in spike probability and the I/O gain (**Fig. S2**).

There are a number of interrelated properties that jointly contribute to determining the I/O gain, and whether or not it changes after synaptic plasticity. Below we first address the mechanisms responsible for the observed changes in the I/O function in response to inhibitory or excitatory plasticity in isolation. Additionally, the issue of I/O gain control is further discussed in the Supplemental Material.

I-LTD

Consider a ‘baseline’ I/O function (blue curve in **Fig. 6A**), and the stimulation intensity (S_{50}) which elicits the EPSP slope that defines the threshold of this I/O curve (**Fig. 6D**; that is, the EPSP slope that generates action potentials with 50% probability). If one induces I-LTD (**Fig. 6A**, red curve) the EPSP slope at S_{50} will remain largely unchanged, since it is mainly determined by the excitatory strength. Yet, the PSP width and height will *increase*; hence the same EPSP slope will yield action potentials with increased probability. To find the new I/O threshold one must *decrease* the stimulation intensity until it yields an EPSP slope where the neuron fires action potentials again with 50% probability (**Fig. 6A**, left red I/O), thus accounting for the left shift of the threshold of the I/O curve. But why does the gain change? Compared with an I/O of the same threshold, but with the same gain as the baseline curve (dark green trace in **Fig. 6A**, see 'E-LTP' below), changes in stimulation intensity will produce a smaller change in the inhibitory conductance (g_{Inh}) because inhibitory synapses are weaker after I-LTD

(**Fig. 6C**, left red). This can also be visualized in **Fig. 6D**, in which the crosses and squares represent the peak IPSC and EPSC amplitudes as function of stimulation intensity. At stimulation intensities straddling 50% firing probability of the I-LTD I/O curve (red line), the red crosses change at a slower rate than the green crosses for the corresponding S_{50} point (yet there is relatively little change in the red and green EPSC amplitudes, squares, see below). Hence, as intensity increases, the rate of change of excitation is higher than that of inhibition (compared to the E-LTP isothreshold case, green lines), resulting in a faster transition from a low to high probability state (i.e., a higher gain).

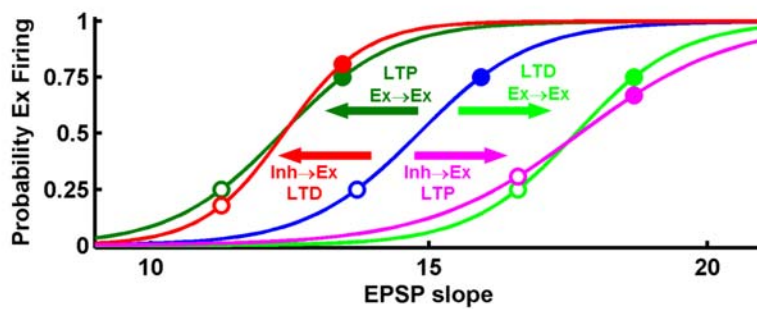
E-LTP

Ex→Ex LTP is similar to Inh→Ex LTD in the sense that both make it easier for the cell to fire an action potential at any given EPSP slope, shifting the I/O curve leftwards (green line, **Fig. 6A**). When one increases the strength of excitatory synapses, the *same* stimulation intensity yields a *bigger* EPSP slope, and increased spike probability. Thus, to return to the initial EPSP slope, one has to *decrease* the stimulation intensity, which has the consequence of decreasing the recruitment of inhibitory neurons and increasing their latency. As a result, the original EPSP slope is now accompanied by less inhibition and has increased probability of generating an action potential, which means that the whole I/O curve has shifted to the left.

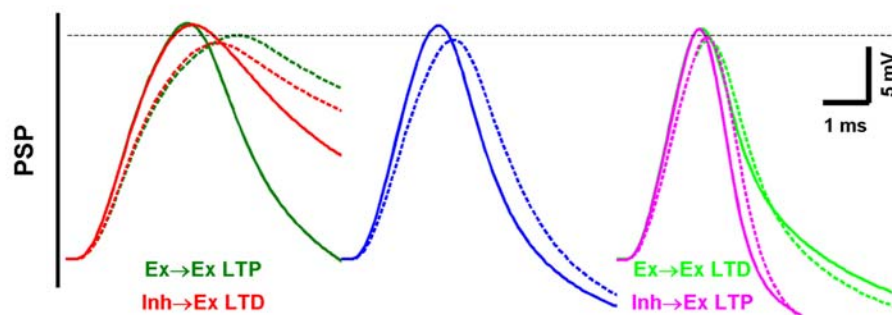
However, in the case of potentiation of excitatory synapses (or conversely Ex→Ex LTD, light green line, **Fig. 6A**), the left shift is qualitatively different from the left shift caused by decreased inhibitory strength given that the gain of the I/O function stays the same. As in the case of I-LTD, E-LTP produces an effective shift in the range of stimulation intensities straddling the I/O threshold (**Fig. 6D**). An important consequence of this is that, even in the absence of plasticity at the inhibitory synapses, there will be an effective

change in the levels of inhibition around the new I/O threshold. As shown in **Fig. 6D** (green crosses) this left shift will result in larger changes in inhibition for a given change in stimulation intensity, in the relevant range of the I/O curve. Specifically, as a result of the nonlinear and asymptotic nature of the IPSC versus stimulation intensity curve, decreasing the relevant stimulation intensities effectively produces an increase in the rate of change in inhibition. Thus, it is possible to maintain the balance between the rate of change of excitation and inhibition even after E-LTP because the IPSC versus stimulation intensity function is now operating in a regime with a higher slope (note the larger change in IPSC amplitudes over the range in which firing probability changes from 25 to 75%, dashed and solid dark green lines, **Fig. 6C**). In other words, the relationship between EPSC and IPSC amplitudes as a function of stimulation intensity is relatively constant for I/Os that underwent excitatory plasticity (as shown in **Fig. S3** for the I/O functions depicted in **Fig. 6**). Note that although the IPSC and EPSC amplitudes are balanced across intensities, higher intensities will still be more effective at eliciting spikes because the changes in EPSC and IPSC latency favor excitation (see Supplementary Material; **Fig S6**) – for example, in the extreme a strong EPSP can generate a spike regardless of inhibitory synaptic strength if voltage crosses spike threshold before the Inh neurons fire.

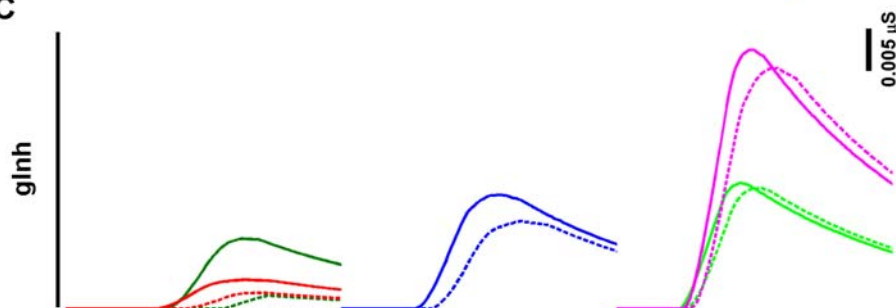
A



B



C



D

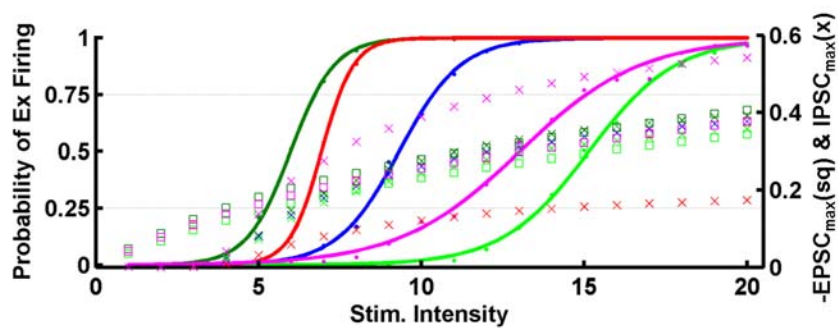


Fig. 6: Mechanisms underlying the change in I/O gain produced by synaptic plasticity.

A) Neuronal I/O functions from the model at different values of Ex→Ex and Inh→Ex synaptic strength. Blue curve is the "baseline", the green curves result from Ex→Ex plasticity and the red/magenta curves from Inh→Ex plasticity. Note that LTD of Inh→Ex and LTP of Ex→Ex produced an equal left shift in threshold, however, inhibitory plasticity also resulted in an *increased* gain; conversely, LTP of Inh→Ex and LTD of Ex→Ex produced the same right shift, with a *decreased* gain in the former case. The points with 0.25 and 0.75 probability of firing are highlighted in the blue and green curves. In the red/magenta curves we highlighted the EPSP slope that yielded 0.25 or 0.75 in the corresponding isothreshold *green curve*.

B) Voltage traces with EPSP slopes highlighted with the circles in panel A (V_m noise and action potentials were removed). Dashed and solid lines represent the PSPs that would yield ~25% and ~75% probability of firing, respectively (see Panel A).

C) Inhibitory conductance traces of the corresponding PSP traces in panel B. Notice that at the same EPSP slopes, the inhibitory change from 0.25-0.75 is smaller for Inh→Ex LTD as compared to Ex→Ex LTP, which causes an I/O function with a higher gain. Conversely, the inhibitory change from 0.25-0.75 in Inh→Ex LTP is bigger as compared to Ex→Ex LTD, which results in an I/O function with decreased gain.

D) Same data as in A) but plotted as a function of stimulus intensity (solid sigmoid curves). The maximum EPSC (squares) and IPSC (crosses) amplitudes are also plotted, in the color corresponding to each of the I/O functions.

Thus, an important factor underlying the isogain bands of **Fig. 1D** is the relationship between IPSCs as a function of stimulation intensity (crosses in **Fig. 6D**) and EPSCs as a function of intensity (squares in **Fig. 6D**). More specifically, these functions scale in an approximately linear fashion over most intensities, consequently, at different intensities the IPSC/EPSC balance is approximately constant. Given that excitatory plasticity does not change the IPSC/EPSC ratio significantly (**Fig. S3**), for the reasons that were mentioned earlier (**Fig. S1**), the change in the relevant range of stimulation intensities caused by excitatory plasticity also does not alter the IPSC/EPSC ratio significantly. If, however, the IPSC versus stimulation intensity function is disrupted in a manner that significantly alters the IPSC/EPSC ratios across intensities then excitatory plasticity will alter the gain of the I/O (see

Supplementary Materials and **Fig. S4**). Thus, the model assumptions regarding the relationship between inhibition and stimulation intensity are crucial. Importantly however, they are supported by experimental findings that demonstrate that synaptic drive increases asymptotically as a function of intensity (Costa et al., 2002; Kushner et al., 2005) and that excitation and inhibition remain balanced across stimulation intensities (Gabernet et al., 2005). Additionally, the fact that our own experimental findings confirm that E-LTP does not change the I/O gain, further supports our model.

It can be seen that since Ex→Ex potentiation shifts the I/O curve leftwards without changing its gain, and that Inh→Ex potentiation can shift the I/O rightwards with a decrease in gain (Fig 6A, magenta curve) that the appropriate mix of both forms of plasticity could produce no change in the threshold together with a decrease in the gain. Thus, simultaneous Ex→Ex and Inh→Ex LTP, as reported by (Froemke et al., 2007), may function to maintain the threshold of a neuron while decreasing its gain (**Fig. 1E, middle; Fig. S2**)

The above discussion of gain control highlights the subtlety and nonlinear nature of even a relatively simple disynaptic circuit, particularly in relation to the dynamic nature of the balance of excitation and inhibition (Marder and Buonomano, 2004). Indeed, it is important to stress that a limitation of the above analysis is that it is actually not the balance of excitation and inhibition at the peak EPSC and IPSC values that governs whether or not a neuron fires, but at earlier and intensity-dependent points near the peak the PSP (Supplemental Data, **Fig S5**). Thus, a detailed and quantitative description of the relative contribution of different factors to gain control, including the latency and jitter of the inhibitory neurons, will benefit from future theoretical studies.

Discussion

We have used theoretical and experimental techniques to examine how changes in the strength of excitatory and/or inhibitory synapses alter the response of neurons to transient synaptic stimulation. A large number of studies have described how long-term plasticity of excitatory and/or inhibitory synapses affect subthreshold responses, however, there has been less focus on how these changes alter the input-output characteristics of neurons – which is what ultimately determines the computational and behavioral relevance of synaptic plasticity. The general intuition regarding LTP of Ex→Ex synapses is that it will increase the likelihood of a given input generating a postsynaptic spike. However, as shown in our simulation, if LTP is accompanied by a parallel increase in the strength of Inh→Ex synapses, additional nonlinear behaviors take place. Specifically, the threshold can remain the same, but the likelihood of eliciting a spike can increase at low intensities, but actually decrease at high intensities (i.e., a decrease in gain; **Fig. 1E, middle; Fig. S2**).

As mentioned in the Introduction, the current study addresses a distinct question from those that characterized the modulation of the response of neurons by different levels or characteristics of background activity (Ho and Destexhe, 2000; Chance et al., 2002; Murphy and Miller, 2003; Shu et al., 2003; Cardin et al., 2008). Because these previous studies were aimed at addressing ‘online’ changes in gain they did not examine the consequences of synaptic plasticity, nor the changes in firing probability in response to synaptic inputs (but see Prescott and De Koninck, 2003). Additionally, studies using direct current injection to emulate excitatory or inhibitory currents do not capture the inherent temporal interactions between excitatory and inhibitory synapses, which are critical in determining the output of neurons (Pouille and Scanziani, 2001; Wehr and Zador, 2003; Marder and Buonomano, 2004; Wilent and Contreras, 2005). Here, the issue of how synaptic plasticity of

excitatory and inhibitory synapses alters spike probability relates to learning and memory and the processing of sensory stimuli. Specifically, in sensory areas, computations often rely on the input-output characteristics of cortical neurons in response to brief sensory stimuli that tend to elicit a single or a few spikes (Kilgard and Merzenich, 1998; Perez-Orive et al., 2002; DeWeese et al., 2003; Tan et al., 2004; Hung et al., 2005; Higley and Contreras, 2006). Changes in I/O threshold as a result of LTP of Ex→Ex synapses have been well documented experimentally (Bliss and Gardner-Medwin, 1973; Bliss and Lomo, 1973; Andersen et al., 1980; Staff and Spruston, 2003) and are due, at least in part, to changes in the relative balance of excitation and inhibition (Marder and Buonomano, 2004), although changes in intrinsic excitability or dendritic integration may also contribute to the shift in I/O threshold (Sourdret et al., 2003; Staff and Spruston, 2003; Frick et al., 2004; Campanac and Debanne, 2008). To the best of our knowledge, this is the first report of synaptic-dependent changes in the gain of the neuronal I/O function, which are primarily linked to inhibitory plasticity.

Excitatory and Inhibitory Plasticity

Postsynaptic potentials elicited by sensory stimuli are almost always composed of an excitatory and inhibitory component (Wehr and Zador, 2003; Tan et al., 2004; Higley and Contreras, 2006). One of the questions posed in the Introduction was what would be the functional and computational difference between increasing the strength of excitatory and decreasing the strength of inhibitory synapses. While the computational role of excitatory plasticity has been embedded within a solid theoretical framework since Hebb (Hebb, 1949; von der Malsburg, 1973; Bienenstock et al., 1982; Miller et al., 1989), the computational role of inhibitory synaptic plasticity remains much more speculative. As with excitatory plasticity, inhibitory plasticity is likely to

play multiple roles both in maintaining the proper homeostatic balance and preventing runaway excitation (Rutherford et al., 1997; Karmarkar and Buonomano, 2006). It is also likely to play a role in mnemonic plasticity (Kim and Linden, 2007), in masking excitatory responses during experience-dependent plasticity (Zheng and Knudsen, 1999; Foeller et al., 2005) or contribute to the development of cortical maps (Hensch, 2004),

Here we propose a more detailed computational framework regarding the function of inhibitory plasticity. Specifically, that in contrast to excitatory plasticity, changes in inhibition allow neurons to control the gain of their I/O function. Indeed the fact that evoked activity generally elicits an EPSC followed by an IPSC (a delay produced by the additionally ‘synaptic step’) ensures the inhibitory plasticity is well suited to control the width of the PSP (- the integration window, Pouille and Scanziani, 2001; Gabernet et al., 2005) and thus the gain of the neural I/O function. An interesting corollary is that excitatory and inhibitory plasticity in parallel may provide a mechanism by which neurons can alter the I/O gain while maintaining their I/O threshold.

Computational Relevance

The computational advantage of controlling the threshold and gain of neurons has been examined in a number of contexts (Laughlin, 1981; Dean et al., 2005). To illustrate how the ability to alter the threshold and/or gain of an I/O function can optimize the encoding of information we provide a simple example in **Figure 7**. We considered a small population of neurons, with the same I/O function, and quantified the information about the intensity of the stimulus (EPSP slope) that is encoded in the response of the population (the total number of spikes). The mutual information (I_m) will depend both on the distribution of the stimulus as well as on the I/O function of the neurons (**Fig. 7A**). For example, for the broad distribution shown in **Fig. 7B** there is an

optimal I/O gain that will allow the neurons to encode 1.83 bits. If the stimulus distribution becomes more narrow (decrease in entropy), the previous gain is no longer optimal – however changing the gain can bring the system back into an optimal range (**Fig. 7C**). Thus, the ability to adjust the gain of the I/O function, while maintaining threshold, would allow neurons to increase their information capacity, which we propose may be achieved by balanced synaptic changes in excitation and inhibition.

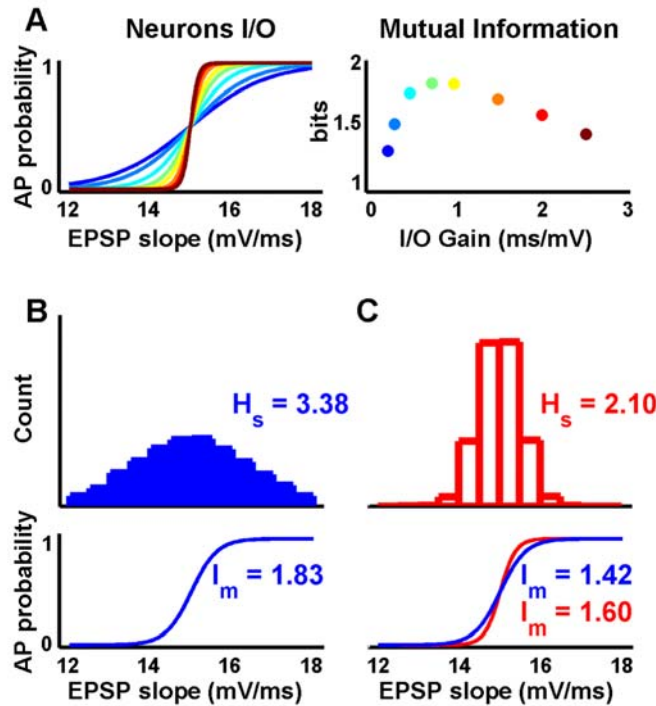


Fig. 7: Neurons can maximize the information transmission by adjusting their I/O function.

A) *Left:* I/O functions with different gains. *Right:* Information that a population of 15 neurons with the same I/Os would be able to convey, as a function of their gain and in response to the Gaussian distributed stimuli depicted in panel B.

B) Plot of the stimulus distribution used in panel A, and the I/O function that maximizes mutual information ($I_m = 1.83$ bits, green curve in panel A). H_s is the entropy of the stimulus, which corresponds to the maximal mutual information.

C) If the stimulus distribution changes (upper panel), the I/O function depicted in panel B would carry less information (blue sigmoid, 1.42 bits). However by adjusting the I/O function the neuron's response can now code for 1.60 bits. Note that the maximal information H_s also varies according to the distribution.

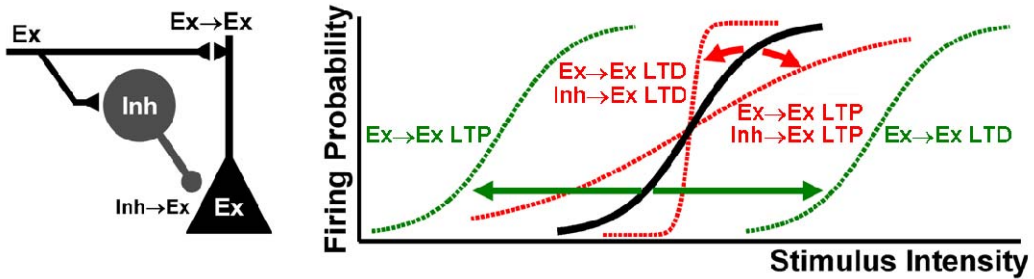


Fig. 8: I/O Threshold and Gain Plasticity.

In disynaptic circuits, plasticity of the excitatory synapses onto a neuron leads to horizontal shifts of the I/O function without changing the gain (*threshold plasticity*, dashed black sigmoids). Balanced changes in excitation and inhibition change the gain of the I/O function without changing the threshold (*gain plasticity*, gray sigmoids). Different combinations of excitatory and inhibitory plasticity can produce arbitrary plasticity of threshold and gain.

Conclusion

Our results indicate that orchestrated regulation of excitatory and inhibitory synaptic strength provides control over both the threshold and gain of I/O functions, which in turn could be used to optimize information processing. If this notion is correct it would imply that a set of learning rules is in place that would endow neurons with two general modes of I/O plasticity. *Threshold plasticity*, consisting primarily of changes in excitation, would leave gain unchanged. *Gain plasticity*, consisting of parallel changes in excitation and inhibition, would allow altering the gain independently of the threshold (**Fig. 8**).

Methodology

Model

Simulations were performed with NEURON (Hines and Carnevale, 1997). Each neuron was simulated as an integrate-and-fire unit. The excitatory unit (Ex) had two compartments, representing the soma and an apical dendrite; inhibitory units (Inh) had a single compartment. The total synaptic weight onto each Inh neuron was distributed so that increases in intensity corresponded to increases in the number of Inh neurons recruited, and progressively decreased their latency (Marder and Buonomano, 2004). I/O curves were determined in the same manner as for experimental intracellular recordings, by measuring the EPSP slope and spike probability at all intensities, and the gain and threshold were determined as described below. Further details and parameters are presented in the Supplemental Material online. We also performed the simulations shown in this paper using a Hodgkin-Huxley implementation of the Ex unit and the results were qualitatively similar (data not shown).

Calculation of the change in inhibitory conductance (Δg_{Inh}) relied on the difference of peak g_{Inh} at the points corresponding to approximately 25 and 75% probability of firing. We used the inhibitory conductance because it is independent of the driving force, and thus of the excitatory component.

Mutual Information. The information transmission simulations were performed in MATLAB. Briefly, stimuli were withdrawn from a normal distribution with variance 2 or 0.25 and activated a population of 15 neurons, each with the same I/O function represented in the figure. Whether or not a neuron spikes in response to a given EPSP was determined directly from the I/O function. The mutual information is given by $I_m = H_s + H_r - H_{sr}$ where

$H_i = -\sum_i P_i \log_2(P_i)$. The response 'r' corresponds to the number of active neurons and 'sr' is the joint probability of the stimulus and the response.

Electrophysiology

Slice preparation. Experiments were performed at a temperature of $31 \pm 1^\circ\text{C}$ on acute 400 μm transverse hippocampal slices from 17- to 28 day old Sprague Dawley rats in standard ACSF (see Supplemental Material online).

Recordings. Electrodes were positioned in area CA1. Whole-cell recordings were considered acceptable if they met the following criteria: resting potential below -55 mV, input resistance larger than 80 M Ω and overshooting action potentials. Sharp recordings were considered acceptable if they met the following criteria: resting potential below -55 mV, input resistance of 30 M Ω , and overshooting action potentials. In tight-seal cell-attached recordings if the seal dropped to <1G Ω the experiment was aborted. Most commonly, seal values were ~5G Ω . A second microelectrode was placed extracellularly, in stratum radiatum positioned along a line perpendicular to the cell body layer, to record fEPSPs.

Electrical stimulation. Electrodes were positioned in the stratum radiatum close to the CA3-CA1 border. In experiments with a control pathway the second electrode was placed in the stratum radiatum towards the subiculum; the test and control pathway were chosen randomly. The distance between the recording and stimulating sites was between 150 and 450 μm . Biphasic, constant current, 100 μsec stimuli were delivered at 10-15 sec intervals (if applicable, out of phase and alternately to each pathway). Stimulation intensities ranged from 30-300 μA .

I/O curves. A series of 60-90 pulses were given at different stimulation intensities, covering a range of responses from subthreshold to supramaximal. I/O curves were constructed by binning the totality of the EPSP (fEPSP) slopes and plotting the centre of the bin versus the percentage of successful action potentials in that bin, for the corresponding experimental condition. The data points were fitted with a sigmoid: $S = 1/(1 + \exp [(E50 - E)/k])$, where E50 is the EPSP (fEPSP) slope that yields action potentials 50% of the times (the I/O threshold). The gain was determined by calculating the slope of the linear portion of the sigmoid (between 0.25 and 0.75).

Pairing Protocol. After completion of the baseline I/O curve, single pulse or 4 pulse (40Hz) extracellular stimulation was paired with cellular depolarization by injecting positive current through the recording electrode for 100 ms, so that 6-10 action potentials were elicited. The delay between the extracellular stimulation and the onset of the depolarization was 2 ms. The pairing was repeated 60 times at 1 or 0.2 Hz. The second I/O function was determined 10 min. after the pairing protocol.

Statistics. For statistical comparisons of I/O curves, we analyzed the change in threshold and gain. For intracellular experiments paired t-tests were performed. The absolute fEPSP values depend on several factors, including distance of the stimulating electrode and placement of the field electrode. For this reason, the data was normalized to baseline in the extracellular experiments and t-tests were performed to assess if the ratio was significantly different from 1; and paired t-tests were performed to compare the control and experimental groups. All values are expressed as mean \pm SEM.

The composition of the solutions used and further experimental details are presented in the Supplemental Material online.



Supplemental Figures

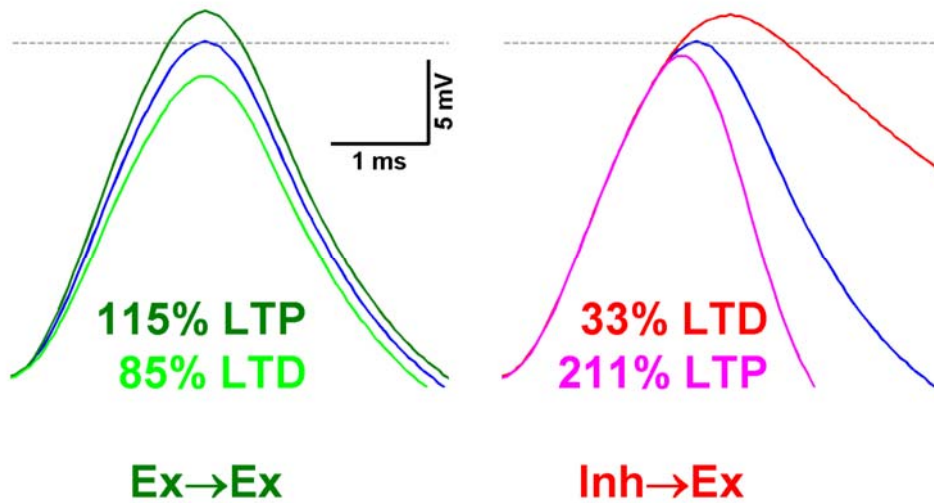


Figure S1: Ex and Inh plasticity differ in their effects on PSP waveforms.

Because inhibition is delayed in relation to excitation, inhibitory plasticity does not change the PSP slope but alters the PSP peak and width. Additionally, relatively small changes in Ex strength compared to Inh strength (measured as changes in conductance) are needed to produce similar changes in the PSP peak. The traces correspond to the levels of plasticity necessary to produce equal shift in the threshold (Fig. 6), measured at the same stimulation intensity (the intensity of the threshold of the 'baseline' blue condition).

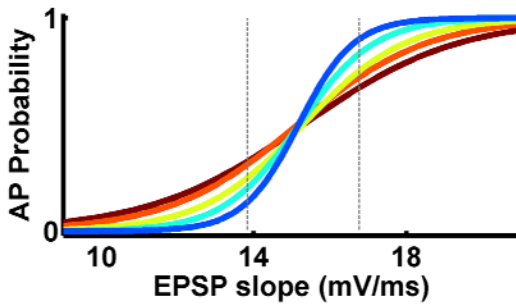
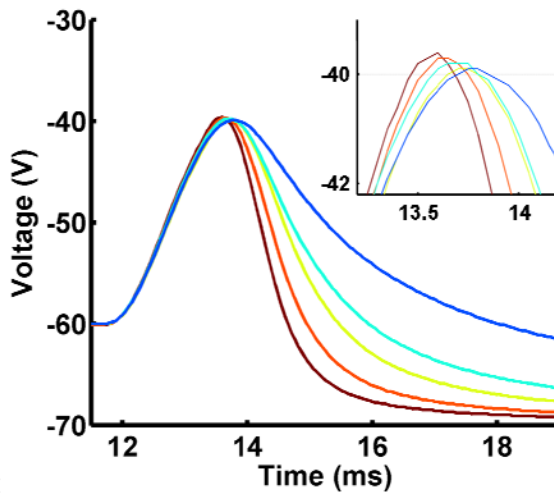
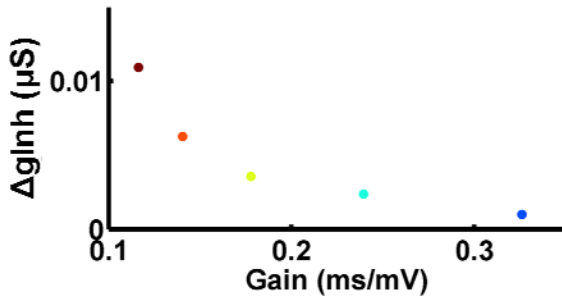
A

Figure S2: Gain control is dependent on PSP width and the rate of change of inhibition.

For iso-threshold curves (A) the spiking probability will be the same at the EPSP slope corresponding to the I/O threshold, however, the integration time window (PSP width) is different due to different inhibition levels (wider PSPs less inhibition) (B). Importantly, the rate of change of inhibition across the same range of EPSP slopes (dashed lines in panel A) is smaller for higher gains. Smaller changes in inhibition across the same EPSP slope range result in sharper gains because the increase in EPSP slope is not accompanied by a proportional increase in inhibition. The brown (low gain) and blue traces (high gain) correspond to strong and weak excitatory and inhibitory synapses, respectively.

B**C**

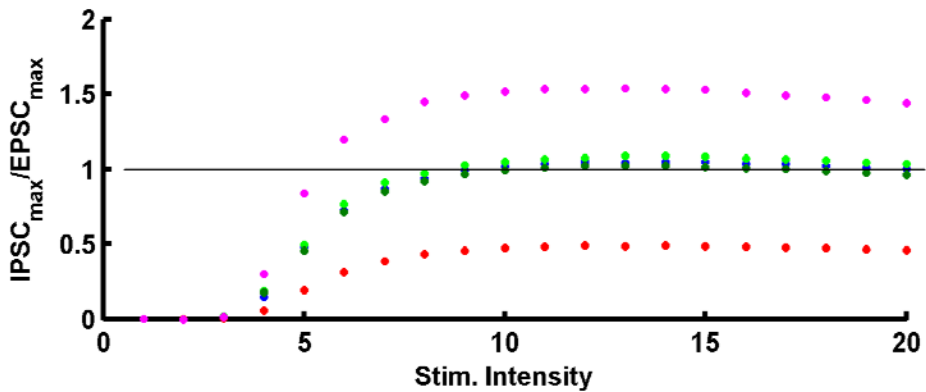


Figure S3: The IPSC/EPSC amplitude ratio is similar after Ex but not Inh plasticity.

Similarly to **Fig. 6**, dark and light green correspond to Ex→Ex LTP and Ex→Ex LTD, and red and magenta to Inh→Ex LTD and Inh→Ex LTP respectively. The IPSC/EPSC amplitude ratio as a function of stimulus intensity changes much more dramatically after Inh plasticity than Ex plasticity (see Supplemental Data text). Towards stimulation intensities where few Inh neurons are active the Inh/Ex balance always favors excitation, additionally in these areas there is variability in the gains of the iso-gain curves.

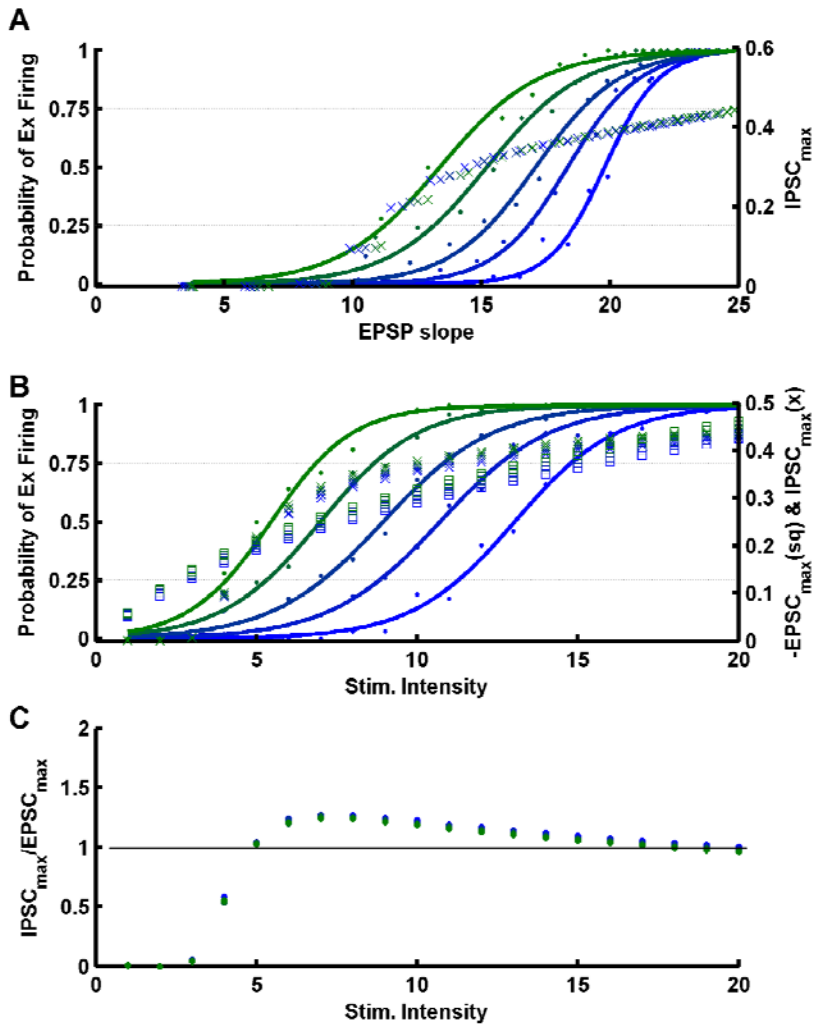


Figure S4: Altering the recruitment of inhibitory neurons prevents the occurrence of isogain curves induced by Ex plasticity.

These I/O curves were obtained after modifying the Ex→Inh synaptic strengths, and thus the recruitment of inhibitory neurons as a function of stimulus intensity. (A) Green corresponds to degrees of LTP and blue to LTD. Note that in panel B, in contrast to **Fig 6D**, for any given I/O curve the relationship between EPSC and IPSC amplitudes changes across stimulation intensities – accounting for the loss of the isogain property after excitatory plasticity. The ratio of Inh to Ex is maximal in intensities of 7 to 8, which is reflected in the $IPSC_{max}/EPSC_{max}$ ratio plotted in C. But for a given intensity, after plasticity there is little change in the ratio, because as explained in the text, small changes in Ex are capable of producing dramatic changes in firing probability (additionally larger EPSPs increase the IPSC amplitude).

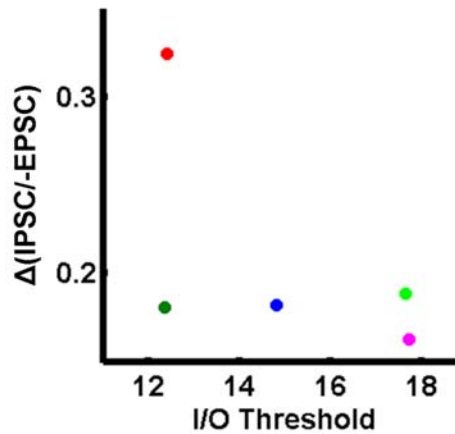


Figure S5: Isogain curves have the same change in IPSC/EPSC ratio at the times of the action potential.

Here the IPSC and EPSC values were measured at the approximate time of an action potential or at the time of the PSP maximum when no action potential occurred. The Y coordinate represents the difference of the IPSC/EPSC ratios, along a fixed range of EPSP slopes that straddled the I/O threshold. The color scheme is the same as in **Fig. 6**. Note that the points with similar Y values (green, blue, light green) are those with similar gains (**Fig. 6A**). As stimulation intensity increases the IPSC/EPSC ratio (again, at the approximate time of the spike) decreases, accounting for the fact that spike probability increases within any given I/O curve. The faster this change occurs (e.g., red point) the higher the gain will be.

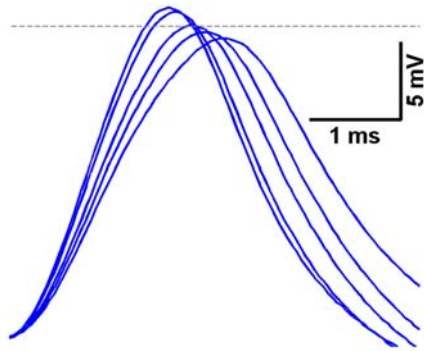


Figure S6: Constant IPSC/EPSC amplitude ratios may still underlie different probabilities of firing.

PSP waveforms for the default 'baseline' curve (shown in blue in **Fig. 6** and **S1**). PSPs corresponding approximately to 10, 25, 50, 75, and 90% firing probability (spikes removed). Note that across this range the peak **IPSC/EPSC amplitude ratio** is the same (see **Fig. S3**), however, because the increases in E_x are more effective in changing the slope and peak, firing probability increases.

Supplemental Information Regarding the Mechanisms Underlying Gain Control

We established that changes in excitatory and inhibitory synaptic strength both shift the threshold of the I/O function while inhibitory plasticity also changes the gain. In other words, excitatory plasticity by itself maintains the gain, thus creating the ‘isogain’ bands shown in **Fig. 1D**. The mechanisms underlying the gain change after inhibitory plasticity and the gain maintenance after excitatory plasticity are the result of a number of interrelated properties including: (1) excitatory and inhibitory synaptic plasticity differentially alter the waveform of the PSP; (2) given that both Ex and Inh plasticity by themselves alter the I/O threshold, there is an effective change in the relevant ‘operating’ stimulation intensity values for the I/O curves; (3) the relationship between net excitation and inhibition as a function of stimulus intensity is also critical to the results observed here.

Q1. What determines the gain of isothreshold I/O curves?

In order to understand the mechanisms underlying gain control it is useful to consider the case where different curves have the same threshold but different gains. **Supplemental Fig. 2** shows an example of PSPs at the same threshold ($P(\text{spike}) = 0.5$; spikes removed) from I/Os with different gains (which were obtained by parallel changes in excitatory and inhibitory synaptic strength). Why are the I/O gains different? As shown in **Fig. S2** (inset), wider PSPs at threshold are related to isothreshold I/Os with higher gain, because a given subsequent increase in EPSP slope will lead to greater increase in $P(\text{spike})$. Specifically, isothreshold curves of high gain have weaker inhibitory synaptic strength (parameter scan in **Fig. 1D**), and thus broader PSPs (as known from experimental findings, e.g., inset of **Fig. 2B**) (Buonomano and

Merzenich, 1998a; Pouille and Scanziani, 2001). As a consequence, across a given Δ EPSP slope, the changes in inhibitory conductances (or IPSCs) will be smaller in higher gain curves (**Fig. S2C**) – precisely because the Inh synapses are weaker (note that the excitatory synapses are also weaker, thus to span the same range of Δ EPSP slopes the stimulation intensity must change more, potentially recruiting more inhibition, however even with this factor, the net effect is that inhibition changes much more slowly, see **Fig. 6C**). Hence, a given increase in EPSP slope is not kept in check by a corresponding increase in inhibition, resulting in a sharp I/O curve. The reverse is true for lower gain I/O functions (high inhibitory strength).

For isothreshold curves, over a fixed range of Δ EPSP slopes we can consider the net change in excitation constant (same EPSP slopes) across different gains. Thus, the change in gain is attributable to the different rate of change of inhibition as a function of stimulus intensity (or EPSP slope); specifically, for high gain curves inhibition changes more slowly over the same range of EPSP slopes. These results establish that, in these conditions, gain control is not a result of changes in shunting inhibition or noise as described previously for I/O functions defined by the firing rate versus injected steady-state current (Chance et al., 2002) (importantly, the results shown in **Fig. S2** are qualitatively similar when noise is removed from the inhibitory neurons).

Q2. Why does I-LTD result in a higher gain I/O curve?

In explaining why excitatory and inhibitory plasticity have different functional consequences it is important to remind the reader that Ex plasticity and Inh plasticity “look” different. That is, as shown in **Fig. S1** and known from experiments (Buonomano and Merzenich, 1998a; Pouille and Scanziani, 2001), Ex plasticity changes the PSP slope and peak, while Inh plasticity does not change the slope but changes the peak (and its timing) and width.

Additionally, it should be clear from this figure that, percent wise, changes in Ex strength are much more effective in altering the shape of the PSP than changes in Inh.

To understand the differential effects of excitatory or inhibitory plasticity on gain control it is useful to compare the case in which both forms of plasticity generate equal shifts in the I/O threshold. Starting from a baseline I/O curve (blue line in **Fig. 6**), why does I-LTD change the gain while a degree of E-LTP that results in the same I/O threshold does not (green and red lines in **Fig. 6**)? To find the new threshold after plasticity both conditions require decreasing stimulation intensity (although the E-LTP case will require a larger decrease in intensity, because the EPSPs are stronger, **Fig. 6D**). In these new operating regimes, the IPSCs change *slower* in the I-LTD case as a function of EPSP slope or stimulation intensity (**Fig. 6C,D**), again due to the weaker inhibitory synaptic strength. In the E-LTP condition the IPSC amplitude does not change much as a function of stimulus intensity (more specifically, g_{Inh} does not change, but IPSC amplitudes change a bit due to the increased driving force). Smaller changes of IPSCs as a function of stimulation intensity (or EPSP slopes) will, in turn, result in increases in gain (this is intuitive because the increases in EPSP slope are not counteracted by a 'parallel' increase in inhibition).

Q3. Why does E-LTP result in the *same gain* as compared to 'baseline'?

As stated above, when the I/O threshold shifts left (after E-LTP or I-LTD) there is an effective shift in the relevant range of stimulation intensities (**Fig. 6D**). An important consequence of this is that, even in the absence of inhibitory synaptic plasticity, there will be an effective change in the levels of inhibition near the new I/O threshold. Because the function that describes IPSC amplitude vs. stimulation intensity increases asymptotically (crosses in

Fig. 6D) a left shift in the operating range will result in larger changes in inhibition for a given change in stimulation intensity. Thus, it is possible to maintain the balance between excitation and inhibition even after E-LTP because the IPSC function is now operating in a regime with a higher slope. Using the curves of **Fig. 6** again as an example, it can be seen in **Fig. 6D** that as a function of stimulation intensity, E-LTP results in a sharper change in the firing probability than baseline. This is because excitatory synapses are stronger, thus a small increase in stimulation intensity should correspond to a greater increase in the EPSP slope and consequently increase the probability of firing. However, notice how the *rate of change* of the IPSC vs. stimulation intensity function at the left shifted operating intensities is also sharper. Ultimately, after the left shift, the ratio of IPSC/EPSC amplitudes at the new operating regime is still similar when compared with the original IPSC/EPSC ratio (at the original operating regime). As described in the Results section the relationship between EPSCs and IPSCs (peak values) as a function of stimulation intensity is relatively constant for I/Os that underwent excitatory plasticity (**Fig. S3**). Note that although the peak IPSC and EPSCs are balanced across intensities, that increased intensities are still more effective at eliciting spikes because the changes in EPSC and IPSC latencies favor excitation (**Fig. S6**). **Fig. S3** shows that the balance between Inh and Ex is fairly constant both across different stimulation intensities and after Ex plasticity. Why is this the case? Ex plasticity does not change the ratio significantly because relatively small changes in Ex strength produce large changes in firing probability and the Inh function does not change at all (additionally, the ratios are measured as currents and the increases in EPSC also increase IPSC amplitude indirectly through driving force). In contrast, as shown in **Fig. S1**, larger changes in inhibitory strength are required to produce an equivalent shift in the I/O threshold and hence the Inh/Ex ratio changes in a much more dramatic fashion.

To highlight the importance of the relationship between inhibition and stimulation intensity and excitation and stimulation intensity, we performed simulations in which the IPSC versus stimulation intensity function was altered in a manner that it no longer parallels the EPSC versus stimulation intensity function. In this case the Inh/Ex ratios are altered as a function of stimulus intensity and isogain curves are not observed after Ex plasticity (**Fig. S4**, thus the different thresholds – different ‘operating values’ – will have different Inh/Ex ratios).

For the sake of completeness it should be pointed out that, as mentioned in the main text, it is actually not the *peak* EPSC and IPSC that determines if a cell fires, but their relationship at earlier time points during near the end of the rising phase of the PSP. Analysis of the ratio of the change in IPSCs and EPSCs (over the same Δ EPSP slope) *at around threshold crossing* reveals similar values for isogain curves, which are different when the gain changes (**Fig. S5**) (these curves will of course not be flat across stimulation intensities). Importantly, analysis of the peak EPSCs and IPSCs amplitudes seems to capture many of the main characteristics of I/O behavior in disynaptic circuits. However, further studies should focus on providing a quantitative description of the trade-off between excitatory and inhibitory latencies and amplitudes, as well as the timing, recruitment and jitter of the inhibitory neuron population in controlling the gain of neurons in response to brief synaptic stimuli.

Q4. Why do threshold points of isothreshold curves have the same probability of firing (50%) if they have different levels of inhibition?

Isothreshold I/O curves are obtained with different combinations of parallel changes in excitatory and inhibitory synaptic weights. The fact that different excitatory synaptic strengths yield the same PSP slope is only

possible due to a corresponding change in stimulation intensity, which will activate more or less excitatory inputs (*lower* excitatory synaptic strengths require *higher* stimulation intensities to yield the same PSP slope). High gain isothreshold I/O curves have higher operating stimulation intensities and as a consequence there will be a shortening of the latency of the evoked inhibition (inhibitory neurons will fire earlier), which is observed in the inset of **Fig. S2B** (specifically, note that the rising phase of the blue PSP started to be affected by inhibition before the others). On the other hand, because inhibitory synapses are also weaker in high gain I/O curves, the "EPSP cut-off" effect is not so dramatic and the overall result is a broader but lower amplitude PSP (as compared with the brown trace in which inhibition kicks in later but it more strongly cuts off the PSP – low I/O gain, strong Ex/Inh synapses, lower stimulation intensity). In summary the combination of high stimulation intensities and weak synaptic strengths (high gain conditions) results in earlier onset of weaker inhibition – producing ‘shorter’ but wider PSPs. Low stimulation intensities and strong synaptic strengths (low gain conditions) result in bigger but narrower PSPs (**Fig. S2B**).

Q5. Additional point related with the behavior of the model

It is important to emphasize how complex and nonlinear even a trivial disynaptic circuit model behaves, specifically with regards to the consequences of changes in latency associated with changes in the stimulation intensity. This situation is well illustrated by the light green and magenta curves of **Fig. 6**, at EPSP slopes $\sim 15\text{mV/ms}$. The magenta curve has stronger inhibitory synapses and elicits bigger IPSCs at all stimulation intensities, so, why is there a higher probability of firing at this point in the I-LTP condition? The explanation has to do with differences in the latency of recruitment of inhibition. Specifically, even though peak IPSCs are much

stronger after I-LTP, the IPSC actually have slightly shorter onset latency after E-LTD. Why is this the case? Because after E-LTD excitatory synapses are weaker, hence higher stimulation intensities are required to achieve the same EPSP slope, thus inhibitory neurons are recruited slightly earlier.



Supplemental Methods

Electrophysiology

Slice preparation. Experiments were performed on acute 400 μm transverse hippocampal slices from 17- to 28 day old Sprague Dawley rats as described previously (Marder and Buonomano, 2003). Briefly, the hippocampus was dissected out and submerged in 1-4°C solution composed of (in mM): 206 sucrose, 2.8 KCl, 2 MgSO₄, 1 MgCl₂, 1.25 NaH₂PO₄, 26 NaHCO₃, 1 CaCl₂, 10 glucose, and 0.4 ascorbic acid. The hippocampus was then placed on an agar block and slices were cut from the dorsal portion using a vibratome (Leica, Nussloch, Germany). Slices were immediately placed in a beaker (at room temperature) filled with oxygenated Artificial Cerebral Spinal Fluid (ACSF) composed of (in mM): 119 NaCl, 2.5 KCl, 1.3 MgSO₄, 1.0 NaH₂PO₄, 26.2 NaHCO₃, 2.5 CaCl₂, and 10 glucose. After an equilibration period of at least 1.5 hr, slices were transferred individually to a submerged recording chamber (RC-26GLP, Warner Instruments) perfused at a rate of 3 ml/min with ACSF maintained at a temperature of 31±1°C. Cells were recorded electrophysiologically from the cell body layer in area CA1 of the hippocampus using blind techniques. Cells were presumed to be pyramidal neurons based on characteristic electrophysiological properties including rapid spike accommodation.

Whole-cell recordings. Patch pipettes were pulled from borosilicate glass (1.5 mm O.D./1.17 mm I.D. Warner Instruments or 1.5 mm O.D./0.86 mm I.D. A-M Systems) using a Flaming/Brown (Sutter Instruments) or a PC-10 (Narishige) electrode puller (4 to 8 M Ω). Cell recordings in area CA1 were considered acceptable if they met the following criteria: resting potential below -55 mV, input resistance larger than 80 M Ω and overshooting action potentials. Internal

solution was composed of (in mM): 100/110 K-gluconate; 20/10 KCl; 4 ATP-Mg; 10 Phosphocreatine; 0.03/0.3 GTP; 10 HEPES and adjusted to a pH of 7.3 with KOH and 290 mOsm by adding sucrose.

Sharp recordings. Micropipettes were pulled from borosilicate glass (1.2 mm O.D./0.68 mm I.D.) using a Flaming/Brown electrode puller (Sutter Instruments). Their resistance when filled with 3M potassium acetate varied from 70 to 90 M Ω . Cell penetrations were considered acceptable if they met the following criteria: resting potential below -55 mV, input resistance of 30 M Ω , and overshooting action potentials.

Tight-seal cell-attached recordings. Pipettes were pulled from borosilicate glass (1.5 mm O.D./0.86 mm I.D. A-M Systems) using a PC-10 (Narishige) electrode puller (~5 M Ω). The procedure to achieve tight-seal configuration was the same as above, but no negative pressure to break-in was applied. If throughout the experiment the seal dropped to <1G Ω the recording was aborted. Most commonly, seal values were around ~5G Ω . A second microelectrode filled with ACSF (3-5 M Ω) was placed extracellularly, in stratum radiatum positioned along a line perpendicular to the cell body layer, to record fEPSPs.

Electrical stimulation. Extracellular stimulation was performed with platinum-iridium bipolar electrodes coated with platinum black (Frederick Haer Co., Bowdoinham, ME). Electrodes were positioned in the stratum radiatum close to the CA3-CA1 border. In experiments with a control pathway the second electrode was placed in the stratum radiatum towards the subiculum; the test and control pathway were chosen randomly. The distance between the recording and stimulating sites was between 150 and 450 μ m. Biphasic, constant current, 100 μ sec stimuli were delivered at 10-15 sec intervals. Stimulation intensities ranged from 30-300 μ A.

I/O curves. Five to twenty minutes after obtaining a seal (extracellular recordings) or breaking in (whole-cell recordings), a series of 60-90 pulses were given at different stimulation intensities, covering a range of responses from subthreshold to supramaximal. Intracellular I/O curves were constructed by binning the totality of the EPSP slopes and plotting the center of the bin versus the percentage of successful action potentials in that bin, for the corresponding experimental condition. Cell-attached I/O curves were constructed in a similar fashion but using fEPSP slopes instead of intracellular EPSP slopes. Curve fitting was done using a custom-written MATLAB program. The program provided the best fit using a sigmoid with two free parameters: $S = 1/(1 + \exp [(E50 - E)/k])$, where E50 is the EPSP or fEPSP slope that yields action potentials 50% of the times (the threshold) and k is inversely related to the linear slope of the sigmoid. The gain was determined by calculating the slope of the linear portion of the sigmoid (between 0.25 and 0.75).

Pharmacology. 2-3 μ M bicuculline methiodide was dissolved in oxygenated ACSF, from a 6mM stock solution prepared in water. A 40 mM picrotoxin stock solution was prepared in DMSO and picrotoxin was added from there to oxygenated ACSF to achieve final concentrations of 10-15 μ M. DMSO concentration in the ACSF did not exceed 0.04%. Drugs were purchased from Sigma, St. Louis, MO. Bicuculline and picrotoxin were 5-10 min. washing in before determining the respective I/O function, and bicuculline was 10-15 min. washing out before determining the washout I/O function. We could not wash out picrotoxin in less than 15 min.

Pairing Protocol. After completion of the baseline I/O curve, single pulse or 4 pulse (40Hz) extracellular stimulation was paired with cellular depolarization by injecting positive current through the recording electrode for 100 ms, so that 6-10 action potentials were elicited. The delay between the extracellular stimulation and the onset of the depolarization was 2 ms. The pairing was

repeated 60 times at 1 or 0.2 Hz. The second I/O function was determined 10 min. after the pairing protocol.

Statistics. For statistical comparisons of I/O curves, we analyzed the change in threshold and gain. For intracellular experiments paired t-tests were performed. The absolute fEPSP values depend on several factors, including distance of the stimulating electrode and placement of the field electrode. For this reason, the data was normalized to baseline in the extracellular experiments and t-tests were performed to assess if the ratio was significantly different from 1; and paired t-tests were performed to compare the control and experimental groups. All values are expressed as mean \pm SEM.

Model

All simulations were performed with NEURON (Hines and Carnevale, 1997). Each unit was simulated as an integrate-and-fire unit. The excitatory (Ex) unit had two compartments, representing the soma and an apical dendrite; inhibitory (Inh) units had a single compartment. The circuit incorporated 20 excitatory inputs, allowing a possible range of intensities from 1 to 20, corresponding to the number of activated inputs. Each input synapsed onto the dendrite of the Ex unit (Ex \rightarrow Ex) and to the 10 Inh units (Ex \rightarrow Inh), which in turn had a single synapse each onto the soma of the Ex unit (Inh \rightarrow Ex) (**Fig. 1A**). The total synaptic weight onto each Inh neuron was differentially distributed so that increases in intensity corresponded to increases in the number of Inh neurons recruited and progressive decrease in their latency (Marder and Buonomano, 2004) to mimic what is observed experimentally. Specifically, the first synapse of each Inh had strength $1.36 \times 10^{-3} \mu\text{S}$ and the remainder $2.1 \times 10^{-4} + i \times 2.95 \times 10^{-5} \mu\text{S}$ for $i = [1 \text{ nInh} - 1]$. The increase in stimulation intensity generates a nonlinear increase in the peak inhibitory conductance

that is well fit by a hyperbolic ratio function

$$(gInh_{peak} = gInh_{peak}^{asympt} \times \left(\frac{Int^n}{Int^n + Int_{50}^n} \right)), \text{ where } Int \text{ is the stimulation}$$

intensity, $gInh_{peak}^{asympt}$ is the function asymptote, n is a constant and Int_{50} is the intensity that yields the half-maximum $gInh_{peak}$. The Ex→Inh synaptic strength constants are robust, however if the drive of the inhibitory neurons is too weak or too strong, then inhibition will be zero or saturate over the relevant range of stimulus intensities, and excitatory plasticity will induce an increase or decrease in gain of the I/O function. Ex→Inh synaptic strength was the same for all simulations presented here (except **Fig. S4**).

The synaptic delays and cellular parameters were chosen to reflect published electrophysiological data on excitatory and inhibitory cells in the hippocampus (Brown et al., 1981; Spruston and Johnston, 1992; Karnup and Stelzer, 1999). Inh units exhibited a lower threshold and faster time constant than Ex units, so they were easier to drive than Ex units, consistent with evidence that single-action potentials in pyramidal neurons can trigger spikes in inhibitory neurons (Miles, 1990; Marshall et al., 2002).

Integrate-and-fire units. Membrane time constants were 30 ms for the Ex unit ($g_{pas} = 0.1 \text{ mS/cm}^2$; $C = 3 \text{ } \mu\text{F/cm}^2$) and 15 ms for the Inh units ($g_{pas} = 0.1 \text{ mS/cm}^2$; $C = 1.5 \text{ } \mu\text{F/cm}^2$). Resting V_m was -60 mV for all the units, the thresholds were -40 mV for the Ex unit and -50 mV for the Inh units, and the reset potentials -53 and -65 mV respectively (to prevent multiple high frequency action potentials in Inh units). A random amount of noise current, withdrawn from an uniform distribution, in the range of $\pm 20 \text{ pA}$ for the Ex unit and $\pm 10 \text{ pA}$ for the Inh units was injected at each time step ($dt = 0.05 \text{ ms}$) and resulted in a voltage SD of 0.35 mV, which is on the upper side of the mean value of the in vitro data we are comparing it to. Increase or decrease in noise levels decrease or increase the gain of I/O functions in the overall,

respectively, but do not affect qualitatively the changes in gain and I/O threshold produced by synaptic plasticity. Noise levels were constant across simulations.

Synapses. The input units were connected to the Ex and Inh units by excitatory synapses with AMPARs, and the Inh units were connected to the Ex unit by inhibitory synapses with GABA_ARs. The synaptic delays were 1.4 ms for Ex→Ex, 1 ms for Ex→Inh and 0.6 ms for Inh→Ex. AMPA and GABA_A synaptic currents were simulated using a kinetic model as described previously (Destexhe et al., 1994; Buonomano, 2000). The reversal potentials were 0 mV for the excitatory synapses (E_{Ex}) and -70 mV for the inhibitory synapses (E_{Inh}). The forward (alpha) and backward (beta) rate constants that determine transmitter binding to receptors were as follows: excitatory synapses: alpha = 1.5 ms⁻¹mM⁻¹, beta = 0.75 ms⁻¹; inhibitory synapses: alpha = 0.5 ms⁻¹mM⁻¹, beta = 0.15 ms⁻¹.

I/O curves. In hippocampal slice experiments, a wide range of intensities, which activate a variable number of Schaffer collateral axons, are used to determine the I/O curves. Thus, the model I/O functions were determined by sequentially activating an increasing number of inputs, corresponding to an increase in stimulation intensity. The lowest intensity was simulated by a spike in a single input, and higher intensities were simulated by recruiting additional input units. Each input unit only fired one spike per trial. At each intensity, the neuron was stimulated 50 times. I/O curves were constructed in the same manner as for experimental intracellular recordings (described above), by measuring the EPSP slope and spike probability at all intensities. The gain and threshold of each I/O curve were also determined in the same manner as the experimental I/O curves.

Acknowledgments

Supported by NIMH (MH60163) and NSF (0543651), and T.P.C. was supported by the Portuguese Science and Technology Foundation. We would like to thank Robert Froemke, Hope Johnson, Rosalina Fonseca, Felix Schweizer and Tom O'Dell for helpful scientific discussions and/or for their comments on earlier versions of this manuscript.

CHAPTER 3

**Short-term plasticity and metaplasticity
of short-term plasticity enhance the
discrimination of spatiotemporal
stimuli in simulated neural networks**

Short-term plasticity and metaplasticity of short-term plasticity enhance the discrimination of spatiotemporal stimuli in simulated neural networks

Tiago P. Carvalho^{1,2} & Dean V. Buonomano^{2,3,4}

¹*Gulbenkian Ph.D. Program in Biomedicine, P-2781-901 Oeiras, Portugal*

²*Departments of Neurobiology and ³Psychology, and ⁴Brain Research Institute, University of California, Los Angeles, CA 90095, USA.*

Correspondence should be addressed to D.V.B. (dbuono@ucla.edu)

Abstract

While short-term synaptic plasticity (STP) is ubiquitously observed in neocortical synapses, its contributions to neural computations are not understood. Here we show that the incorporation of STP into simple neural network models significantly enhances their ability to discriminate spatiotemporal stimuli. Additionally, we propose that STP itself undergoes long-term plasticity, and show that discrimination of temporal patterns is further enhanced by metaplasticity of STP. We present an extension to traditional associative forms of long-term synaptic plasticity in which synapses can ‘learn’ *when* to be weak or strong – e.g., when a postsynaptic cell fires towards the end of a train of presynaptic pulses short-term facilitation should be expressed, however if the postsynaptic cell fires at the beginning of the train, then depression should occur. This form of temporal synaptic plasticity allows simple feed-forward networks to solve computational problems that are otherwise unsolvable.

Introduction

It is well established that synapses are plastic and that their contribution to information transmission can decrease or increase in an activity-dependent manner (Malenka and Bear, 2004; Caporale and Dan, 2008). However, another ubiquitous property of synapses is the sensitivity to the history of their prior activity, a phenomenon called short-term synaptic plasticity (STP), in which the effective synaptic strength between two neurons dynamically decreases or increases in a use-dependent manner, on a time scale on the order of tens to hundreds of milliseconds. Indeed, STP is a defining feature of neocortical synapses, and has been proposed to contribute to a number of different functional roles including temporal processing (Buonomano and Merzenich, 1995; Buonomano, 2000), working memory (Mongillo et al., 2008) and gain control (Chance et al., 1998; Galarreta and Hestrin, 1998).

Excitatory synapses between neocortical neurons exhibit short-term depression and facilitation (Reyes and Sakmann, 1999; Cheetham et al., 2007; Hardingham et al., 2007), and both types of STP are believed to be produced primarily by presynaptic mechanisms (Zucker and Regehr, 2002). Short-term synaptic depression may arise from the depletion of the readily releasable pool of synaptic vesicles (Schneggenburger et al., 2002), while short-term synaptic facilitation is associated with the accumulation of residual calcium in the presynaptic terminal, which can enhance subsequent transmitter release (Katz and Miledi, 1968; Burnashev and Rozov, 2005).

In the brain, neurons express multiple forms of STP in a synapse-specific manner, which suggests there may be a continuum of possible 'flavors' of STP that lie in between purely depressing and purely facilitating synapses (passing through compound forms that may initially facilitate and then depress on consecutive action potentials (Markram et al., 1998; Dittman

et al., 2000; Gupta et al., 2000; Rozov et al., 2001). A number of different mathematical models have been shown to capture the diversity of types of short-term synaptic plasticity (Gingrich and Byrne, 1985; Varela et al., 1997; Markram et al., 1998).

It is well established that STP can change after the induction of LTP or LTD in neocortical synapses (Markram and Tsodyks, 1996; Bender et al., 2006; Hardingham et al., 2007), and that it differs at different developmental stages (Reyes and Sakmann, 1999; Zhang, 2004) and among different cortical areas (Atzori et al., 2001). However, it remains unknown whether STP itself is controlled by specific learning rules; e.g., can a synapse switch from depressing to facilitating, or adjust the temporal profile of depression or facilitation, to better process time-varying stimuli?

Here, we first show that STP is necessary to solve even simple computational problems, and that it enhances the discrimination of more complex spatiotemporal patterns. In addition, we propose that STP itself may be governed by specific learning rules, and that such a form of synapse-specific temporal plasticity further enhances the computational ability of cortical circuits to process spatiotemporal patterns.

Methodology

To examine the contribution of STP to the discrimination of spatiotemporal stimuli we used a simple feed-forward network, in which the afferents convey the time-varying patterns generated by the stimuli. These inputs synapse onto integrate-and-fire postsynaptic neurons which act as the classifiers.

We implemented pre- and postsynaptic learning rules in an essentially independent manner. The presynaptic learning rule, ‘Temporal Synaptic Plasticity’ (see below), governs the dynamics of short-term synaptic plasticity – determining not only whether short-term depression or short-term facilitation is induced but also their respective temporal profiles. The postsynaptic learning rule is responsible for governing the traditional postsynaptic ‘weight’ of the synapse. Here we considered a conventional form of associative synaptic plasticity (STDP, **Figs. 3** and **4**), or the tempotron learning rule (**Figs. 2** and **5**) (Gutig and Sompolinsky, 2006). However, since the mechanisms of STP and STDP are not fully understood, and because postsynaptic mechanisms may contribute to STP (Rozov and Burnashev, 1999; Bagal et al., 2005) it is also possible that postsynaptic mechanisms are involved in determining the short-term synaptic dynamics.

Model neuron: Postsynaptic neurons were modeled as conductance based integrate and fire (IAF) units:

$$(1) \quad \frac{dV(t)}{dt} = -g_L \cdot V + g_{Ex}(E_{Ex} - V) + g_{Inh}(E_{Inh} - V)$$

where $g_L = 0.1$ (0.05 in **Figs. 1** and **2**), $E_{Ex} = 3$ and $E_{Inh} = -3$. If $V(t) > 1$ a spike was elicited and $V(t+dt)$ was reset to 0. Upon arrival of a presynaptic action

potential gEx and gInh increased by the effective synaptic efficacy (see below) and decayed exponentially back to zero with time constant $\tau_{Ex} = \tau_{Inh} = 5$ ms. For the experiments shown in **Figs. 2** and **5**, a ‘noise current’ withdrawn from a normal distribution with mean 0 and standard deviation 0.015 was also present.

Simulation of short-term synaptic plasticity (STP): STP was simulated as described previously (Markram et al., 1998; Maass and Markram, 2002). This model of STP is characterized by three parameters, U , τ_R and τ_F , which represent the fraction of synaptic efficacy used by the first action potential (AP) in a train, the time constant of recovery from depression (R), and the time constant of synaptic facilitation (F). At any point in time, R and F of each synapse are described by the following equations:

$$(2) \quad R(t) = 1 + \left(R(t_{pre}) - R(t_{pre}) \cdot F(t_{pre}) - 1 \right) \cdot \exp\left(\frac{-\Delta t}{\tau_R} \right)$$

$$(3) \quad F(t) = U + F(t_{pre}) \cdot (1 - U) \cdot \exp\left(\frac{-\Delta t}{\tau_F} \right)$$

The initial values of R and F are 1 and U, respectively. Δt represents the time since the last presynaptic spike t_{pre} represents the time of the last presynaptic spike. If there is a presynaptic spike at time t, immediately after synaptic release F(t) is increased by $U(1-F(t))$ and subsequently recovers back to U with time constant τ_F . Hence, F is related to the degree of facilitation and its initial value (U) represents an unfacilitated synapse. R is related to the degree of depression, and recovers to 1 with time constant τ_R . Presynaptic efficacy was determined by the product of R(t) and F(t). Total effective synaptic efficacy was obtained by multiplying the presynaptic efficacy with the postsynaptic

weight, w (see STDP below). In **Fig. 1C** $U = 0.5$; $\tau_R = 1$ or 25 ms and $\tau_F = 1$ ms. In **Fig. 3B** the weights w were 1.00 and 0.08 for the "PPF only" and "PPD only" conditions, respectively.

Temporal Synaptic Plasticity (TSP): There are a number of different potential implementations for the plasticity of the U , τ_R and τ_F variables. For the results shown in **Fig. 4** we used an implementation in which it was assumed that at the time of the positively reinforced postsynaptic spike it is desirable that both the running values of presynaptic variables R and F be relatively high. That is, R should have been largely recovered and F should still be significantly elevated, representing the presence of facilitation. The equilibrium based equations described below drive the three variables towards steady states that favor facilitation at the time of the reinforced postsynaptic spike.

We hypothesized that the changes in U , τ_R and τ_F should depend on the level of activity of the presynaptic terminal at the time of the postsynaptic spike, t_{post} . The variable $S_i(t)$ reflects the amount of activity at the presynaptic terminal i , and can be thought of as a saturating presynaptic Ca^{2+} sensor. S_i changes according to:

$$(4) \quad \frac{dS_i(t)}{dt} = -\frac{S_i(t)}{\tau_s} + \frac{(S_{\max} - S_i(t)) \cdot \sum_n \delta(t - t_i^{(n)})}{S_{\max}}$$

Where τ_s and S_{\max} represent the decay time constant and maximal value of S , respectively. The presynaptic spike train at synapse i is represented by $\sum_n \delta(t - t_i^{(n)})$, where the Dirac function $\delta(t)$ equals 0 at all values except when there is a presynaptic spike at time t , when it equals 1.

At the time of the postsynaptic spike the presynaptic variable U_i (which in this model relates to P_r) was updated by:

$$(5) \quad \Delta U_i = \begin{cases} (U_{\max} - F_i(t_{pre} - dt)) \cdot \alpha_U & \text{if } 0 < S_i(t_{post}) \leq 1 \\ (\overline{F_U} - F_i(t_{pre} - dt)) \cdot \alpha_U & \text{if } S_i(t_{post}) > 1 \end{cases}$$

Where $\overline{F_U}$ corresponds to the equilibrium value of F at the time of the last presynaptic spike. t_{pre} represents the time of the last presynaptic spike to precede t_{post} . Thus if the postsynaptic spike occurs after one presynaptic spike ($S < 1$) U will converge towards U_{\max} , and favor PPD, if it occurs after more than one presynaptic spike ($S > 1$) it will converge towards $\overline{F_U}$. $F_i(t_{pre}-dt)$ equals the value of F immediately before the time of the last presynaptic spike.

Similarly, plasticity of the time constant variables τ_R and τ_F were governed according to:

$$(6) \quad \Delta \tau R_i = (R_i(t_{pre} - dt) - [1 - \overline{R_+}]) \cdot \alpha_{\lambda R_+} \quad \text{if } S_i(t_{post}) > 1$$

$$(7) \quad \Delta \tau F_i = (\overline{F_+} - FN_i(t_{pre} - dt)) \cdot \alpha_{\lambda F_+} \quad \text{if } S_i(t_{post}) > 1$$

Where $FN(t) = \frac{F(t) - U_i}{U_i}$, which represents the normalized value of the

facilitated state. $\overline{R_+}$ and $\overline{F_+}$ are related to the equilibrium values of R and F at the time of the postsynaptic spike, respectively. α_U , $\alpha_{\lambda D_+}$ and $\alpha_{\lambda F_+}$ are gain constants.

In **Fig. 5A**, where we use Poisson stimuli, the time of the ‘desired’ postsynaptic spike is unknown, hence we used the tempotron learning rule (see below) to govern postsynaptic plasticity and determine the time of positive or negative reinforcement. Accordingly, if a neuron did not fire to a positive pattern, U was changed according to Eq. 5, and τ_R and τ_F :

$$(8) \quad \Delta \tau_{R_i} = \left(R_i(t_{pre} - dt) - \left[1 - \overline{R_+} \times S_i(t_{pre} - dt) \right] \right) \cdot \alpha_{\tau_{R+}} \quad \text{if } S_i(t_{post}) > 1$$

$$(9) \quad \Delta \tau_{F_i} = \left(\overline{F_+} - \frac{FN_i(t_{pre} - dt)}{S_i(t_{pre} - dt)} \right) \cdot \alpha_{\tau_{F+}} \quad \text{if } S_i(t_{post}) > 1$$

Where t_{post} is the time of the maximal postsynaptic voltage. Given the presence of trains of spikes at each input the target equilibrium state of the variables τ_R and τ_F are dependent on the presynaptic activity levels ($S_i(t)$). This is the general form of the TSP learning rule, which also capture the rule used above.

Conversely, if a neuron fired an action potential to a negative pattern τ_R and τ_F were updated according to:

$$(10) \quad \Delta \tau_{R_i} = \left(R_i(t_{pre} - dt) - \overline{R_-} \right) \cdot \alpha_{\tau_{R-}} \quad \text{if } R_i(t_{pre} - dt) < \left(1 - \overline{R_+} \times S_i(t_{pre} - dt) \right)$$

$$(11) \quad \Delta \tau_{F_i} = \left(\overline{F_-} - \frac{FN(t_{pre} - dt)}{S_i(t_{pre} - dt)} \right) \cdot \alpha_{\tau_{F-}} \quad \text{if } R_i(t_{pre} - dt) \geq \left(1 - \overline{R_+} \times S_i(t_{pre} - dt) \right)$$

Where $\overline{F_-}$ and $\overline{R_-}$ are equivalent to $\overline{R_+}$ and $\overline{F_+}$ during negative reinforcement, and t_{post} denotes the time of the postsynaptic action potential. As with the case of the errors to the positive pattern, this was only true if $S_i(t_{post}) > 1$.

Both pre- and postsynaptic plasticity were modulated with a kernel that equals 1 at t_{post} and decays to 0 for the preceding time points (with time constant τ_K) – thus preventing plasticity of short-term plasticity at synapses that fired significantly before the postsynaptic spike. U was bounded between [0.10 0.90], $\Delta \tau_F$ and $\Delta \tau_R$ between [1 1200] and Δw was divided by U to normalize the changes in synaptic strength.

The desired steady-state values and gain constants used in the simulations presented here were determined empirically, and are presented in Table 1. For visualization purposes and to maximize the difference in the peaks among the different intervals (to the extent allowed by the STP model itself) we used $\overline{F_U} = 0.65$, $\overline{R_+} = 0.05$ and $\overline{F_+} = 0.37$ in **Fig. 4**.

Spike timing-dependent plasticity: STDP was implemented according to (Song et al., 2000):

$$(12) \quad \Delta w_i = \begin{cases} -A_d e^{\Delta t / \tau_d} & \Delta t < 0 \\ A_p e^{-\Delta t / \tau_p} & \Delta t \geq 0 \end{cases}$$

Where w_i is assumed to be controlling the synaptic weight and $\Delta t = t_{\text{post}} - t_{\text{pre}}$. In both **Fig. 3B** and **Fig. 4B-D** initial weights were 0.05 and $A_p = A_d = 5 \times 10^{-4}$, $\tau_p = 30$ ms and $\tau_d = 40$ ms. During training the postsynaptic neuron was depolarized 20 ms after the last spike of pathway P1 (**Fig. 3C**) or 5 ms after the last spike of the target interval (**Fig. 4**).

Supervised learning rule: In **Figs. 2** and **5** we used tempotron learning rule (Gutig and Sompolinsky, 2006). Neurons had 10 incoming synapses, with initial strength [0 0.01] withdrawn from a uniform distribution. The learning rate was 10^{-3} and in **Fig. 5** the synaptic weights were bounded between [10^{-9} and 0.15], so there were no inhibitory synapses. Neurons were allowed to learn the respective Poisson pattern for an average of 500 presentations of each stimulus (see bellow).

Poisson spike trains: Stimuli were composed of 10 inputs and the duration of each pattern was 250 ms. At each time point the presence or absence of a spike was drawn from a uniform distribution, and set to yield an average rate of [10 12.5 15 17.5 20] Hz (**Fig. 2**) or 20Hz (**Fig. 5**). A relative refractory period of 5 ms was imposed, which recovered with a time constant of 2 ms. Each stimulus set consisted of five Poisson patterns which were presented pseudo-randomly, for a total of 5x500 presentations. During testing the stimuli were presented in order and the reverse of the patterns used for training were included. 10 or 20 of these sets were built with different seeds (**Figs. 2** and **5**, respectively).

Statistics: In **Figs. 2C** and **5B** the error bars represent the standard error to mean. The presented p-value results from t-tests performed pair wise among groups.

$\overline{F_U}$	0.5
$\overline{R_+}$	0.1
$\overline{F_+}$	0.4
$\overline{R_-}$	0.2
$\overline{F_-}$	0.2
α_U	0.05
$\alpha_{\tau R+}$	10
$\alpha_{\tau F+}$	10
$\alpha_{\tau R-}$	25
$\alpha_{\tau F-}$	20
τ_K	10 ms
τ_S	1000 ms
S_{\max}	4

Table 1: Values of the constants used in the computer simulations.

Results

We first considered a ‘toy’ problem in which the task of a single conductance-based integrate-and-fire neuron (see Methods) is to distinguish between input patterns conveyed by two presynaptic neurons, A and B. Each pattern consisted of two spikes 25 ms apart, thus, there are four possible patterns: AA, AB, BA or BB (**Fig. 1A**). The goal of the postsynaptic neuron is to respond *exclusively* to the AB pattern; i.e., generate an action potential when AB, but not the other patterns, is presented. One can intuit that there is no solution to this task (when static synapses are used) because any weight vector $[w_A, w_B]$ that produces a spike to AB will also spike in response to AA or BB. The behavior of the postsynaptic neuron to the four different stimulus over the relevant range of synaptic weights, w_A and w_B , is shown in **Fig. 1C** (top). For each pair of synaptic weights we presented the four stimuli and represented in color *which stimuli* yielded an action potential. If, for a given w_A and w_B , the neuron fired only to the AA stimulus (and not AB, BA and BB) that coordinate would be red. If it fired to AA and BA the coordinate would be pink, and so on, according to the color cube in **Fig. 1B**.

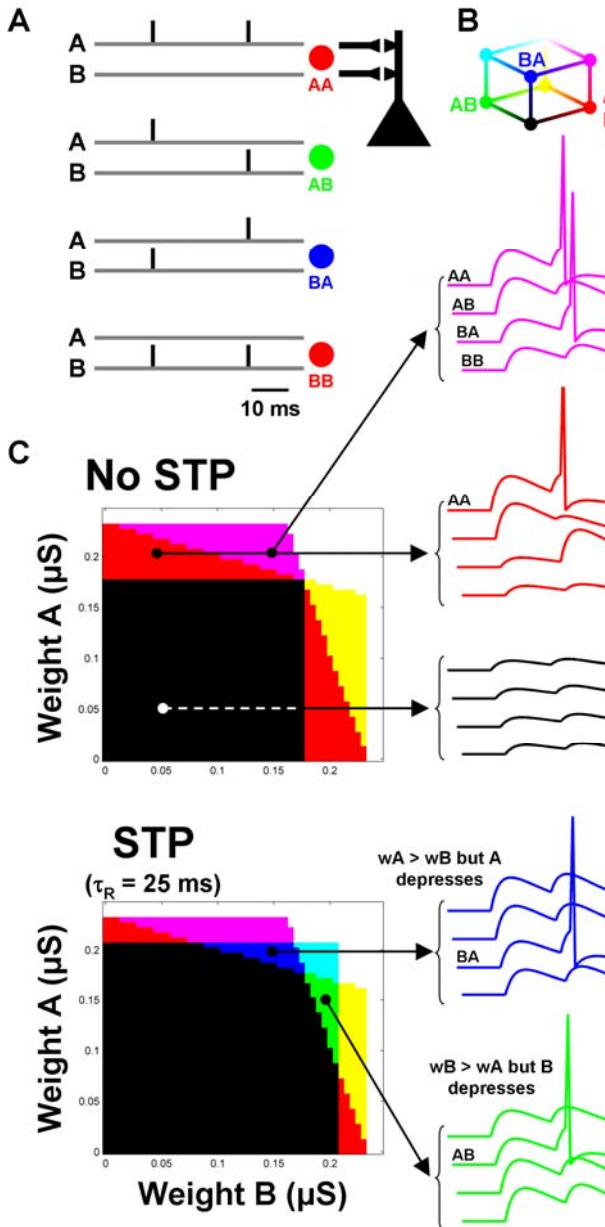


Figure 1: Classical synaptic plasticity alone cannot solve the XAB problem.

A) XAB problem: One neuron receives two inputs (A and B) and its goal is to fire an action potential exclusively to the sequence AB (but not AA, BA or BB).

B) Figure legend: The colors correspond to *which* stimuli the neuron fired. If the neuron fired exclusively to AB we colored the response green (bottom green voltage traces of C). Firing exclusively to AA or exclusively to BB was colored red. Thus, according to the cube, if the neuron fires to BA and AA the response is colored pink (and so on for the other possible combinations).

C) Parameter scan of the synaptic weights of inputs A and B. For each combination of synaptic weights, the 4 possible stimuli were presented consecutively. Some sample voltage traces are illustrated on the right, colored according to which stimuli the neuron fired (color cube). TOP, No STP: In black the weights are too weak so the neuron never fires an action potential. In red the weight of input A is strong so the neuron fires exclusively to the sequence AA (or exclusively to BB if B is strong). Notice that there are no

combinations of weights that provide a response exclusively to BA (or AB). BOTTOM, STP: If the synapses exhibit paired-pulse depression the neuron can exclusively respond to BA (blue) (or AB, green). Essentially, short term depression prevents the neuron from firing to AA in a region where before it was firing to AA *and* BA (notice the color changed from pink to blue) allowing an exclusively BA response (or, conversely, preventing to fire to BB, yellow to green, allowing for an exclusively AB response).

In **Fig. 1C** (top) it can be seen that the ‘exclusively BA’ solution cannot be achieved because the postsynaptic neuron will also fire in response to AA (pink voltage traces, on the right), thus, one can see that the presence of short-term depression could prevent this. Accordingly, we implemented moderate levels of short-term synaptic depression in the same model ($\tau_R = 25$ ms, see Methods) and re-run the parameter scan (**Fig. 1C**, bottom). Importantly, now there are regions of the synaptic space in which it is possible to detect exclusively AB (green) or BA (blue). This is possible because some coordinates that were firing before to AA *and* BA (pink) or BB *and* AB (yellow), now fire exclusively to BA or AB because the synaptic responses to the second pulse in AA or BB depress. This toy problem provides an example of a task which cannot be solved by a simple feed-forward network with ‘static’ synapses (that do not exhibit STP).

STP improves forward versus reverse selectivity by establishing temporal asymmetry

Next we analyzed the computational advantages of endowing synapses with STP in tasks based on the discrimination of complex spatiotemporal patterns. Neurons were trained to discriminate Poisson spike patterns (**Fig. 2A**, left) by adjusting the synaptic weights according to a supervised learning rule (Gutig and Sompolinsky, 2006). In brief, if the postsynaptic neuron did not fire to the target (‘positive’) stimulus the weights of the synapses whose activity contributed to the maximum voltage were increased in a manner proportionally to that contribution (see Methods). On the other hand, if the postsynaptic neuron fires at any point during a ‘negative’ stimulus the synaptic weights of each synapse are decreased in proportion to their contribution to the incorrect spike.

At each trial we randomly presented one of five Poisson spike patterns (each pattern consisted of 10 inputs) with average firing rates ranging from 10 to 20 Hz (see Methods). We used different mean spike rates to make the problem more challenging; specifically, it is difficult to generate selective responses to low-frequency patterns. The goal of the output neuron is to adjust its 10 synaptic weights in a manner that it fires an action potential selectively to its target Poisson pattern. In the absence of STP, the tempotron learning rule performed very well, yielding 1-2% errors (**Fig. 2B**). The inclusion of synaptic STP (the same STP parameters for the 10 synapses), whether depressing or facilitatory, did not alter the learning procedure significantly.

However, when we tested performance not only in response to the 5 original Poisson stimuli, but to their reverse patterns as well, the performance degraded significantly to $42\pm 2\%$ errors (an error is a failure to detect the positive pattern or firing to any of the non-target patterns, **Fig. 2C**, blue solid bar). Analyzing the errors in more detail reveals that the neuron is mostly firing specifically to the negative patterns that are the reverse of the positive target patterns (**Fig. 2C**, blue dotted bar, $38\pm 2\%$). Analysis of the times of the postsynaptic action potential in the forward and reverse patterns indicates approximately symmetric spike times (**Sup. Fig. 1**, left histograms). The lack of selectivity to the forward versus reverse patterns indicates that discrimination relies in large part not on the temporal structure of the stimulus, but on the detection of synchronous spikes characteristic of a particular stimulus. The presence of STP significantly increased the discrimination of forward versus reverse spatiotemporal patterns. Specifically, short-term depression ($U=0.5$; $\tau_R=400$ and $\tau_F=1$ ms) produced $16\pm 3\%$ errors (of which only $3\pm 1\%$ are specific to the reverse of the positive pattern, **Fig. 2C**, solid and dotted bars respectively) and short-term facilitation $28\pm 3\%$ errors ($18\pm 3\%$ to the reverse).

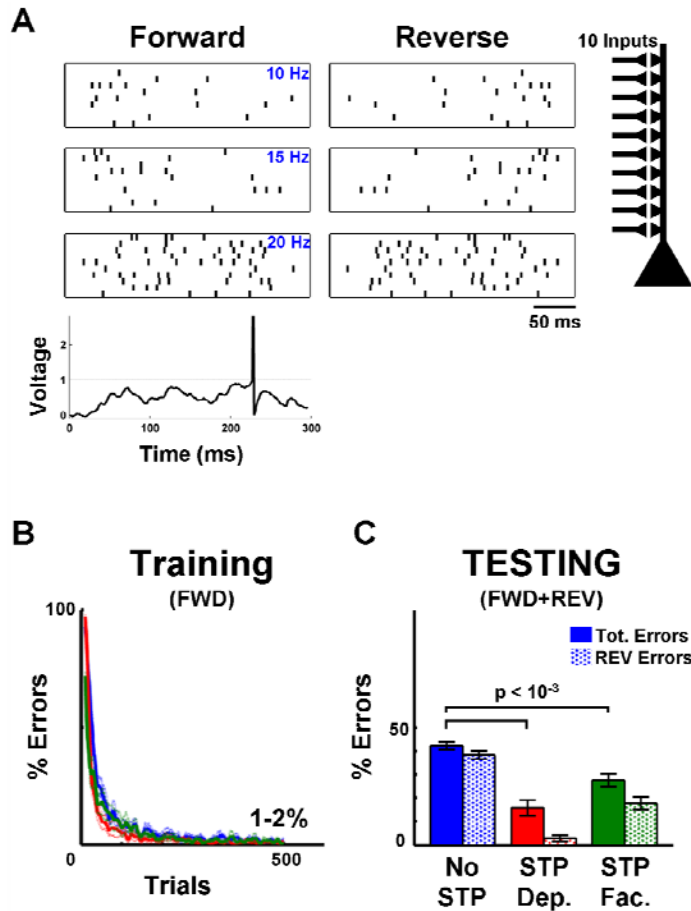
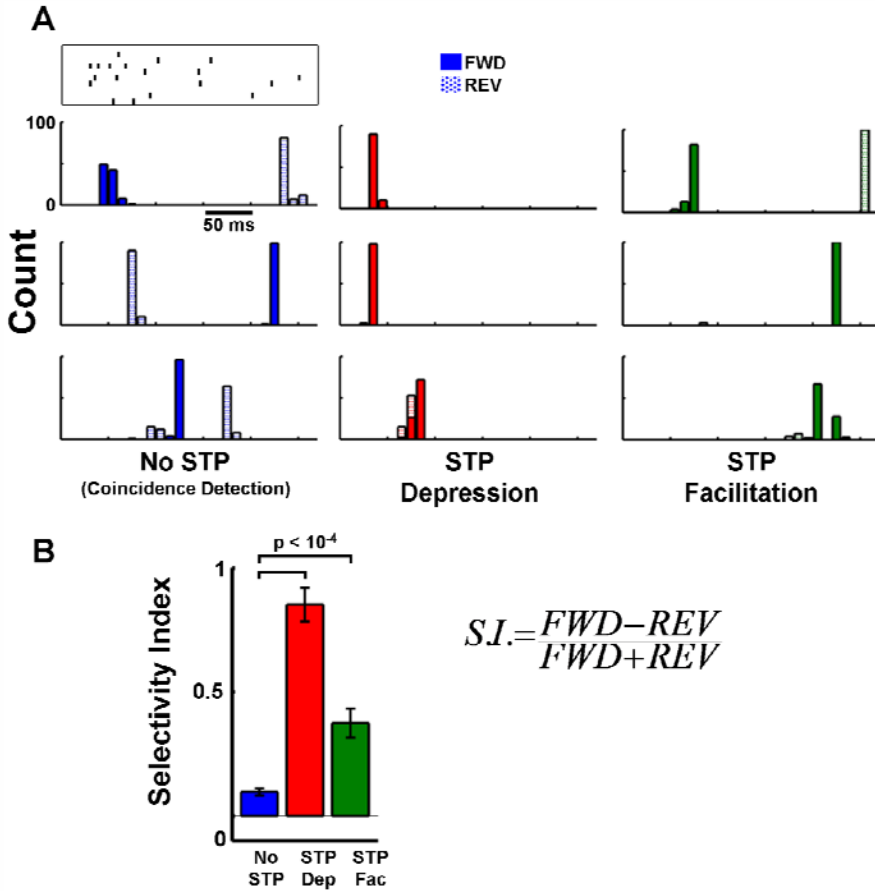


Figure 2: Short-term plasticity improves forward versus reverse selectivity of spatiotemporal Poisson patterns.

A) Poisson patterns: Each training set consists of 5 FWD Poisson patterns with rates ranging from 10-20Hz. Each pattern has 10 inputs which synapse to one post-synaptic neuron whose goal is to fire an action potential selectively, to just one of the patterns (supervised learning, see text). The bottom trace depicts an example of the voltage in response to the 20Hz pattern shown.

B) Performance during training on the FWD patterns. Blue line depicts learning without short-term plasticity and the red and green lines depict learning with some levels of depression and facilitation, respectively (see text).

C) Performance during testing, when the reverse of the patterns used for training were included in the stimulus set. Short-term plasticity, whether depression or potentiation, enhances pattern selectivity. Solid bars quantify total errors. Dotted bars quantify the errors when the neuron fired to the reverse of the target pattern ($n = 10$).



Supplemental Figure 1: STP establishes a temporal asymmetry.

A) Histograms of the spike times of the neuron during testing, when the forward and reverse patterns are presented (solid and dotted bars, respectively). Each row represents a different sample stimulus pattern. Columns depict different STP conditions (the same as in **Fig. 2**). Notice how static synapses (no STP) have nearly symmetric spike time histograms when the FWD and REV stimuli are presented. Short-term depression or facilitation break that symmetry. The spike raster at the top depicts a 10 Hz FWD stimulus, which leads to the response of the solid bars in the first row.

B) Selectivity Index. The selectivity index quantifies the selectivity of the response towards the trained pattern, with regard to its reverse. A value of 1 means that training resulted in responses exclusively to the trained pattern. A value of 0 signifies that the neuron responds both to the trained pattern and to its reverse.

STP is intrinsically temporal and allows synapses to carry a history of their recent past events. We have shown that a corollary of this property is that when a stimulus is reversed, the pattern perceived by the neuron will be effectively different from a simple mirror image of the original. The results above suggest that STP improves selectivity of forward versus reverse stimuli by breaking the symmetry when a pattern is reversed (**Sup. Fig. 1**, red and green histograms). Note that we chose to train the network on the forward patterns, and test it on the untrained reverse patterns, in order to parallel experimental findings. For example, in songbirds, HVC neurons respond selectively to the forward song, but not to the reverse song, even though the bird was presumably never exposed to the reverse song in its lifetime (Doupe, 1997).

Metaplasticity of Short-term Plasticity: Solving the shift problem

The previous results show that STP improves the discrimination of spatiotemporal stimuli. In these simulations the synapses were dynamic (they exhibited STP), however, STP itself was static; i.e. it was hardwired into the synapses and did not exhibit any adaptation or learning related to the stimuli being decoded. Additionally, each synapse in the network exhibited qualitatively and quantitatively the same form of STP. We next asked if different types of STP at different synapses could further enhance performance, and whether there are suitable learning rules to guide STP into regimes that optimize neural computations.

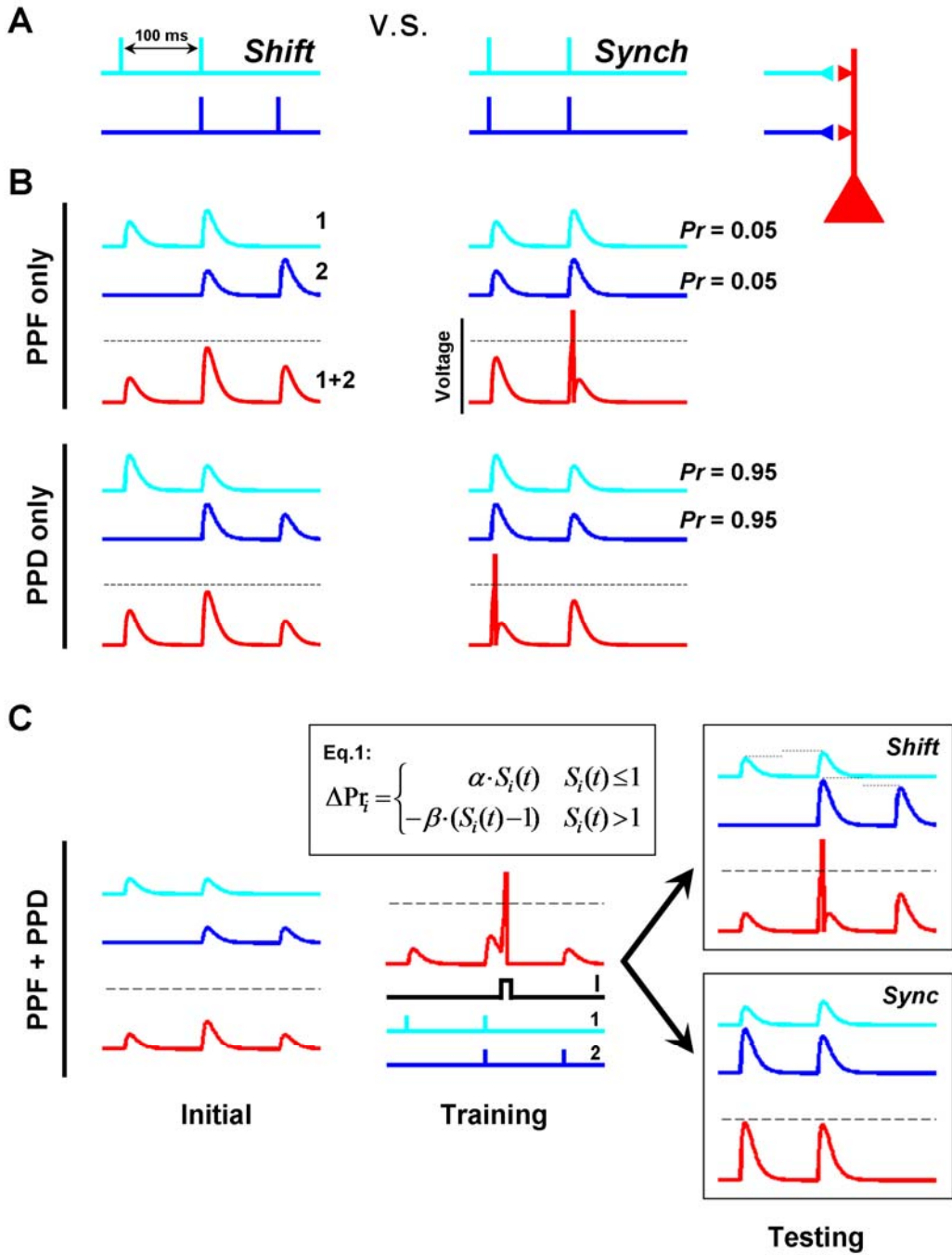


Figure 3: Metaplasticity of short-term plasticity.

A) Shift Problem. The goal is to discriminate between the shift (top row, left) and synchronous patterns (top row, right).

B) Same STP in both inputs does not solve the shift problem. The traces depict the voltage contribution of each input (light and dark blue) to the total postsynaptic voltage (red). Paired-pulse facilitation or paired-pulse depression in both inputs cannot solve the problem because the neuron's peak response (red trace) will always be to the second or first pulse of the *Synch* pattern, respectively. Each input exhibits PPF or PPD depending on whether its synapse has a low or high Pr, respectively.

C) Eq.1. A simple learning rule that adjusts the probability of release (Pr) at each synaptic terminal solves the shift problem. S is a variable that reflects the number of presynaptic spikes (see Methods). Bottom: Pairing postsynaptic depolarization (I) – which acts as the ‘supervisor’ – with the coincident presynaptic spikes of the Shift pattern results in PPF at synapse 1 and PPD at synapse 2, in addition to conventional postsynaptic LTP at both synapses. The rationale is that the time of postsynaptic depolarization in relation to a presynaptic spike train determines whether those synapses will show PPD (early pairing) or PPF (late pairing). By pairing postsynaptic depolarization with either the first or second spikes of the synchronous pattern the postsynaptic neuron will also learn to respond selectively to it (not shown).

To address this issue we initially considered another toy problem that a simple feed-forward network with static synapses cannot solve. In the “shift problem” each of two input neurons fire twice with a 100 ms interspike interval, onto a single postsynaptic neuron; in the *shift* pattern the onset of the first input neuron occurs 100 ms before that of input 2, while in the *synchronous* pattern both inputs fire at the same time (**Fig. 3A**). The goal of the neuron is to fire exclusively to the shift pattern but not the synchronous. This problem cannot be solved, even if synapses exhibit STP dynamics (of the same kind, **Fig. 3B**).

On the other hand, there are possible solutions if the different synapses exhibit qualitatively different forms of STP. For example, the postsynaptic neuron can respond selectively to the shift pattern if Input 1 exhibits paired-pulse facilitation (PPF) and input 2 paired-pulse depression (PPD) (**Fig. 3C**, right panels).

One of the determinants of whether a synapse exhibits PPF or PPD is the presynaptic probability of vesicle release (Pr) – high and low Pr values are associated with PPD and PPF, respectively (Debanne et al., 1996; Dobrunz and Stevens, 1997). It is possible for the simple circuit presented in **Fig. 3A** to solve the shift problem if we assume the presence of a physiological learning rule that controls Pr , together with conventional STDP (assumed to be governing postsynaptic efficacy) (**Fig. 3C**). For example, we implemented a rule that altered Pr as expressed in Eq. 1: if the presynaptic neuron has only spiked once before the postsynaptic spike ($S \leq 1$) Pr increases (favoring PPD), in contrast if it has spiked more than once ($S > 1$) Pr decreases (favoring PPF). As it can be seen on the right panels of **Fig. 3C**, physiologically plausible Eq. 1 combined with STDP guides synapses towards suitable synaptic weights and an appropriate combination of PPF and PPD that lead the neuron to fire to the shift but not to the synchronous patterns, as desired.

Temporal Synaptic Plasticity: A Novel Learning Rule for Metaplasticity of STP

The actual mechanisms underlying STP remain incompletely understood and rely on a number of properties in addition to Pr (Zucker and Regehr, 2002). Nevertheless, as implemented in the above simulation, STP is often modeled by two time- and activity-dependent variables that determine the presynaptic *effective* synaptic strength: R , which represents the fraction of synaptic resources available; and F , which represents the fraction of R that is actually used at each release event. Hence, the presynaptic *effective* synaptic strength is given by the product of R and F (see Methods, Markram et al., 1998). R and F are modulated by three parameters: U (related to Pr), τ_R (time constant of recovery from depression) and τ_F (time constant of synaptic facilitation). A learning rule that governs these three STP parameters and

takes into account the recent history of presynaptic activity at the time of the postsynaptic spike can not only control whether PPD or PPF is expressed, but also the *timing* at which the voltage peaks (**Fig. 4**, see Methods). As an example, we considered the case in which a neuron receives only one input, which is activated twice, with an interval of 50, 100 or 200 ms between pulses. The goal is to train the neuron to become selective to the middle (100 ms) interval, by repetitively pairing the second pre-synaptic spike of this interval with post-synaptic depolarization (**Fig. 4A**, right), which adjusts both the synaptic weight and the STP parameters (see Methods).

This rule for metaplasticity of STP performs well and finds a solution that, *at the time of the paired spike*, causes the synapse to be mostly recovered from depression while not displaying exaggerated levels of facilitation (**Fig. 4B**, R and F, top right). For example, if initially the neuron did not fire to the second pulse of the 100 ms interval, because the synapse had not recovered yet from the first pulse, then τR would be decreased so that recovery from depression (R) would occur faster. Parallely, if there was too little facilitation at the time of the second pulse then τF would be increased so that facilitation (F) contributed to generate an action potential at the time of the pairing (**Fig. 4B**, left panel). This model is based on equilibrium values for R and F, *at the time of the paired spike*. Otherwise, if the synapse recovers too quickly from depression the neuron would also fire to the second pulse of the shorter (50 ms) interval; or, conversely, if there was too much facilitation the neuron would fire to the second pulse of the 200 ms interval as well, thus loosing the ability to be interval selective.

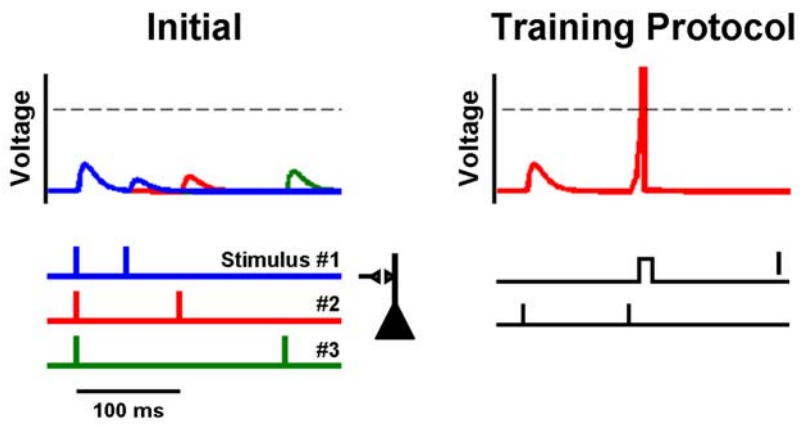
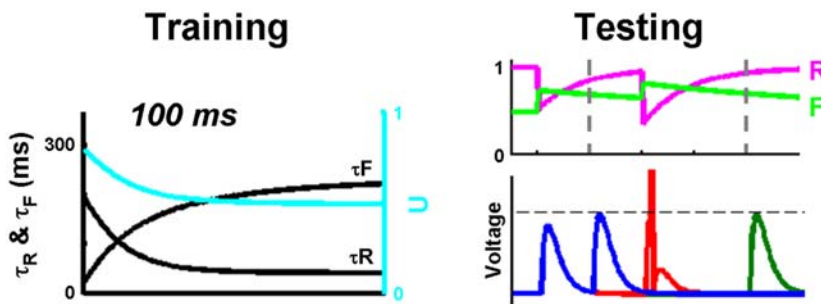
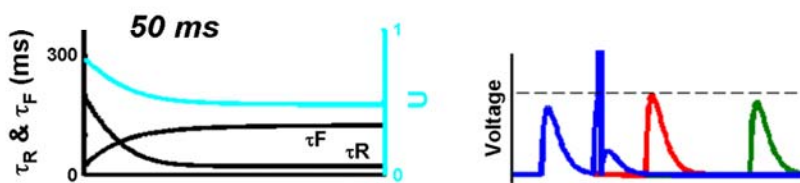
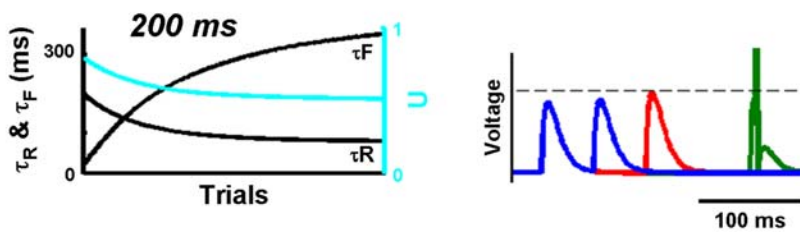
A**B****C****D**

Figure 4: Temporal synaptic plasticity can produce interval selective responses.

A) Selective discrimination of a medium duration interval. Left: The model neuron receives only one input pathway, which is stimulated with 3 different patterns (paired-pulse intervals of 50, 100 or 200 ms). Right: The 100 ms interval is reinforced by depolarizing the neuron after the arrival of the second spike. The synaptic weight is adjusted according to STDP.

B) Training selectivity to a 100 ms interval. Left: Values of the parameters U , τ_R and τ_F during training. Right: In the end of training, the parameters are such that paired-pulse facilitation peaks at approximately 100 ms, thus creating a neuron that fires preferentially to the trained interval (voltage traces). TOP: In this case the solution achieved 'intermediate' values of τ_R and τ_F such that at 50 ms the synapse is still recovering (R) and there is not too much facilitation at 200 ms (F).

C and D) Left: as in B). Right: Responses after training to the short (50 ms) and long (200 ms) intervals.

Similarly, if the postsynaptic spike is paired with the second presynaptic spike of a 50 ms interval, τ_R and τ_F settle at relatively small values, whereas for a 200 ms interval, they settle at higher values (**Fig. 4C,D**) such that the neuron fires exclusively to the target interval.

Temporal Synaptic Plasticity Applied to the Discrimination of Poisson Spike Patterns

The same STP learning rule enhances the ability of model neurons to discriminate complex spatiotemporal patterns (**Fig. 5**). Initially, neurons were trained to discriminate forward Poisson patterns (20 Hz) with the tempotron learning rule (Gutig and Sompolinsky, 2006), and tested in the same manner as described in **Fig. 2**, by including the reverse patterns. Similarly to what has been shown, in the absence of STP and temporal synaptic plasticity, neurons were responsive to the untrained reverse stimuli ($37 \pm 2\%$ total errors, **Fig. 5**, blue bar).

In a second set of experiments, random STP parameters were included at *each* of the synapses and the postsynaptic neuron was trained as above (while the STP parameters themselves were held constant during training). This procedure increased spatiotemporal selectivity significantly ($28\pm 2\%$ errors, green bar).

In a third set of simulations that were initiated with the same random STP parameters, training with the tempotron together with temporal synaptic plasticity, which modifies the STP parameters of each synapse individually, dramatically decreased the total number of errors ($8\pm 2\%$, red bar). At the end of these simulations, the STP parameters of each synapse were shuffled across synapses, and then trained with the tempotron alone (i.e., the shuffled STP values were held constant during training). This procedure resulted in increased percentage of errors ($31\pm 4\%$, orange bar), similar to the levels of the 'Random STP / No TSP' condition (green bar). This important control shows that temporal synaptic plasticity can optimize the discriminatory selectivity of simple feed-forward networks in a synapse specific manner and that this effect is not due the distribution of STP parameters – that is, performance relies on specific types of STP at the appropriate synapses.

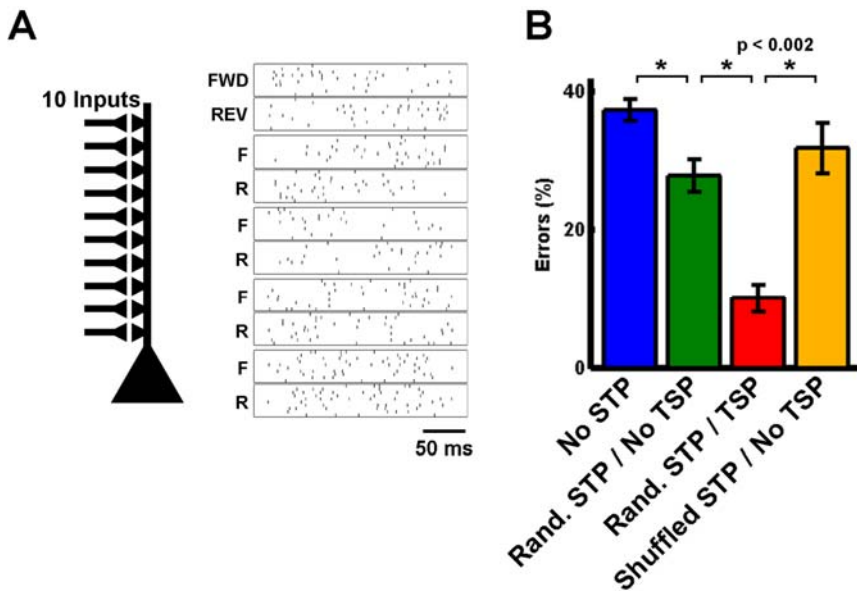


Figure 5: Temporal synaptic plasticity enhances the discrimination of complex spatiotemporal patterns.

A) Discrimination of Poisson spike patterns: Schematics of the circuit and sample Poisson patterns (20 Hz). Neurons were trained to detect exclusively one forward stimulus (FWD) and tested on the dataset that included the reverses (REV).

B) Percentage of errors during testing: Notice that the inclusion of synapses with random (but static) STP values before training improves performance significantly (green). However, using Temporal Synaptic Plasticity (TSP) to tune STP further decreases the number of errors (red). In orange is depicted the percentage of errors when the model is re-trained using the shuffled STP values obtained after training with TSP ($n = 20$).

Discussion

The results presented here highlight the computational advantages of endowing synapses with short-term plasticity. We presented concrete toy computations that cannot be performed without STP and demonstrated that it significantly increases spatiotemporal pattern selectivity. We showed that STP and metaplasticity of STP provide a built-in temporal asymmetry that ensures that the forward and reverse stimuli are easily distinguishable – a characteristic of spatiotemporal selective cells observed *in vivo* (Doupe, 1997), and an observation consistent with the lack of perceptual similarity between forward and reversed stimuli, such as speech.

The general hypothesis presented here is that the relative timing of the pre- and postsynaptic spikes do not simply modulate long-term plasticity, as established by STDP (Debanne et al., 1994; Markram et al., 1997; Bi and Poo, 1998), but may serve as a ‘teacher’ signal to determine whether the synapse should be depressing or facilitating, as well as the time course of these forms of short-term synaptic plasticity. The simplest experimental prediction of this hypothesis is that when pairing postsynaptic activity with a train of presynaptic spikes, the position of the postsynaptic spikes should shape short-term plasticity in a predictable manner. For example, a postsynaptic spike paired with the first or last of a pair of presynaptic spike should favor PPD and PPF, respectively; because the contribution of the EPSP to the postsynaptic spike would be optimized by depression (increased use of presynaptic efficacy) if the post spike occurs early, or by facilitation if the post spike occurs late. It should be noted that this prediction has been tested at least twice in CA1 synapses with negative results (Buonomano et al., 1997; Buonomano, 1999). However, since these studies were performed it has been established that CA1 and neocortical LTP appear to be fundamentally different, for example neocortical

STDP relies on presynaptic changes and a complex biochemical network potentially involving metabotropic glutamate receptors, endocannabinoids, nitric oxide, and presynaptic NMDA receptors (Bender et al., 2006; Sjostrom et al., 2007; Rodriguez-Moreno and Paulsen, 2008). Furthermore, any experimental test of this hypothesis should take into account that plasticity of short-term plasticity may require de-novo protein synthesis and thus emerge only a few hours after induction (Huang et al., 1994).

Short-term synaptic depression and facilitation are caused directly or indirectly by the action of calcium ions within the presynaptic terminal (Zucker and Regehr, 2002; Mochida et al., 2008). A recent alternative is that, in some systems, depression and facilitation may be caused by common mechanisms involving Ca^{2+} -dependent regulation of Ca^{2+} sensor proteins that modulate the presynaptic calcium channels responsible for triggering transmitter release (Mochida et al., 2008). This unifying and interesting hypothesis could open the possibility for bidirectional modulation of short-term plasticity through the modulation of Ca^{2+} sensor proteins (CaS).

Temporal synaptic plasticity extends traditional Hebbian plasticity into the temporal domain by proposing that synapses learn not only whether they should be strong or weak, but *when* they should be strong. This feature could play an important adaptive role in allowing synapses to tune themselves according to experience, in a fashion that improves temporal computations and the processing of time-varying stimuli. The presence of two learning rules operating in parallel may help explain the complexity of neocortical associative plasticity and why in some instances the same induction protocol can induce either LTD or LTP (Ismailov et al., 2004; Hardingham et al., 2007). Additionally, the presence of two independent learning rules governing pre- and postsynaptic efficacy provide a framework to understand the current neocortical plasticity experimental data which indicates the presence of parallel pre- and postsynaptic changes under control of a complex network of

biochemical processes (Bender et al., 2006; Sjostrom et al., 2007; Rodriguez-Moreno and Paulsen, 2008).



Acknowledgements

Supported by NIMH (MH60163), and T.P.C. was supported by the Portuguese Science and Technology Foundation. We would like to thank Felix Schweizer, Hope Johnson and Weixiang Chen for their comments on earlier versions of this manuscript.



CHAPTER 4

Final Discussion



The brain's ability to learn and perform complex computations relies in large part on the strength of the connections between neurons. Here, two well known properties of biological neural networks that govern synaptic strength were considered: long-term (Chapter 1) and short-term (Chapter 2) synaptic plasticity. It was shown, using a combination of experiments and computer simulations, how the dynamics of synaptic plasticity may determine the *output* of neurons, thus establishing a link between subcellular phenomena and neural computations.

It is not the strength of each synapse in isolation that determines what computation occurs, but the net interaction between many excitatory and inhibitory synapses. Specifically, the role of a neuron in a computation is determined by whether or not it fires an action potential, which depends on the information conveyed by excitatory and inhibitory synapses activated by a particular stimulus. Here, it was established how changes in excitatory and inhibitory synaptic strength interact to shape the behavior of a neuron, and thus its role in information processing. If synaptic plasticity is believed to be involved in learning and memory, it cannot be overstated the importance of understanding in detail its consequences in the output of neurons.

Specifically, it was shown that excitatory synaptic plasticity can control the threshold of neuronal I/O functions, while balanced changes in excitatory and inhibitory synaptic strength determine the gain. One issue that was not considered was the *timing* of the action potential. It was shown that the gain of a neuron's I/O function is intimately related with the width of the integration window, which in turn is known to be directly related with the timing and jitter of the action potential (Pouille and Scanziani, 2001). Sharper I/O responses will have good threshold detection characteristics but on the other hand, given that the integration window is wide, will have later and more variable spike times. Shallower I/O responses are not so precise regarding the intensity of the eliciting stimulus, but they have the advantage that they are sensitive to a

broader dynamic range of inputs and in addition have earlier and more accurate spike times.

This work may contribute to the understanding of why excitation and inhibition are co-tuned in vivo. However, future work remains to be done to determine the learning rules that lead to the development of these microcircuits and their balanced regimes.

Regarding short-term synaptic plasticity, we provided specific examples of computations that could benefit from this ubiquitous phenomenon. In the simulations, however, we modeled STP as continuous variations in synaptic strength and, in reality, synaptic transmission is quantal and probabilistic (Debanne et al., 1996; Dobrunz and Stevens, 1997). Our simplification is reasonable if one assumes multiple release sites per neuron or a representation of the average activity of multiple release events. Nevertheless it could be interesting to attempt to model vesicle release as a probabilistic event on a trial by trial basis. It may help in the discrimination of spatiotemporal patterns, as it could allow for a broader, combinatorial, sampling of the parameter space (Seung, 2003).

In addition, it should be noted that some of the presented toy problems are not meant to be faithful representations of what happens in vivo; they should be seen simply as illustrations of the computations that could potentially be performed. For example, it was shown that short-term plasticity coupled with spike-timing dependent plasticity could lead a single neuron to perform interval discrimination and become interval selective. This is highly unlikely, and indeed it has been proposed that these type of computations are performed by the brain not at the single neuron level but in the high-dimensional state of neural networks, using physiological time-varying properties, of which STP is an example (Karmarkar and Buonomano, 2007).

Nevertheless, we presented a novel approach which consists in using synapse specific STP in neural network models to improve the discrimination of spatiotemporal patterns. Importantly we provide a learning rule that adjusts the magnitude and temporal profile of STP in an attempt to further optimize the performance of stimulus discrimination. In principle, this approach could be applied to more complex tasks such as speech recognition.

Above any particular result, it is expected that the work presented here will increase the awareness that understanding the brain requires that well characterized synaptic and cellular properties be placed in a global context. Specifically, it is the balance of excitation and inhibition together, as well as the dynamic changes in synaptic strength, that determine in a highly interactive and nonlinear fashion whether a neuron will fire in response to its input. It is expected that the work presented here is of interest to cellular electrophysiologists, system neuroscientists, computational neuroscientists and the learning and memory community in general, because all changes in behavior are ultimately a product of changes in the firing of neurons embedded within complex neural networks.

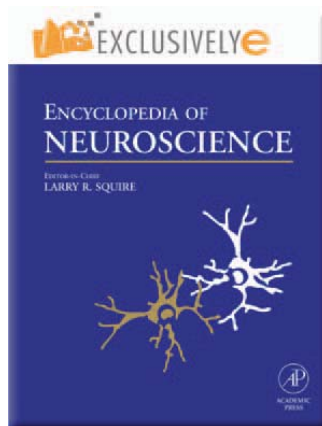


APPENDIX A

Spike-Timing-Dependent Plasticity (STDP)

Provided for non-commercial research and educational use.
Not for reproduction, distribution or commercial use.

This article was originally published in the *Encyclopedia of Neuroscience* published by Elsevier, and the attached copy is provided by Elsevier for the author's benefit and for the benefit of the author's institution, for non-commercial research and educational use including without limitation use in instruction at your institution, sending it to specific colleagues who you know, and providing a copy to your institution's administrator.



All other uses, reproduction and distribution, including without limitation commercial reprints, selling or licensing copies or access, or posting on open internet sites, your personal or institution's website or repository, are prohibited. For exceptions, permission may be sought for such use through Elsevier's permissions site at:

<http://www.elsevier.com/locate/permissionusematerial>

Buonomano D V and Carvalho T P (2009) Spike-Timing-Dependent Plasticity (STDP). In: Squire LR (ed.) *Encyclopedia of Neuroscience*, volume 9, pp. 265-268. Oxford: Academic Press.

Spike-Timing-Dependent Plasticity (STDP)

D V Buonomano and T P Carvalho, University of California, Los Angeles, CA, USA

© 2009 Elsevier Ltd. All rights reserved.

Introduction

Spike-timing-dependent plasticity (STDP) refers to a form of associative synaptic plasticity in which the temporal order of the presynaptic and postsynaptic action potentials determines the direction of plasticity, that is, whether synaptic depression or potentiation is induced. In the most common form of STDP, long-term potentiation (LTP) is induced if the presynaptic spike precedes the postsynaptic spike (pre→post). In contrast, if the postsynaptic spike happens before the presynaptic spike (post→pre), then long-term depression (LTD) is induced. In addition to the order of the pre- and postsynaptic spike, STDP is sensitive to the interspike interval (ISI), the time elapsed between the two spikes. In general, short intervals produce maximal plasticity, while longer intervals produce little or no change in synaptic strength.

STDP represents an important form of synaptic plasticity for both experimental and computational reasons. Experimentally, LTP and LTD have often been induced by distinct protocols, and the relationship between these protocols as well as their physiological relevance has not always been clear. STDP formalizes the conditions for the induction of both LTP and LTD into a single learning rule. STDP is attractive as a computational learning rule because the direction of synaptic plasticity reflects the causal relationship between pre- and postsynaptic activity. If the presynaptic spike consistently precedes a postsynaptic spike, it is likely that the former contributes in eliciting the latter, and this contribution will be 'reinforced' through potentiation. In contrast, if the presynaptic spike consistently fires after the postsynaptic spike, no causal relationship between pre- and postsynaptic activity is present, and depression will ensue.

STDP and Hebbian Plasticity

The psychologist Donald Hebb postulated that if a presynaptic neuron "repeatedly or persistently takes part in firing" a postsynaptic neuron the synapse between them would be potentiated. This form of plasticity has come to be known as Hebbian or associative synaptic plasticity. However, Hebb's original postulate left two important issues unaddressed. First, what is the learning rule that underlies

'decreases' in synaptic strength? Second, what is the effective time window between pre- and postsynaptic activity that will result in potentiation? STDP addresses both these issues by establishing the specific conditions and temporal requirements for the induction of both LTP and LTD.

In a typical protocol, a single presynaptic spike is repetitively (e.g., every 1 s for 1 min) elicited 0–25 ms before or after a postsynaptic action potential. Here, intervals consisting of pre→post pairings will be defined as 'positive' ISIs, while post→pre pairings will be referred to as 'negative' ISIs. By examining the direction and magnitude of plasticity over a range of ISIs, we can plot the so-called 'STDP function' (change in synaptic strength vs. ISI), schematized in [Figure 1](#). The STDP function characterizes plasticity at a given synapse, and represents the 'time windows' for the induction of both LTP (green) and LTD (red). Because both LTP and LTD are maximal for short intervals, differences of only a few milliseconds result in a sharp discontinuity at ~0 ms. In addition to the amplitude and duration of both time windows, another important feature of the STDP function is their ratio. For example, under the simplified assumption that pre- and postsynaptic spikes occur in isolation and randomly at all possible ISIs, one can see that if the LTP and LTD windows are equal in area there will be no net change in the overall synaptic strength. However, if the LTD area is larger than its LTP counterpart, random pre- and postsynaptic events will lead to a decrease in synaptic strength toward zero. Conversely, synaptic strength will saturate if the LTP area is larger. While not all the experimental data are in agreement, it is clear that in some cases the STDP functions do exhibit larger LTD windows, and thus are consistent with a potential role of STDP in synaptic competition (see below).

STDP functions similar to the one schematized in [Figure 1](#) have been characterized in a number of different preparations including excitatory neocortical synapses, the retinotectal projection in *Xenopus*, and dissociated hippocampal cell cultures. Nevertheless, STDP is not universally observed, and thus the following points should be noted.

1. Not all synapses seem to undergo STDP in response to the pairing of single pre- and postsynaptic action potentials. For example, most evidence suggests that pairing of single pre- and postsynaptic spikes in the Schaffer-collateral→CA1 synapse in hippocampal slices does not result in synaptic changes that follow a function similar to the one depicted in [Figure 1](#). At these synapses, the induction of LTP seems to require a burst of postsynaptic spikes.

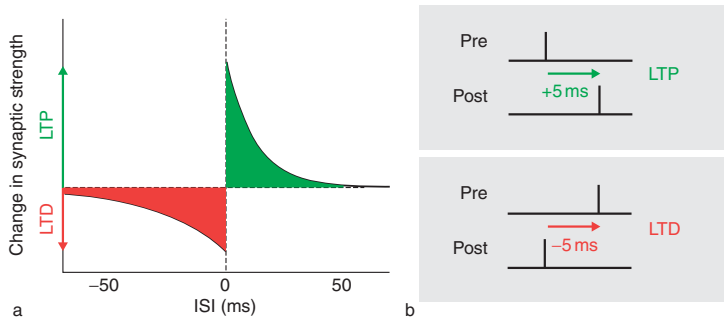


Figure 1 (a) A hypothetical STDP function is depicted. Positive or negative interstimulus intervals give rise to LTP or LTD, respectively. No appreciable plasticity is induced at the synapse for large ISIs. Note the sharp discontinuity at 0, and that a longer-lasting LTD window is depicted. (b) A positive ISI is defined as the time interval between an initial presynaptic spike and a consecutive postsynaptic spike, which will lead to LTP. For negative ISIs, the postsynaptic cell fires before the presynaptic, and LTD will ensue.

- The shape of the STDP function is highly variable. The peak or total area of the LTP and LTD windows are dependent not only on the types of synapses being examined, but on the exact induction protocol, pre- and postsynaptic cell type, and even on the position of the synapse along the dendritic arbor.
- The standard STDP function is based on isolated single pre- and postsynaptic spikes, and does not necessarily describe synaptic plasticity in response to more complex patterns of activity.

Linearity of STDP

What would happen if the presynaptic spike consistently preceded and followed the postsynaptic spike by ISIs that individually would contribute with the same, but opposite, amount of LTP and LTD? If the result of such an experiment yielded no change in the synaptic strength, it would be said that individual ISIs were independent and that the contributions of each of the intervals summate linearly. In contrast, if, for instance, LTP was observed, STDP would be nonlinear and LTP would be dominant. Under experimental conditions, it is possible to constrain the spike patterns to single isolated spikes; however, *in vivo* data show that bursts of spikes or complex ongoing temporal patterns of spikes are commonly elicited in response to a given stimuli. Thus, in order to understand the computational role of STDP *in vivo*, it is necessary to address the issue of linearity or nonlinearity of STDP, and define the rules governing plasticity in response to complex patterns of pre- and postsynaptic activity.

Experimental studies have examined the issue of linearity by using protocols with spike triplets (e.g., pre→post→pre or post→pre→post) or quadruplets. It is clear that STDP is not strictly linear; however, the precise nature of the interaction of complex spike patterns on the LTP and LTD components of

STDP is still emerging. Empirically determining the higher-order features of STDP is a challenging task, because the potential arrangements of spike patterns undergo a combinatorial explosion. Thus, a detailed understanding of the higher-order properties of STDP will likely rely on the elucidation of the underlying mechanisms. Specifically, if the critical cellular, synaptic, and biochemical mechanisms governing STDP can be quantitatively characterized, it should be possible to accurately predict the direction and magnitude of synaptic plasticity in response to any arbitrary patterns of pre- and postsynaptic spikes.

Mechanisms

Over the past decades, considerable emphasis has been placed on elucidating the mechanisms underlying LTP and LTD; similar efforts are currently focused on understanding the mechanisms underlying STDP. Two critical features of STDP must be accounted for at the mechanistic level:

- Order.* How can a synapse detect differences of a few milliseconds regarding the temporal order of presynaptic and postsynaptic spikes, and account for the sharp discontinuity observed at approximately 0 ms ISIs?
- Interval.* Independently of the issue of temporal order, what are the mechanisms that allow synapses to be sensitive to the pre→post and post→pre intervals? Specifically, why does a long positive (or negative) ISI produce little LTP (or LTD), while a short interval produce stronger LTP (or LTD)?

The mechanisms responsible for the interval sensitivity of the LTP component of STDP are generally accepted as being the same as those underlying associative LTP. Specifically, the *N*-methyl-D-aspartate (NMDA) receptors function as coincidence detectors of pre- and postsynaptic activity. A presynaptic spike

results in the release of glutamate, which binds to the NMDA receptor. Subsequent depolarization caused by a postsynaptic spike produces a voltage-dependent extrusion of the Mg^{2+} ion that impedes Ca^{2+} influx at rest. Only when both of these events occur in close temporal proximity will the NMDA channels allow the critical influx of Ca^{2+} . Since glutamate can remain bound to the NMDA receptor for at least tens of milliseconds, if the postsynaptic spike occurs shortly after the presynaptic event, glutamate will still be bound and Ca^{2+} influx will ensue. Thus, it appears that the binding kinetics of the NMDA receptor can account for the timing of the LTP window of STDP. Specifically, at large positive ISIs, little or no glutamate will remain bound to the postsynaptic NMDA receptor resulting in little or no LTP; however, at short intervals, maximal glutamate will be bound, and high levels of Ca^{2+} influx will be achieved, thus inducing maximal LTP. Consistently, there is robust experimental data showing that the blockade of NMDA receptors blocks the LTP component of STDP. For these reasons, the properties of the NMDA receptor likely underlie both the order and interval sensitivity components of STDP potentiation.

It is not immediately clear how the NMDA receptors could account for both the interval and order sensitivity of the LTD window of STDP. If the postsynaptic neuron fires before the presynaptic one, the membrane of the postsynaptic cell should have returned to close to its resting potential before glutamate is released from the presynaptic terminal (particularly for long negative ISIs); thus, the released glutamate should be ineffective in leading to Ca^{2+} influx. It could be argued that a small degree of Ca^{2+} influx occurs in response to a presynaptic action potential even when it occurs after a postsynaptic spike, and that this is sufficient for the induction of LTD. This argument, however, leads to a scenario in which presynaptic stimulation by itself could induce LTD (which is generally not the case).

Conflicting results have been reported regarding the ability of NMDA antagonists to block the LTD component of STDP; however, at least in some preparations, it seems clear that postsynaptic NMDA receptors are not involved in the induction of LTD in response to post→pre pairings. If NMDA receptors are not necessary for detecting the order and interval of negative ISIs, a second coincidence detector would be required, that is, the presence of a postsynaptic followed by a presynaptic spike must be detected by another biochemical pathway that triggers the induction of LTD. This two-coincidence detector model of STDP assumes the presence of a second biochemical locus that is capable of detecting the order and interval of post→pre spikes. One candidate mechanism

for the second coincidence detector is the metabotropic glutamate receptor pathway. In this model, post→pre spiking leads to a low-level Ca^{2+} rise entering through voltage-dependent Ca^{2+} channels (VDCCs) that would prime the activation of the G-protein-mediated cascade, which would in turn be triggered by the presynaptic action potential via metabotropic glutamate receptors.

Computational Relevance and Correlates of STDP *In Vivo*

Competition

In general, computational models of cortical plasticity require two critical components: (1) an associative form of synaptic plasticity that allows correlated inputs to be strengthened and (2) competition, which is required to prevent neurons from responding to multiple sets of correlated patterns (stimuli). In contrast to other models, it has been proposed that STDP may be able to satisfy both these conditions with a single learning rule.

In its simplest sense, in STDP, competition arises between synapses that fire before and after a postsynaptic spike. Synapses from presynaptic neurons that fire before the postsynaptic action potential will be strengthened and take control of the postsynaptic behavior, while the synapses from neurons that fire later will be weakened. A competitive role for STDP predicts that the area of the LTD window should be larger than that of LTP. As mentioned above, this insures that in response to random background activity the net synaptic change is negative. While STDP can clearly implement competition between synapses, it should be stressed that the competition is dependent on the temporal relationship between the stimuli, that is, for different sets of correlated inputs to compete they must occur in close temporal proximity. If the two stimuli are separated by an interval well outside the STDP window, there can be no interaction (and thus no competition) between stimuli over these time frames (note that LTD produced by spontaneous activity would be common to both stimuli). Thus, while STDP does provide a potential mechanism for competition, it does not by itself provide a universal one.

Computational Relevance and Neural Correlates of STDP *In Vivo*

In vitro STDP is generally studied by directly eliciting action potentials in the pre- and postsynaptic neurons. However, a number of studies have examined the putative *in vivo* correlates of STDP in the context of external stimuli. The order sensitivity of STDP

predicts that if two stimuli, A and B, are reliably presented in the order A→B and in close temporal proximity, a receptive field asymmetry should develop. Specifically, responses to A should increase and those to B decrease. Indeed, several experimental studies have measured stimulus-induced shifts in receptive fields in response to exposure to ordered stimuli. These include experiments in which the stimuli A and B corresponded to orientation of bars of light, visual position, or spatial receptive (i.e., the receptive fields of hippocampal place cells). Taken together, these results support the notion that STDP operates *in vivo*, and plays an important role in shaping neural responses.

While STDP likely contributes to the order-sensitive shifts in receptive field properties, it does not generate order selectivity. In the above example, consistent pairing of stimuli A→B results in strengthening of synapses driven by stimulus A and weakening of those from B, but nevertheless the neuronal response to A→B should be approximately equal to the response to B→A. Thus, the order sensitivity of STDP does not by itself generate order-selective neuronal responses.

Experience-dependent changes in the receptive fields of cortical neurons have also been interpreted in the context of STDP. For example, plasticity can be induced by cutting all but one whisker of the mystacial pad of a rat. In the barrel of a cut whisker, two changes are observed: a decreased response to the normally dominant whisker and an increased response to the spared whisker. It has been proposed that STDP can contribute to this phenomenon. Specifically, the decreased response of layer II/III pyramidal neurons to the previously dominant whisker appears to be due to LTD of synapses from layer IV. It has been shown that this LTD is consistent with STDP and the order of activation of these neurons. Specifically, in the deprived barrel, L-II/III pyramidal neurons may fire before the L-IV neurons, resulting in LTD.

Timing

STDP is highly sensitive to the interval between the pre- and postsynaptic spikes; however, the role of STDP in generating timed responses remains unclear. If a presynaptic spike consistently occurs 25 ms before the postsynaptic spike, the synaptic strength between the two neurons will increase. Assuming that this potentiation can influence cell firing, the postsynaptic neuron will spike at progressively shorter latencies, until the synaptic strength saturates or the interval decreases toward the monosynaptic delay latency. Thus, the original temporal interval used in the training is not effectively reproduced. As a result, STDP

maintains the order of activation and favors early responses, but the patterns produced after STDP do not capture the temporal structure of the training stimuli. Nevertheless, STDP could take part in setting up specific spatiotemporal patterns of network activity that could play a role in temporal processing.

See also: Adult Cortical Plasticity; Developmental Synaptic Plasticity: LTP, LTD, and Synapse Formation and Elimination; Hebbian Plasticity; Long-Term Depression: Cerebellum; Long-Term Depression (LTD): Metabotropic Glutamate Receptor (mGluR) and NMDAR-Dependent Forms; Long-Term Potentiation (LTP): NMDA Receptor Role; Long-Term Potentiation and Long-Term Depression in Experience-Dependent Plasticity; Long-Term Potentiation (LTP); Metabotropic Glutamate Receptors (mGluRs): Functions; Spike-Timing-Dependent Plasticity Models; Synaptic Plasticity: Learning and Memory in Normal Aging.

Further Reading

- Abbott LF and Nelson SB (2000) Synaptic plasticity: Taming the beast. *Nature Neuroscience* 3: 1178–1183.
- Bender VA, Bender KJ, Brasier DJ, and Feldman DE (2006) Two coincidence detectors for spike timing-dependent plasticity in somatosensory cortex. *Journal of Neuroscience* 26: 4166–4177.
- Bi G-Q and Poo M-M (1998) Synaptic modifications in cultured hippocampal neurons: Dependence on spike timing, synaptic strength, and postsynaptic cell type. *Journal of Neuroscience* 18: 10464–10472.
- Bi G-Q and Poo M-M (2000) Synaptic modification by correlated activity: Hebb's postulate revisited. *Annual Review of Neuroscience* 24: 139–166 (Review).
- Dan Y and Poo MM (2004) Spike timing-dependent plasticity of neural circuits. *Neuron* 44: 23–30.
- Debanne D, Gähwiler BH, and Thompson SM (1994) Asynchronous presynaptic and postsynaptic activity induces associative long-term depression in area CA1 of the rat hippocampus *in vitro*. *Proceedings of the National Academy of Sciences of the United States of America* 91: 1148–1152.
- Feldman DE (2000) Timing-based LTP and LTD at vertical inputs to layer II/III pyramidal cells in rat barrel cortex. *Neuron* 27: 45–56.
- Karmarkar UR and Buonomano DV (2002) A model of spike-timing dependent plasticity: One or two coincidence detectors? *Journal of Neurophysiology* 88: 507–513.
- Levy WB and Steward O (1983) Temporal contiguity requirements for long-term associative potentiation/depression in the hippocampus. *Neuroscience* 8: 791–797.
- Markram H, Lubke J, Frotscher M, and Sakmann B (1997) Regulation of synaptic efficacy by coincidence of postsynaptic APs and EPSPs. *Science* 275: 213–215.
- Mehta MR, Quirk MC, and Wilson MA (2000) Experience-dependent asymmetric shape of hippocampal receptive fields. *Neuron* 25: 707–715.
- Song S, Miller KD, and Abbott LF (2000) Competitive Hebbian learning through spike-timing-dependent synaptic plasticity. *Nature Neuroscience* 9: 919–926.
- Yao H and Dan Y (2001) Stimulus timing-dependent plasticity in cortical processing of orientation. *Neuron* 2: 315–323.
- Zhang LI, Huizhong WT, Holt CE, and Poo M-M (1998) A critical window for cooperation and competition among developing retinotectal synapses. *Nature* 395: 37–44.

APPENDIX B

Neural Dynamics in Organotypic Cortical Networks



Summary

A large body of data has focused on the transmission of information from one neuron to another; however, little is known about the flow of information through polysynaptic chains of recurrently connected neurons. Commonly, studies of neuronal dynamics have been performed in cultures that grow on multi-electrode arrays which, by definition, do not maintain the physiological network structure (Beggs and Plenz, 2003; Eytan et al., 2003; van Pelt et al., 2005). Additionally, these types of studies usually rely on the recording of the average activity of many cells (local field potentials) and often analyze activity patterns in the scale of seconds to hours overlooking events that may occur at a finer and cortically relevant time scale.

Within the cortical network in vitro model systems, organotypic slices growing on top of a porous membrane (Stoppini et al., 1991) provide a valid representation of the cortical in vivo system, as they preserve most of the native anatomical cortical structure in a thick 3D organization (which dissociated or roller tube neuronal cultures do not) and develop endogenous spontaneous activity (acute slices show little or no spontaneous activity) (Johnson and Buonomano, 2007). It has been shown that in this system the development of the cortical anatomy, structure and physiology resembles satisfactorily the in vivo development (Gahwiler et al., 1997; De Simoni et al., 2003).

Here, it was attempted to characterize the propagation of activity in cortical circuits in vitro, by using multi-electrode extracellular recordings to simultaneously record from tens of cells individually. While the preliminary data seemed promising, most often the slices would develop "bursts" of synchronized neuronal activity which rendered the sorting of individual units impractical. So far there may still be no reports in the literature that analyze the dynamics of multiple single-units in organotypic slices.

The global activity patterns that these organotypic cultures develop were characterized, and it is shown that the structure of these patterns is not hardwired as they can be modified developmentally through pharmacological manipulations.

Methods

Organotypic slice preparation

Organotypic slices were prepared using the interface method (Stoppini et al., 1991; Buonomano, 2003). Sprague Dawley rats (7 d of age) were anesthetized with isoflurane and decapitated. The brain was removed and placed in chilled cutting media. Coronal slices (400 μm thickness) containing primary somatosensory or auditory cortex were cut using a vibratome and placed on Millipore (Billerica, MA) filters (MillicellCM) with 1 ml of culture media. Culture media was changed 1 and 24 h after cutting and every 2–3 d thereafter. Cutting media consisted of Eagle's minimum essential medium (EMEM; catalog number 15-010; MediaTech, Herndon, VA) plus 3 mM MgCl_2 , 10 mM glucose, 25 mM HEPES, and 10 mM Tris base. Culture media consisted of EMEM plus 4 mM glutamine, 0.6 mM CaCl_2 , 1.85 mM MgSO_4 , 30 mM glucose, 30 mM HEPES, 0.5 mM ascorbic acid, 20% horse serum, 10 U/L penicillin, and 10 g/L streptomycin. In some experiments the total Mg^{2+} concentration in the culture media was 10 mM. Slices were incubated in 5% CO_2 at 35°C and used while 3-week old.

Electrophysiology

Experiments were performed in “culture media artificial CSF” (CM-ACSF) composed of (in mM) 125 NaCl, 5.1 KCl, 2.6 MgSO_4 , 26.1 NaHCO_3 , 1 NaH_2PO_4 , 25 glucose, and 2.6 CaCl_2 . CM-ACSF matches the concentration of the ions in the culture media and differs from “classical” ACSF in KCl (2.5 mM) and MgSO_4 (2 mM) (Stoppini et al., 1991). The internal solution for whole-cell recordings contained (in mM) 100 K-gluconate, 20 KCl, 4 ATP-Mg, 10 phospho-creatine, 0.03 GTP-Na, and 10 HEPES and was adjusted to pH 7.3

and 300 mOsm. Intracellular recordings were made from regular-spiking, supragranular pyramidal neurons (Dong and Buonomano, 2005) located ~500 μm from the external surface of the cortex using infrared differential interference contrast visualization. Intracellular data was acquired at 10 kHz and low passed at 1.5 kHz.

Extracellular activity was acquired with a 10-channel Dagan Ex-1000 amplifier (Dagan Co, MN), with a FHC 4-electrode matrix (platinum-iridium, spacing between electrodes 250 μm FHC, Bowdoin, ME) and wires in the stereotrode configuration (wires twisted in pairs). By bundling the electrodes in pairs, each wire in a given pair will record similar, but slightly different, deviations in the local potential caused by neuronal activity. The small differences result in a different waveform recorded by each electrode in the stereotrode, and this effect is used to increase the accuracy of the spike sorting. Stereotrodes were made by twisting two platinum/iridium wires (Kanthal, diameter: 0.0007"; coating: PAC) and evenly heating them with a heat gun, until the coating is partially melted which confers some stiffness, and then fitted into a polyimide tube (Phelps Dodge, ID: 0.0044", OD: 0.0060"). One of the ends of the bundle was then slightly burned, to fully remove the PAC coating, and each individual wire was soldered to the headstage adaptor. The other end of the bundle, which will penetrate the slice, was cut at an angle with a sharp scissor and placed in gold plating solution (Sifco Selectron), where current pulses were applied in order to obtain a final impedance of approximately 200 Kohm through each of the wires. The bundle was finally mounted in a holder and connected to the amplifier headstage. The signal was amplified 10.000x, sampled at 10-25kHz and bandpassed between 300Hz – 3kHz to allow for the isolation of the single unit responses. The data acquisition and analysis were done with custom-written MATLAB software, except for the spike sorting procedure where we used MClust (MClust-3.3, A. D. Redish et al.) to cluster putative neuronal single units.

When necessary, slices were stimulated with bipolar electrodes (2-electrode matrix, platinum-iridium, 150 μm spacing, FHC, Bowdoin, ME) placed in LII/III-IV and single bipolar ± 100 μs pulses (up to 150 μA) were applied every 10-20 s to elicit synaptic responses.

Quantification of spontaneous activity

For each slice, a minimum of 5 min of spontaneous activity was recorded. Spontaneous events were defined as those in which the 10 point moving average of the sum of the voltage potential of the 10 recording electrodes crossed a threshold of 30 μV . Extracellular events separated by less than 20 ms were merged.



Results

Multi-Unit Extracellular Recordings

A single extracellular electrode can potentially record the activity of many (up to ~10) different neurons and most of the times it is desirable to cluster the spike waveforms in an attempt to sort the spikes that belong to each neuron. Essentially, spike sorting groups the spike waveforms by similarity and the underlying assumption is that similar waveforms should relate to the same neuron.

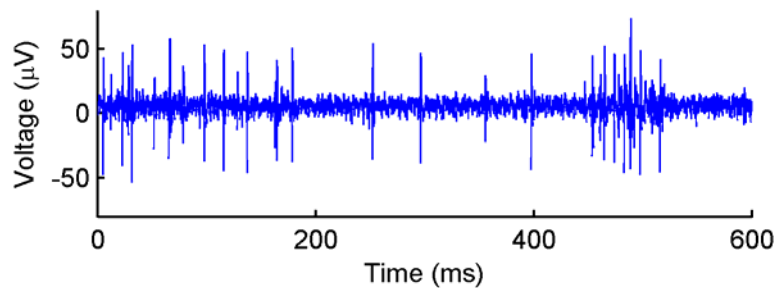


Figure 1 – Example of an extracellular recording (one electrode only).

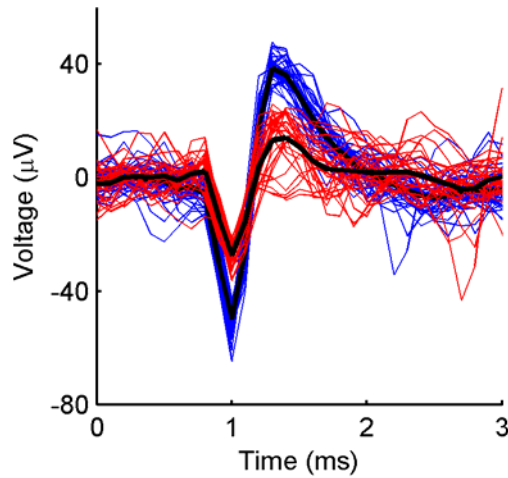


Figure 2 – Sample waveforms from the trace above, which were colored according to similarity.

In reality it is possible that similar waveforms belong to different neurons, if they are approximately equidistant from the recording electrode. The accuracy of detection can thus be improved by using bundles of two electrodes (stereotrodes) and performing the unit identification taking in consideration the waveforms recorded by both electrodes simultaneously. Figure 3 depicts the clustering results of one such sorting procedure where 4 different putative units were identified by the clustering algorithm (see Methods).

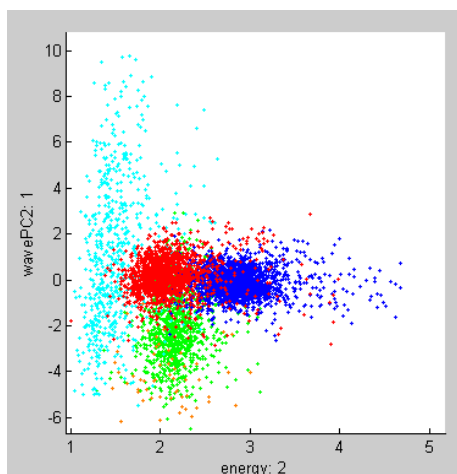


Figure 3 – Clustering results from waveforms recorded from 2 electrodes in the stereotrode configuration. Each point depicts a pair of waveforms (one from each electrode) and the different colors depict putative individual units.

Once the units have been isolated it is possible to know when each neuron fired action potentials, and this revealed very diverse neuronal behavior in response to extracellular stimulation (Figure 4).

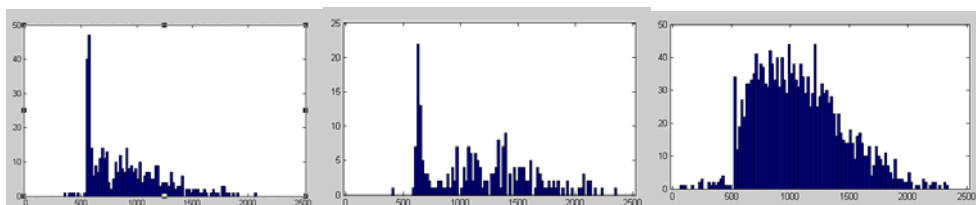


Figure 4 – Diversity of neuronal responses. Sample histograms showing the cumulative activity of 3 putatively different units following a stimulation pulse (at 500 ms). The unit on the left fires preferentially ~30-50 ms after the pulse and the unit on the center ~130 ms after the pulse. The unit on the right has a much higher firing rate but does not show any clear peak (x-axis: Time (ms), bin size: 20 ms; y-axis: Count).

One of the questions that could be asked is whether neuronal activity propagates randomly through these recurrent neuronal networks or whether there is some degree of re-activation of the polysynaptic pathways. Figure 5 depicts a cross-correlation of the spike times of the first two units shown in Figure 4. This data suggests that unit 2 tends to fire 70 ms after unit 1, even though both cells are spatially close to each other (both located in the vicinity of the extracellular recording electrode).

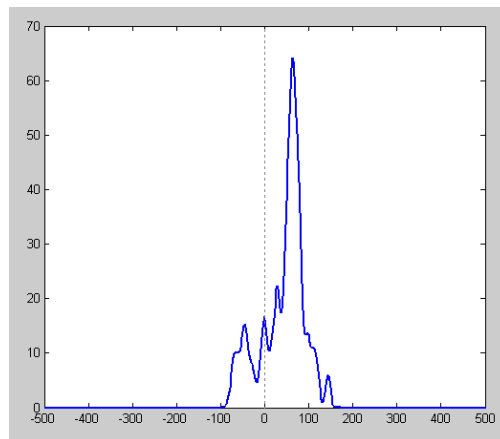


Figure 5 – Cross-correlation of the spike times from two first units shown above. There is a clear peak at ~70ms which suggests that unit 2 tends to fire 70 ms after unit 1.

Dynamics of Organotypic Networks: Synchronized Bursts

‘Active’ cortical processing is believed to rely on desynchronized, sparse and transient network activity (Durstewitz and Deco, 2008) and the initial expectations were to record extracellularly the activity of multiple individual neurons. Instead, it was observed that organotypic slices develop mostly long periods of silent network activity followed by short episodes when there is a “burst” of correlated activity across the whole slice (lasting from tens to hundreds milliseconds) (Figure 6).

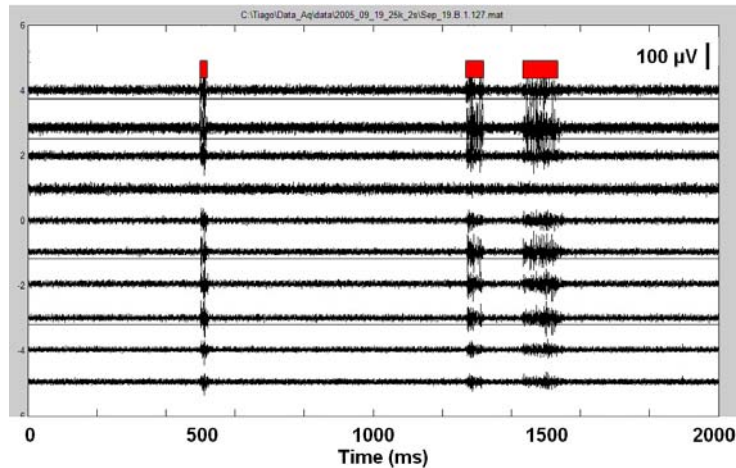


Figure 6 – Example of a 2-second extracellular multi-unit recording. The four uppermost voltage traces correspond to activity recorded using single electrodes from the FHC matrix. The six lowermost traces reflect activity recorded from the electrodes bundled in pairs (stereotrodes). Despite the fact that the electrodes were positioned in different cortical locations, the neuronal activity arises and terminates nearly simultaneously in 9 out of the 10 electrodes. The red boxes on top indicate the periods of what was qualified as a “burst” of activity (see below).

This highly synchronized activity profile renders the task of sorting spikes of single cells unfeasible because if multiple neurons are firing action potentials *simultaneously* the effects in the extracellular potential will *summate* which renders the classification of individual units unpractical (Figure 7).

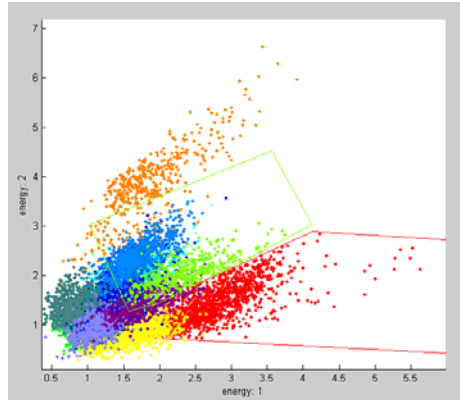


Figure 7 – Example of the MClust cluster cutting window. The recorded waveforms form a continuum and the isolation of individual cluster is ambiguous..

Nevertheless, neuronal activity clusters into short lived, well defined periods, suggesting that there are rules in place that shape cortical networks to respond in such manner. Furthermore, it could be insightful to understand why and how the network spontaneously evolves onto this burst mode in the incubator as, given that the network is devoid of external inputs, it might unravel the “default” intrinsic rules that regulate cortical activity development. Hence, these activity patterns were characterized and quantified.

A “burst” was defined as the period during which the summation of neuronal activity across all the electrodes is above a pre-determined threshold (Methods). Once bursts were detected the following properties were quantified:

- Burst Duration – the time elapsed between the onset of a burst and its end;
- Inter-burst Interval – the period between the end of a burst and the onset of the next one;

- Percentage ON Time – the relative time the cortical network spends in the burst mode;
- Burst Rate – the number of bursts per unit time;

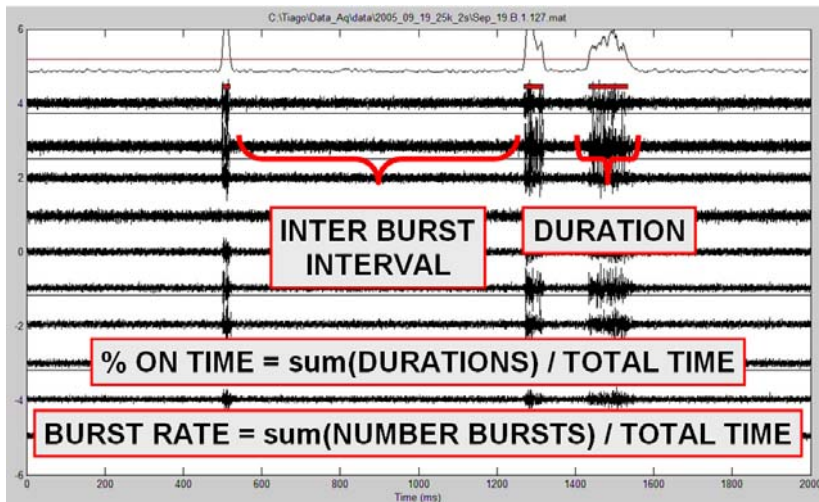


Figure 8 – Same data as before, displaying the properties that were quantified for each slice. The top line depicts a moving average of the sum of the 10 channels.

These patterns of activity seem to be independent of the recording electrode position and occur slice wide. The results of these experiments are summarized in Figure 9.

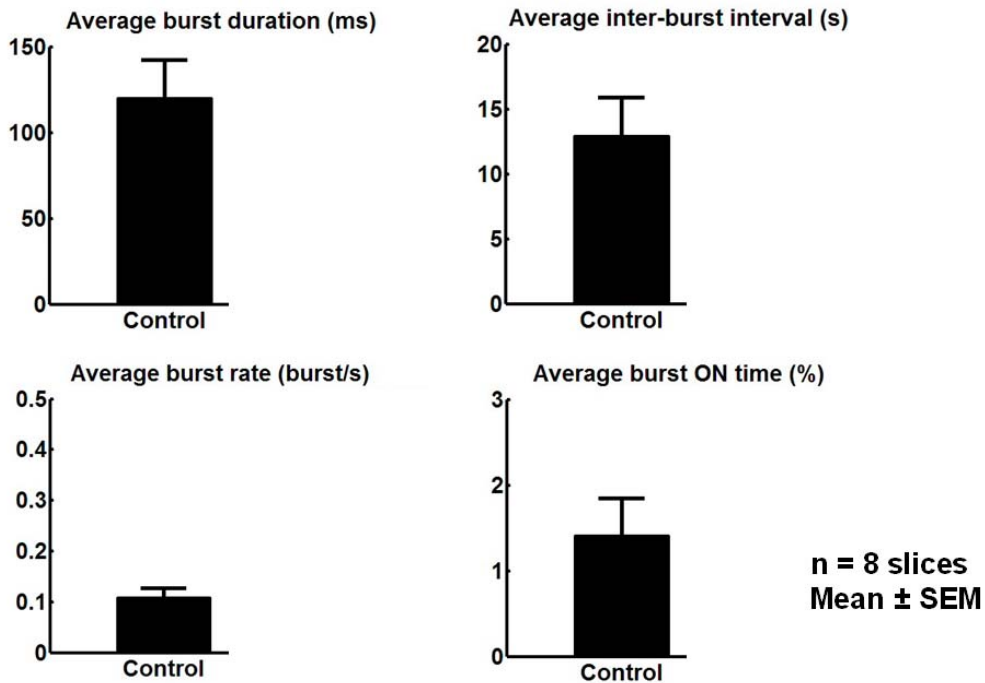


Figure 9 – Group data from slices cultured in standard conditions.

These results suggest that in an organotypic slice, deprived of any external input, the cortical network spontaneously evolves into a mode in which there are bursts of highly synchronized activity that last approximately about 120 ms, re-occurring every 10-15 s. Next, we asked the question: is it possible to perturb the development of these bursts?

Pharmacological Perturbation of the Development of Cortical Bursts

Several forms of long-term synaptic plasticity depend on calcium entry through glutamatergic NMDA channels (Malenka and Bear, 2004; Caporale and Dan, 2008). However, when glutamate binds and the channel opens there is still a magnesium ion blocking the pore, the extrusion of which is voltage

sensitive and required for calcium to flow into the cell (Nowak et al., 1984). Magnesium is an ion that is present in the culture media under normal conditions (2.6 mM) but increasing its concentration should interfere with the normal functioning of NMDA channels. Hence, in an attempt to perturb the development of the neural dynamics, through putative perturbations of long-term synaptic plasticity, the magnesium concentration in the culture media was increased to a total of 10 mM for two days prior the recording session.

In agreement with the hypothesis above, significant changes in the profile of the network activity were observed (Figure 10). High magnesium in the culture medium seems to lead to a “breakdown” of the bursts: neuronal activity gets shorter in duration but more frequent. Interestingly, however, it was not possible to find statistically significant changes in the average burst ON time, even though there is a visible trend towards a difference. The existence of clear changes in the bursts characteristics paralleled by an overall maintenance of the total active time may suggest the existence of homeostatic mechanisms that ensure that the overall network activity is kept within approximately constant levels.

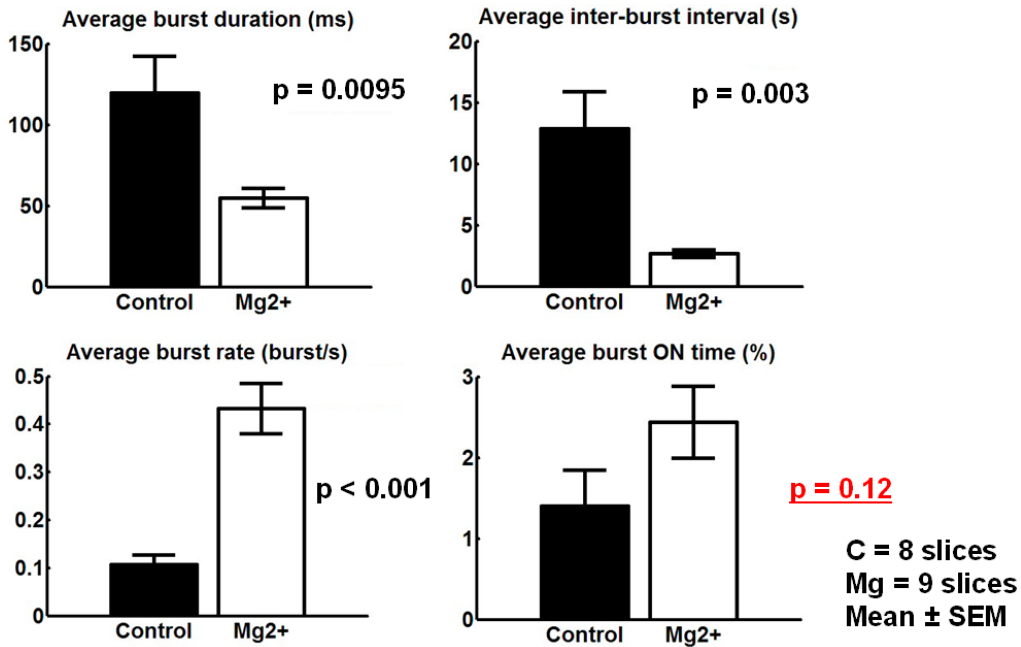


Figure 10 – Comparison of the burst properties between slices grown under standard culture conditions and cultures grown in high Mg²⁺ for two days prior recording. The black bars are the same as presented in Figure 9. p-values are indicated (t-test).

While more experiments would have to be performed to elucidate the mechanisms responsible for these changes, these results establish that the global patterns of activity in cortical networks are modifiable.

The experiments above analyzed exclusively extracellular data but, what is the neurons' subthreshold behavior, during bursts and between bursts?

Intracellular Recordings in Organotypic Slices

Presented below are isolated and non-quantitated examples of some phenomena observed in these slices.

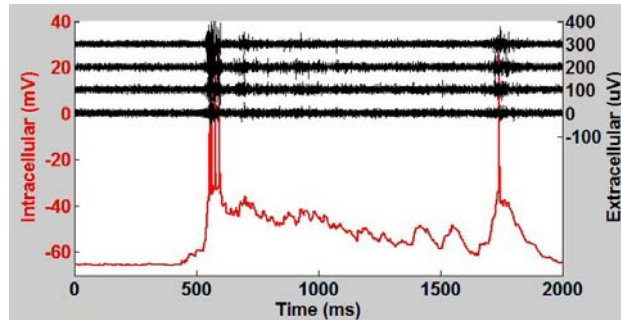


Figure 11 – Simultaneous extracellular and intracellular recordings from a slice grown in control conditions. During the extracellular bursts the neuron's resting membrane potential is depolarized and fires action potentials. Between bursts there are no action potentials, even though the membrane is depolarized for hundreds of milliseconds.

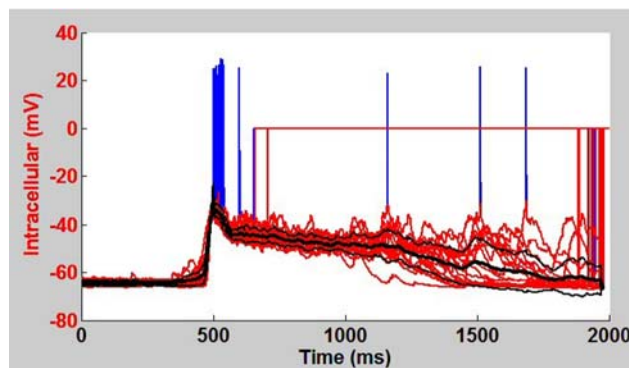


Figure 12 – The same intracellular recording as above but with several overlapped intracellular voltage traces. The traces were aligned at the rising phase of the PSP at -45 mV. The black traces depict mean (thick trace) \pm SEM (thin traces) of the subthreshold responses (colored red). This example suggests that the overall subthreshold profile may repeat multiple times.

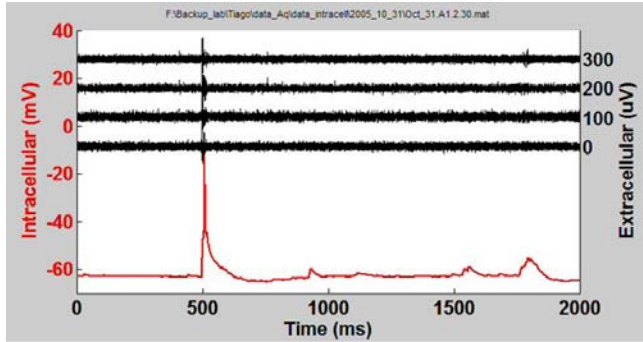


Figure 13 – Same procedure as in Figure 11 but from a slice cultured in 10 mM magnesium, for two days prior to recording. The extracellular bursts are shorter in duration and the intracellular response is remarkably shorter too.

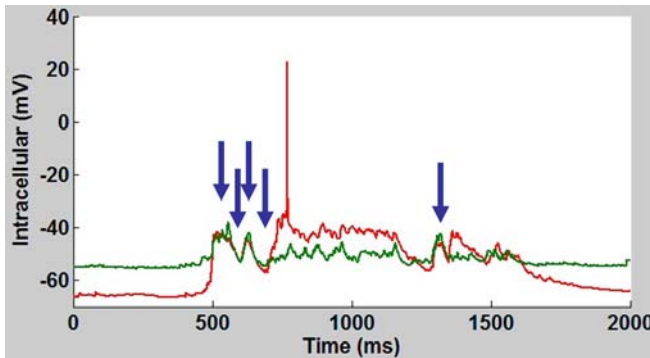


Figure 14 – Simultaneous intracellular paired recordings from two cells in a control cultured slice. The arrows point to events in the voltage trace that appear to have similar onset times, which may suggest some degree of correlation of subthreshold responses in different cells (Buonomano 2000).

Discussion

The original goal of simultaneously recording from tens of multiple single units was not achieved satisfactorily due to the development of synchronized extracellular burst activity, which does not allow the resolution of individual spike waveforms. In principle it could be possible to increase the impedance of the recording electrodes to record from less neurons, but given that active cortical processing may rely on desynchronized activity this goal was not pursued.

Nevertheless, the work presented here characterized the global patterns of cortical activity developed in organotypic slices. The results shown with the manipulation of the culture media (increased Mg^{2+}) are a proof of principle that some statistics of spontaneous activity patterns are plastic and can be modified. It is interesting that the overall level of activity was not altered significantly, possibly supporting the existence of active mechanisms of homeostatic plasticity. However, while the present work showed how the composition of the culture media influences the development of spontaneous activity patterns, the mechanisms through which it occurs are still unknown. If these results are to be pursued further it would be important to directly determine the role of NMDA receptors, if any. Their involvement is speculative at the present, but they could be a likely candidate given their dependence on magnesium.

As a final remark, it is intriguing that while the organotypic protocol is well established, the ionic composition of the culture media is different from 'standard' ACSF (and it has just been shown how the media composition is critical for development). It could be worth to culture organotypic slices in media that mimics the physiological cerebro-spinal fluid and just see if the development is different from the current conditions. In addition, it is known that chronic stimulation of organotypic slices decreases overall levels of

spontaneous activity (Johnson and Buonomano, 2007), and that random electrical stimulation of cortical networks results in overall desynchronization of neuronal activity (Wagenaar et al., 2005). Possibly, a physiological culture media coupled with external stimulation could yield desynchronized sparse activity that would better mimic active cortical processing, allowing extracellular recordings to resolve tens of single units and making possible an analysis of cortical processing and information propagation at the level of many single cells.

REFERENCES

- Abbott LF, Regehr WG (2004) Synaptic computation. *Nature* 431:796-803.
- Abbott LF, Varela JA, Sen K, Nelson SB (1997) Synaptic depression and cortical gain control. *Science* 275:220-224.
- Abraham WC, Gustafsson B, Wigstrom H (1987) Long-term potentiation involves enhanced synaptic excitation relative to synaptic inhibition in guinea-pig hippocampus. *J Physiol* 394:367-380.
- Andersen P, Sundberg SH, Sveen O, Swann JW, Wigstrom H (1980) Possible mechanisms for long-lasting potentiation of synaptic transmission in hippocampal slices from guinea-pigs. *J Physiol* 302:463-482.
- Atzori M, Lei S, Evans DI, Kanold PO, Phillips-Tansey E, McIntyre O, McBain CJ (2001) Differential synaptic processing separates stationary from transient inputs to the auditory cortex. *Nat Neurosci* 4:1230-1237.
- Bagal AA, Kao JP, Tang CM, Thompson SM (2005) Long-term potentiation of exogenous glutamate responses at single dendritic spines. *Proc Natl Acad Sci U S A* 102:14434-14439.
- Barrionuevo G, Brown TH (1983) Associative long-term potentiation in hippocampal slices. *Proc Natl Acad Sci U S A* 80:7347-7351.
- Beaulieu C, Kisvarday Z, Somogyi P, Cynader M, Cowey A (1992) Quantitative distribution of GABA-immunopositive and -immunonegative neurons and synapses in the monkey striate cortex (area 17). *Cereb Cortex* 2:295-309.
- Beggs JM, Plenz D (2003) Neuronal avalanches in neocortical circuits. *J Neurosci* 23:11167-11177.
- Bender VA, Bender KJ, Brasier DJ, Feldman DE (2006) Two coincidence detectors for spike timing-dependent plasticity in somatosensory cortex. *J Neurosci* 26:4166-4177.
- Bi GQ, Poo MM (1998) Synaptic modifications in cultured hippocampal neurons: dependence on spike timing, synaptic strength, and postsynaptic cell type. *J Neurosci* 18:10464-10472.
- Bienenstock EL, Cooper LN, Munro PW (1982) Theory for the development of neuron selectivity: orientation specificity and binocular interaction in visual cortex. *J Neurosci* 2:32-48.

-
- Bliss TV, Gardner-Medwin AR (1973) Long-lasting potentiation of synaptic transmission in the dentate area of the unanaesthetized rabbit following stimulation of the perforant path. *J Physiol* 232:357-374.
- Bliss TV, Lomo T (1973) Long-lasting potentiation of synaptic transmission in the dentate area of the anaesthetized rabbit following stimulation of the perforant path. *J Physiol* 232:331-356.
- Bliss TV, Goddard GV, Riives M (1983) Reduction of long-term potentiation in the dentate gyrus of the rat following selective depletion of monoamines. *J Physiol* 334:475-491.
- Brock LG, Coombs JS, Eccles JC (1952a) The recording of potentials from motoneurons with an intracellular electrode. *J Physiol* 117:431-460.
- Brock LG, Coombs JS, Eccles JC (1952b) The nature of the monosynaptic excitatory and inhibitory processes in the spinal cord. *Proc R Soc Lond B Biol Sci* 140:170-176.
- Brown TH, Fricke RA, Perkel DH (1981) Passive electrical constants in three classes of hippocampal neurons. *J Neurophysiol* 46:812-827.
- Buonomano DV (1999) Distinct functional types of associative long-term potentiation in neocortical and hippocampal pyramidal neurons. *J Neurosci* 19:6748-6754.
- Buonomano DV (2000) Decoding temporal information: A model based on short-term synaptic plasticity. *J Neurosci* 20:1129-1141.
- Buonomano DV (2003) Timing of neural responses in cortical organotypic slices. *Proc Natl Acad Sci U S A* 100:4897-4902.
- Buonomano DV, Merzenich MM (1995) Temporal information transformed into a spatial code by a neural network with realistic properties. *Science* 267:1028-1030.
- Buonomano DV, Merzenich MM (1998a) Net interaction between different forms of short-term synaptic plasticity and slow-IPSPs in the hippocampus and auditory cortex. *J Neurophysiol* 80:1765-1774.
- Buonomano DV, Merzenich MM (1998b) Cortical plasticity: from synapses to maps. *Annu Rev Neurosci* 21:149-186.
- Buonomano DV, Hickmott PW, Merzenich MM (1997) Context-sensitive synaptic plasticity and temporal-to-spatial transformations in hippocampal slices. *Proc Natl Acad Sci U S A* 94:10403-10408.

- Burnashev N, Rozov A (2005) Presynaptic Ca²⁺ dynamics, Ca²⁺ buffers and synaptic efficacy. *Cell Calcium* 37:489-495.
- Byrne JH (2003) *Learning & Memory*, 2nd Edition: Thomson Gale.
- Campanac E, Debanne D (2008) Spike timing-dependent plasticity: a learning rule for dendritic integration in rat CA1 pyramidal neurons. *J Physiol* 586:779-793.
- Caporale N, Dan Y (2008) Spike timing-dependent plasticity: a Hebbian learning rule. *Annu Rev Neurosci* 31:25-46.
- Cardin JA, Palmer LA, Contreras D (2008) Cellular mechanisms underlying stimulus-dependent gain modulation in primary visual cortex neurons in vivo. *Neuron* 59:150-160.
- Chance FS, Nelson SB, Abbott LF (1998) Synaptic depression and the temporal response characteristics of V1 cells. *J Neurosci* 18:4785-4799.
- Chance FS, Abbott LF, Reyes AD (2002) Gain modulation from background synaptic input. *Neuron* 35:773-782.
- Chavez-Noriega LE, Halliwell JV, Bliss TV (1990) A decrease in firing threshold observed after induction of the EPSP-spike (E-S) component of long-term potentiation in rat hippocampal slices. *Exp Brain Res* 79:633-641.
- Cheetham CE, Hammond MS, Edwards CE, Finnerty GT (2007) Sensory experience alters cortical connectivity and synaptic function site specifically. *J Neurosci* 27:3456-3465.
- Chevaleyre V, Castillo PE (2003) Heterosynaptic LTD of hippocampal GABAergic synapses: a novel role of endocannabinoids in regulating excitability. *Neuron* 38:461-472.
- Costa RM, Federov NB, Kogan JH, Murphy GG, Stern J, Ohno M, Kucherlapati R, Jacks T, Silva AJ (2002) Mechanism for the learning deficits in a mouse model of neurofibromatosis type 1. *Nature* 415:526-530.
- Czerner TB (2001) *What Makes You Tick? The Brain in Plain English*. New York: John Wiley & Sons, Inc.
- Damásio AR (1994) *Descartes' Error: Emotion, Reason, and the Human Brain*. New York: Penguin Putnam.

-
- Daoudal G, Debanne D (2003) Long-term plasticity of intrinsic excitability: learning rules and mechanisms. *Learn Mem* 10:456-465.
- De Simoni A, Griesinger CB, Edwards FA (2003) Development of rat CA1 neurones in acute versus organotypic slices: role of experience in synaptic morphology and activity. *J Physiol* 550:135-147.
- Dean I, Harper NS, McAlpine D (2005) Neural population coding of sound level adapts to stimulus statistics. *Nat Neurosci* 8:1684-1689.
- Debanne D, Gähwiler BH, Thompson SM (1994) Asynchronous pre- and postsynaptic activity induces associative long-term depression in area CA1 of the rat hippocampus in vitro. *Proc Natl Acad Sci U S A* 91:1148-1152.
- Debanne D, Guerineau NC, Gähwiler BH, Thompson SM (1996) Paired-pulse facilitation and depression at unitary synapses in rat hippocampus: quantal fluctuation affects subsequent release. *J Physiol* 491 (Pt 1):163-176.
- Destexhe A, Pare D (1999) Impact of network activity on the integrative properties of neocortical pyramidal neurons in vivo. *J Neurophysiol* 81:1531-1547.
- Destexhe A, Mainen ZF, Sejnowski TJ (1994) An efficient method for computing synaptic conductances based on a kinetic model of receptor binding. *Neural Comput* 6:14:18.
- DeWeese MR, Wehr M, Zador AM (2003) Binary spiking in auditory cortex. *J Neurosci* 23:7940-7949.
- Dittman JS, Kreitzer AC, Regehr WG (2000) Interplay between facilitation, depression, and residual calcium at three presynaptic terminals. *J Neurosci* 20:1374-1385.
- Dobrunz LE, Stevens CF (1997) Heterogeneity of release probability, facilitation, and depletion at central synapses. *Neuron* 18:995-1008.
- Dong HW, Buonomano DV (2005) A technique for repeated recordings in cortical organotypic slices. *J Neurosci Methods* 146:69-75.
- Doupe AJ (1997) Song- and order-selective neurons in the songbird anterior forebrain and their emergence during vocal development. *J Neurosci* 17:1147-1167.

- Dudek SM, Bear MF (1992) Homosynaptic long-term depression in area CA1 of hippocampus and effects of N-methyl-D-aspartate receptor blockade. *Proc Natl Acad Sci U S A* 89:4363-4367.
- Durstewitz D, Deco G (2008) Computational significance of transient dynamics in cortical networks. *Eur J Neurosci* 27:217-227.
- Eccles JC, Mac FW (1949) Actions of anti-cholinesterases on endplate potential of frog muscle. *J Neurophysiol* 12:59-80.
- Eccles JC, Katz B, Kuffler SW (1941) Nature of the 'end-plate potential' in curarized muscle. *J Neurophysiol* 5:362-387.
- Eytan D, Brenner N, Marom S (2003) Selective adaptation in networks of cortical neurons. *J Neurosci* 23:9349-9356.
- Foeller E, Celikel T, Feldman DE (2005) Inhibitory sharpening of receptive fields contributes to whisker map plasticity in rat somatosensory cortex. *J Neurophysiol* 94:4387-4400.
- Freund TF, Buzsaki G (1996) Interneurons of the hippocampus. *Hippocampus* 6:347-470.
- Frick A, Magee J, Johnston D (2004) LTP is accompanied by an enhanced local excitability of pyramidal neuron dendrites. *Nat Neurosci* 7:126-135.
- Froemke RC, Merzenich MM, Schreiner CE (2007) A synaptic memory trace for cortical receptive field plasticity. *Nature* 450:425-429.
- Gabernet L, Jadhav SP, Feldman DE, Carandini M, Scanziani M (2005) Somatosensory integration controlled by dynamic thalamocortical feed-forward inhibition. *Neuron* 48:315-327.
- Gahwiler BH, Capogna M, Debanne D, McKinney RA, Thompson SM (1997) Organotypic slice cultures: a technique has come of age. *Trends Neurosci* 20:471-477.
- Gaiarsa JL, Caillard O, Ben-Ari Y (2002) Long-term plasticity at GABAergic and glycinergic synapses: mechanisms and functional significance. *Trends Neurosci* 25:564-570.
- Galarreta M, Hestrin S (1998) Frequency-dependent synaptic depression and the balance of excitation and inhibition in the neocortex. *Nat Neurosci* 1:587-594.

-
- Gingrich KJ, Byrne JH (1985) Simulation of synaptic depression, posttetanic potentiation, and presynaptic facilitation of synaptic potentials from sensory neurons mediating gill-withdrawal reflex in *Aplysia*. *J Neurophysiol* 53:652-669.
- Gupta A, Wang Y, Markram H (2000) Organizing principles for a diversity of GABAergic interneurons and synapses in the neocortex. *Science* 287:273-278.
- Gustafsson B, Wigstrom H, Abraham WC, Huang YY (1987) Long-term potentiation in the hippocampus using depolarizing current pulses as the conditioning stimulus to single volley synaptic potentials. *J Neurosci* 7:774-780.
- Gutig R, Sompolinsky H (2006) The tempotron: a neuron that learns spike timing-based decisions. *Nat Neurosci* 9:420-428.
- Hardingham NR, Hardingham GE, Fox KD, Jack JJ (2007) Presynaptic efficacy directs normalization of synaptic strength in layer 2/3 rat neocortex after paired activity. *J Neurophysiol* 97:2965-2975.
- Hebb DO (1949) *Organization of behavior*. New York: Wiley.
- Hensch TK (2004) Critical period regulation. *Annu Rev Neurosci* 27:549-579.
- Higley MJ, Contreras D (2006) Balanced excitation and inhibition determine spike timing during frequency adaptation. *J Neurosci* 26:448-457.
- Hines ML, Carnevale NT (1997) The NEURON simulation environment. *Neural Comput* 9:1179-1209.
- Hirsch JA, Alonso JM, Reid RC, Martinez LM (1998) Synaptic integration in striate cortical simple cells. *J Neurosci* 18:9517-9528.
- Ho N, Destexhe A (2000) Synaptic background activity enhances the responsiveness of neocortical pyramidal neurons. *J Neurophysiol* 84:1488-1496.
- Houweling AR, Brecht M (2008) Behavioural report of single neuron stimulation in somatosensory cortex. *Nature* 451:65-68.
- Huang YY, Li XC, Kandel ER (1994) cAMP contributes to mossy fiber LTP by initiating both a covalently mediated early phase and macromolecular synthesis-dependent late phase. *Cell* 79:69-79.

- Hung CP, Kreiman G, Poggio T, DiCarlo JJ (2005) Fast readout of object identity from macaque inferior temporal cortex. *Science* 310:863-866.
- Ismailov I, Kalikulov D, Inoue T, Friedlander MJ (2004) The kinetic profile of intracellular calcium predicts long-term potentiation and long-term depression. *J Neurosci* 24:9847-9861.
- Johnson HA, Buonomano DV (2007) Development and plasticity of spontaneous activity and Up states in cortical organotypic slices. *J Neurosci* 27:5915-5925.
- Kairiss EW, Abraham WC, Bilkey DK, Goddard GV (1987) Field potential evidence for long-term potentiation of feed-forward inhibition in the rat dentate gyrus. *Brain Research* 401:87-94.
- Kandel ER, Schwartz JH (1985) *Principles of Neural Science*, 2nd Edition: Elsevier.
- Karmarkar UR, Buonomano DV (2006) Different forms of homeostatic plasticity are engaged with distinct temporal profiles. *Eur J Neurosci* 23:1575-1584.
- Karmarkar UR, Buonomano DV (2007) Timing in the absence of clocks: encoding time in neural network states. *Neuron* 53:427-438.
- Karnup S, Stelzer A (1999) Temporal overlap of excitatory and inhibitory afferent input in guinea-pig CA1 pyramidal cells. *J Physiol* 516 (Pt 2):485-504.
- Kato K, Clifford DB, Zorumski CF (1993) Long-term potentiation during whole-cell recording in rat hippocampal slices. *Neuroscience* 53:39-47.
- Katz B, Miledi R (1968) The role of calcium in neuromuscular facilitation. *J Physiol* 195:481-492.
- Kilgard MP, Merzenich MM (1998) Plasticity of temporal information processing in the primary auditory cortex. *Nat Neurosci* 1:727-731.
- Kim SJ, Linden DJ (2007) Ubiquitous plasticity and memory storage. *Neuron* 56:582-592.
- Komatsu Y (1994) Age-dependent long-term potentiation of inhibitory synaptic transmission in rat visual cortex. *J Neurosci* 14:6488-6499.
- Kushner SA, Elgersma Y, Murphy GG, Jaarsma D, van Woerden GM, Hojjati MR, Cui Y, LeBoutillier JC, Marrone DF, Choi ES, De Zeeuw CI, Petit

-
- TL, Pozzo-Miller L, Silva AJ (2005) Modulation of presynaptic plasticity and learning by the H-ras/extracellular signal-regulated kinase/synapsin I signaling pathway. *J Neurosci* 25:9721-9734.
- Lamsa K, Heeroma JH, Kullmann DM (2005) Hebbian LTP in feed-forward inhibitory interneurons and the temporal fidelity of input discrimination. *Nat Neurosci* 8:916-924.
- Lapid E, Ulrich R, Rammsayer T (2008) On estimating the difference limen in duration discrimination tasks: a comparison of the 2AFC and the reminder task. *Percept Psychophys* 70:291-305.
- Laughlin S (1981) A simple coding procedure enhances a neuron's information capacity. *Z Naturforsch [C]* 36:910-912.
- Losonczy A, Makara JK, Magee JC (2008) Compartmentalized dendritic plasticity and input feature storage in neurons. *Nature* 452:436-441.
- Lu YM, Mansuy IM, Kandel ER, Roder J (2000) Calcineurin-mediated LTD of GABAergic inhibition underlies the increased excitability of CA1 neurons associated with LTP. *Neuron* 26:197-205.
- Maass W, Markram H (2002) Synapses as dynamic memory buffers. *Neural Netw* 15:155-161.
- Maffei L, Fiorentini A (1973) The visual cortex as a spatial frequency analyser. *Vision Res* 13:1255-1267.
- Malenka RC, Bear MF (2004) LTP and LTD: an embarrassment of riches. *Neuron* 44:5-21.
- Marder CP, Buonomano DV (2003) Differential effects of short- and long-term potentiation on cell firing in the CA1 region of the hippocampus. *J Neurosci* 23:112-121.
- Marder CP, Buonomano DV (2004) Timing and balance of inhibition enhance the effect of long-term potentiation on cell firing. *J Neurosci* 24:8873-8884.
- Markram H, Tsodyks M (1996) Redistribution of synaptic efficacy between neocortical pyramidal neurons. *Nature* 382:807-810.
- Markram H, Wang Y, Tsodyks M (1998) Differential signaling via the same axon of neocortical pyramidal neurons. *Proc Natl Acad Sci U S A* 95:5323-5328.

- Markram H, Lubke J, Frotscher M, Sakmann B (1997) Regulation of synaptic efficacy by coincidence of postsynaptic APs and EPSPs. *Science* 275:213-215.
- Marshall L, Henze DA, Hirase H, Leinekugel X, Dragoi G, Buzsaki G (2002) Hippocampal pyramidal cell-interneuron spike transmission is frequency dependent and responsible for place modulation of interneuron discharge. *J Neurosci* 22:RC197.
- Martin SJ, Grimwood PD, Morris RG (2000) Synaptic plasticity and memory: an evaluation of the hypothesis. *Annu Rev Neurosci* 23:649-711.
- McAdams CJ, Reid RC (2005) Attention modulates the responses of simple cells in monkey primary visual cortex. *J Neurosci* 25:11023-11033.
- McCormick DA, Wang Z, Huguenard J (1993) Neurotransmitter control of neocortical neuronal activity and excitability. *Cereb Cortex* 3:387-398.
- McLean HA, Caillard O, Ben-Ari Y, Gaiarsa JL (1996) Bidirectional plasticity expressed by GABAergic synapses in the neonatal rat hippocampus. *J Physiol* 496 (Pt 2):471-477.
- Miles R (1990) Variation in strength of inhibitory synapses in the CA3 region of guinea-pig hippocampus in vitro. *J Physiol* 431:659-676.
- Miles R (2000) Perspectives: neurobiology. Diversity in inhibition. *Science* 287:244-246.
- Miller KD, Keller JB, Stryker MP (1989) Ocular dominance column development: analysis and simulation. *Science* 245:605-615.
- Mochida S, Few AP, Scheuer T, Catterall WA (2008) Regulation of presynaptic Ca(V)2.1 channels by Ca²⁺ sensor proteins mediates short-term synaptic plasticity. *Neuron* 57:210-216.
- Mongillo G, Barak O, Tsodyks M (2008) Synaptic theory of working memory. *Science* 319:1543-1546.
- Morrone MC, Ross J, Burr D (2005) Saccadic eye movements cause compression of time as well as space. *Nat Neurosci* 8:950-954.
- Mountcastle VB, Powell TP (1959) Neural mechanisms subserving cutaneous sensibility, with special reference to the role of afferent inhibition in sensory perception and discrimination. *Bull Johns Hopkins Hosp* 105:201-232.

-
- Murphy BK, Miller KD (2003) Multiplicative gain changes are induced by excitation or inhibition alone. *J Neurosci* 23:10040-10051.
- Nowak L, Bregestovski P, Ascher P, Herbet A, Prochiantz A (1984) Magnesium gates glutamate-activated channels in mouse central neurones. *Nature* 307:462-465.
- Pennartz CM, Kitai ST (1991) Hippocampal inputs to identified neurons in an in vitro slice preparation of the rat nucleus accumbens: evidence for feed-forward inhibition. *J Neurosci* 11:2838-2847.
- Perez-Orive J, Mazor O, Turner GC, Cassenaer S, Wilson RI, Laurent G (2002) Oscillations and sparsening of odor representations in the mushroom body. *Science* 297:359-365.
- Perkins KL (2006) Cell-attached voltage-clamp and current-clamp recording and stimulation techniques in brain slices. *J Neurosci Methods* 154:1-18.
- Pouille F, Scanziani M (2001) Enforcement of temporal fidelity in pyramidal cells by somatic feed-forward inhibition. *Science* 293:1159-1163.
- Prescott SA, De Koninck Y (2003) Gain control of firing rate by shunting inhibition: roles of synaptic noise and dendritic saturation. *Proc Natl Acad Sci U S A* 100:2076-2081.
- Rabinovich M, Huerta R, Laurent G (2008) Neuroscience. Transient dynamics for neural processing. *Science* 321:48-50.
- Reyes A, Sakmann B (1999) Developmental switch in the short-term modification of unitary EPSPs evoked in layer 2/3 and layer 5 pyramidal neurons of rat neocortex. *J Neurosci* 19:3827-3835.
- Reyes A, Lujan R, Rozov A, Burnashev N, Somogyi P, Sakmann B (1998) Target-cell-specific facilitation and depression in neocortical circuits. *Nat Neurosci* 1:279-285.
- Robinson HP, Kawai N (1993) Injection of digitally synthesized synaptic conductance transients to measure the integrative properties of neurons. *J Neurosci Methods* 49:157-165.
- Rodriguez-Moreno A, Paulsen O (2008) Spike timing-dependent long-term depression requires presynaptic NMDA receptors. *Nat Neurosci* 11:744-745.

- Rolls ET, Tovee MJ (1994) Processing speed in the cerebral cortex and the neurophysiology of visual masking. *Proc Biol Sci* 257:9-15.
- Rosenmund C, Stevens CF (1996) Definition of the readily releasable pool of vesicles at hippocampal synapses. *Neuron* 16:1197-1207.
- Rozov A, Burnashev N (1999) Polyamine-dependent facilitation of postsynaptic AMPA receptors counteracts paired-pulse depression. *Nature* 401:594-598.
- Rozov A, Burnashev N, Sakmann B, Neher E (2001) Transmitter release modulation by intracellular Ca²⁺ buffers in facilitating and depressing nerve terminals of pyramidal cells in layer 2/3 of the rat neocortex indicates a target cell-specific difference in presynaptic calcium dynamics. *J Physiol* 531:807-826.
- Rumelhart DE, McClelland JL, University of California San Diego. PDP Research Group. (1986) *Parallel distributed processing : explorations in the microstructure of cognition*. Cambridge, Mass.: MIT Press.
- Rutherford LC, DeWan A, Lauer HM, Turrigiano GG (1997) Brain-derived neurotrophic factor mediates the activity-dependent regulation of inhibition in neocortical cultures. *J Neurosci* 17:4527-4535.
- Salinas E, Thier P (2000) Gain modulation: a major computational principle of the central nervous system. *Neuron* 27:15-21.
- Schneggenburger R, Sakaba T, Neher E (2002) Vesicle pools and short-term synaptic depression: lessons from a large synapse. *Trends Neurosci* 25:206-212.
- Seung HS (2003) Learning in spiking neural networks by reinforcement of stochastic synaptic transmission. *Neuron* 40:1063-1073.
- Sharp AA, O'Neil MB, Abbott LF, Marder E (1993) The dynamic clamp: artificial conductances in biological neurons. *Trends Neurosci* 16:389-394.
- Shepherd GM (1994) *Neurobiology*, 3rd Edition: Oxford University Press.
- Shew T, Yip S, Sastry BR (2000) Mechanisms involved in tetanus-induced potentiation of fast IPSCs in rat hippocampal CA1 neurons. *J Neurophysiol* 83:3388-3401.
- Shu Y, Hasenstaub A, Badoual M, Bal T, McCormick DA (2003) Barrages of synaptic activity control the gain and sensitivity of cortical neurons. *J Neurosci* 23:10388-10401.

-
- Sjostrom PJ, Turrigiano GG, Nelson SB (2007) Multiple forms of long-term plasticity at unitary neocortical layer 5 synapses. *Neuropharmacology* 52:176-184.
- Song S, Miller KD, Abbott LF (2000) Competitive Hebbian learning through spike-timing-dependent synaptic plasticity. *Nat Neurosci* 3:919-926.
- Sourdet V, Russier M, Daoudal G, Ankri N, Debanne D (2003) Long-term enhancement of neuronal excitability and temporal fidelity mediated by metabotropic glutamate receptor subtype 5. *J Neurosci* 23:10238-10248.
- Spruston N, Johnston D (1992) Perforated patch-clamp analysis of the passive membrane properties of three classes of hippocampal neurons. *J Neurophysiol* 67:508-529.
- Staff NP, Spruston N (2003) Intracellular correlate of EPSP-spike potentiation in CA1 pyramidal neurons is controlled by GABAergic modulation. *Hippocampus* 13:801-805.
- Staley K, Smith R (2001) A new form of feedback at the GABA(A) receptor. *Nat Neurosci* 4:674-676.
- Steriade M (2001) Impact of network activities on neuronal properties in corticothalamic systems. *J Neurophysiol* 86:1-39.
- Steriade M, Timofeev I, Grenier F (2001) Natural waking and sleep states: a view from inside neocortical neurons. *J Neurophysiol* 85:1969-1985.
- Stevens CF (2005) Consciousness: Crick and the claustrum. *Nature* 435:1040-1041.
- Stoppini L, Buchs PA, Muller D (1991) A simple method for organotypic cultures of nervous tissue. *J Neurosci Methods* 37:173-182.
- Sullivan JM (2007) A simple depletion model of the readily releasable pool of synaptic vesicles cannot account for paired-pulse depression. *J Neurophysiol* 97:948-950.
- Tan AY, Zhang LI, Merzenich MM, Schreiner CE (2004) Tone-evoked excitatory and inhibitory synaptic conductances of primary auditory cortex neurons. *J Neurophysiol* 92:630-643.
- Thorpe S, Fize D, Marlot C (1996) Speed of processing in the human visual system. *Nature* 381:520-522.

- Trotter Y, Celebrini S (1999) Gaze direction controls response gain in primary visual-cortex neurons. *Nature* 398:239-242.
- van Pelt J, Vajda I, Wolters PS, Corner MA, Ramakers GJ (2005) Dynamics and plasticity in developing neuronal networks in vitro. *Prog Brain Res* 147:173-188.
- Varela JA, Sen K, Gibson J, Fost J, Abbott LF, Nelson SB (1997) A quantitative description of short-term plasticity at excitatory synapses in layer 2/3 of rat primary visual cortex. *J Neurosci* 17:7926-7940.
- von der Malsburg C (1973) Self-organization of orientation sensitive cells in the striate cortex. *Kybernetik* 14:85-100.
- Wagenaar DA, Madhavan R, Pine J, Potter SM (2005) Controlling bursting in cortical cultures with closed-loop multi-electrode stimulation. *J Neurosci* 25:680-688.
- Wang X, Lu T, Snider RK, Liang L (2005) Sustained firing in auditory cortex evoked by preferred stimuli. *Nature* 435:341-346.
- Wehr M, Zador AM (2003) Balanced inhibition underlies tuning and sharpens spike timing in auditory cortex. *Nature* 426:442-446.
- Wigstrom H, Gustafsson B (1985) Facilitation of hippocampal long-lasting potentiation by GABA antagonists. *Acta Physiol Scand* 125:159-172.
- Wilent WB, Contreras D (2005) Dynamics of excitation and inhibition underlying stimulus selectivity in rat somatosensory cortex. *Nat Neurosci* 8:1364-1370.
- Wright SH (2004) Generation of resting membrane potential. *Adv Physiol Educ* 28:139-142.
- Xie Z, Yip S, Morishita W, Sastry BR (1995) Tetanus-induced potentiation of inhibitory postsynaptic potentials in hippocampal CA1 neurons. *Can J Physiol Pharmacol* 73:1706-1713.
- Xu J, Kang N, Jiang L, Nedergaard M, Kang J (2005) Activity-dependent long-term potentiation of intrinsic excitability in hippocampal CA1 pyramidal neurons. *J Neurosci* 25:1750-1760.
- Zalutsky RA, Nicoll RA (1990) Comparison of two forms of long-term potentiation in single hippocampal neurons. *Science* 248:1619-1624.

-
- Zhang L, Spigelman I, Carlen PL (1991) Development of GABA-mediated, chloride-dependent inhibition in CA1 pyramidal neurones of immature rat hippocampal slices. *J Physiol* 444:25-49.
- Zhang ZW (2004) Maturation of layer V pyramidal neurons in the rat prefrontal cortex: intrinsic properties and synaptic function. *J Neurophysiol* 91:1171-1182.
- Zheng W, Knudsen EI (1999) Functional selection of adaptive auditory space map by GABAA-mediated inhibition. *Science* 284:962-965.
- Zucker RS, Regehr WG (2002) Short-term synaptic plasticity. *Annu Rev Physiol* 64:355-405.